Asset and Liability Management: Optimization using Least-Squares Monte Carlo

Master's thesis in Mathematical Statistics

By

SANNA BRANDEL

Supervisor:
Prof. Magnus Wiktorsson

LUNDS UNIVERSITET

Faculty of Mathematical Statistics
2018

Abstract

This thesis aims to examine an efficient asset and liability management method under Solvency II regulations, and to find an optimization framework that takes complex interactions between assets and liabilities into account. The investigated approach consists of a least-squares Monte Carlo method, where least-squares regression is used to obtain a proxy function for future net asset values. A fairly close approximation is achieved, and the computational burden is significantly reduced compared to a traditional full nested Monte Carlo simulation method. By allocating capital into several asset classes with different risk attributes, the effects on the risk adjusted net asset value are studied when moving from low to high risk assets. Restrictions on risk and asset return are introduced, and an optimal allocation compatible with the Solvency capital requirement is obtained. For comparison, a similar study is conducted using a mean-variance optimization approach.

Keywords: Asset and liability management, Solvency capital requirement, least-squares Monte Carlo, nested Monte Carlo simulation, risk-adjusted net asset value, mean-variance optimization

Acknowledgements

I would like to express my gratitude to Prof. Magnus Wiktorsson at the Department of Mathematical Statistics, Lund University, for his guidance and valuable advice. Furthermore, I would like to thank my supervisors, Lars Larsson and Edvard Sjögren, at Kidbrooke Advisory for their support and useful inputs, and for the opportunity to realize this thesis.

Contents

List of Abbreviations

ALM ..... Asset and liability management

ATS ..... Affine term structure

B-S ..... Black-Scholes

CIR ..... Cox-Ingersoll-Ross

CVaR ..... Conditional value-at-risk

EIOPA ..... European insurance and occupational pensions authority

LARS ..... Least angle regression

LS ..... Least-squares

LSMC ..... Least-squares Monte Carlo

MJD ..... Merton jump diffusion

MVO ..... Mean-variance optimization

NAV ..... Net asset value

QE ..... Quadratic exponential

RANAV ..... Risk adjusted net asset value

RAROC ..... Risk adjusted return on capital

SCR ..... Solvency capital requirement

SDE ..... Stochastic differential equation

VA ..... Variable annuity

VaR ..... Value-at-risk

ZCB ..... Zero coupon bond

Chapter 1

Introduction

In the insurance industry, risk-based capital requirements are continuously being revised as part of the Solvency II framework. One key aspect of the framework is the Solvency capital requirement (SCR), i.e. the measure of risk defined by the capital required under Solvency II principles. To satisfy this aspect of the regulatory framework, insurers are required to determine their risk capital for a one-year time horizon. A factor that can greatly impact an insurer's SCR is an efficient asset and liability management (ALM) method. An impact on the SCR will in turn impact the risk adjusted net asset value, affecting the solvency of the insurer. Large losses as a result of asset-liability mismatches can thereby be avoided by applying basic ALM techniques (Gilbert, 2017).

Although primarily viewed as a risk mitigation exercise, many insurers aim to exercise ALM as a strategic decision-making framework. In these cases, investment strategies related to the assets and liabilities are implemented to achieve financial objectives beyond risk management. The implementation is however an issue to many insurers, to a large extent due to inefficient methods underlying their numerical computations.

Some widely applied approaches are traditional asset allocation methodologies, such as the Markowitz mean-variance optimization (MVO). However, there are several well-known limitations to the MVO framework. Traditionally, only the asset side of the balance sheet is optimized, meaning complex interactions between assets and liabilities are not taken into account. Secondly, the standard deviation, i.e. the risk measure considered in a MVO framework, assumes a symmetric distribution. As this is not a common attribute in return distributions, standard deviation fails to sufficiently capture the full risk picture.

In this thesis, an approach where the insurer's portfolio performance is defined by the net assets, rather than just the assets, will be examined. Instead of the MVO standard deviation, the value-at-risk (VaR) will be the risk measure considered in this approach. VaR provides additional information on the maximum loss, and holds no assumptions on distributional symmetry, making it in many regards preferable to standard deviation. Additionally, the one-year VaR at a 99.5% confidence level is considered in SCR calculations, meaning this choice of risk measure makes ALM calculations compatible under Solvency II regulations.

The liability structure will in this thesis be determined by implementing a replicating portfolio approach, using basic financial instruments. The considered approach is selected due to its increasing popularity, and it is currently used by an increasing number of insurers (Hermans and Waaijer, 2013). The type of insurance products considered here are unit-linked with embedded guarantees. The liabilities are therefore set to replicate a class of variable annuities that hold the desired pay-off structure. A similar approach can been seen in e.g. Cathcart (2012) and Bacinello et al. (2011), where insurance products with the considered attributes are valuated.

The implementation will consist of a stochastic simulation approach called the least-squares Monte Carlo (LSMC) method. An advantage to stochastic simulation is the possibility of examining future economic scenarios over time and analyzing the resulting distribution. As the ALM workflow involves projecting the balance sheet of an insurance company forward in time, this method will be used to provide future economic scenarios from which expected net asset values can be obtained. Economic scenario generation, in turn, is well aligned with the philosophy of Solvency II, and currently the method most of the large insurers implement in their SCR calculations (Cathcart, 2012).

To account for the embedded optionality present in the liability structure, a nested stochastic simulation

approach is required. This approach can be summarized in two steps; first, outer scenarios are generated under real world measure. Following this, the instruments are valued using inner scenarios, simulated under risk neutral measure. As the SCR is calculated over a 99.5% confidence level, tail accuracy is of essence, meaning a very large number of valuation scenarios are required. Consequently, a full nested Monte Carlo simulation becomes extremely computationally costly (Cathcart, 2012).

The scope of implementing the LSMC method in ALM calculations is to obtain a proxy function for future net asset values from the nested simulated economic scenarios, using a far smaller amount of inner scenarios. By utilizing the cross-sectional information between inner and outer scenarios the accuracy of the approximations remains high, while the required runtime is greatly reduced in comparison to a full nested simulation.

The LSMC method has gained popularity in the financial field due to its substantial advantages. It was originally proposed by Longstaff and Schwartz (2001) in the context of American option pricing, and it has since been applied for a number of different implementations. For a setting closer to this thesis, see e.g. Bauer et al. (2010), where the LSMC method is applied to obtain a framework for SCR calculations.

The significant gain in computational efficiency from using the LSMC regressed proxy function, rather than a full nested simulation, allows for evaluations that are extremely fast in comparison. This facilitates the study of the effects from moving capital between asset classes, and enables the implementation of a time efficient ALM optimization framework. Consequently, optimal investment strategies can be applied to reach financial objectives, in addition to the required risk mitigation under Solvency II regulations. The financial objective will in this thesis consist of the maximization of the risk adjusted net asset value, by optimally allocating investments between several asset classes with different risk attributes. The optimization will be performed subject to some minimum return requirement and SCR-based risk constraint.

As a complement to the main optimization framework, an MVO approach concerning the entire NAV rather than just the asset side will be implemented. The intention is to compare the results between frameworks, which can provide useful insights on the impact of the considered risk measure.

1.1 Background

This section serves to briefly introduce the reader to some concepts central to the thesis. Beginning with an introduction to asset and liability management, the section proceeds with a definition of the Solvency capital requirement. This is followed by a short summary of the main financial risks associated with the assets and liabilities of an insurance undertaking.

1.1.1 Asset and Liability Management

The Society of Actuaries ALM Principles Task Force 2004 provides the following definition for asset and liability management (ALM):

"Asset Liability Management is the ongoing process of formulating, implementing, monitoring, and revising strategies related to assets and liabilities to achieve financial objectives, for a given set of risk tolerances and constraints."

In short, the goal of ALM is to manage the financial risk exposure associated with assets backing liabilities. As this risk exposure is a function of both assets and liabilities, risk mitigation concerning the entire balance sheet is a key focus of ALM. Relative risk is therefore of greater importance to an insurer than absolute risk. To illustrate this, have a look at the following example (Gilbert, 2017):

Consider a highly volatile asset portfolio whose market value is prone to large swings. This implies that the portfolio has a high absolute risk. However, this portfolio is also backing liabilities whose value changes by the same amount for a given change in a financial variable. This leads to the relative risk of the portfolio, associated with both assets and liabilities, being of more importance than the absolute risk, associated only with assets.

The example emphasizes the inappropriateness of implementing a management approach for insurance portfolios focusing solely on the asset side of the balance sheet. Managing assets separately against a benchmark, rather than directly against the liabilities, is not effective in an ALM point of view. This implementation would possibly yield a portfolio with a higher return on assets, but with far more increasing liabilities and, consequently, capital requirements.

Another important feature of the ALM process is the measurement of risk exposure. A popular approach is to calculate the distribution of the assets and liabilities by using stochastic simulation. An advantage to this method is the possibility of examining future economic scenarios over time, and testing impacts of ALM strategies.

Following the risk measurement, it remains to determine how the risks should be managed. Company culture, the nature of the liabilities and the regulatory environment all influence how the financial risks associated with the assets and liabilities are measured and managed. For some insurers, ALM is viewed as a risk mitigation exercise primarily and the goal is simply to ensure that all risk exposures are within the approved risk limits. In the case considered in this thesis, ALM is executed as a strategic decision-making framework. Beyond risk mitigation, optimal investment strategies related to the assets and liabilities are implemented to achieve financial objectives. Said financial objective will in this thesis consist of the maximization of the risk adjusted net asset value under Solvency II regulations, subject to some constraints on minimum return and risk.

1.1.2 The Solvency Capital Requirement

Solvency II is a European regulation introduced in 2009, which establishes the restrictions of risk management for insurance undertakings. The Solvency capital requirement (SCR) is part of the Pillar 1 requirements of the Solvency II framework. This aspect of the regulatory framework demands that the amount of available financial resources of an insurer should cover its overall financial requirements. This enables the insurer to absorb significant losses, which in turn gives reasonable assurance to policyholders and beneficiaries that payment obligations will be met.

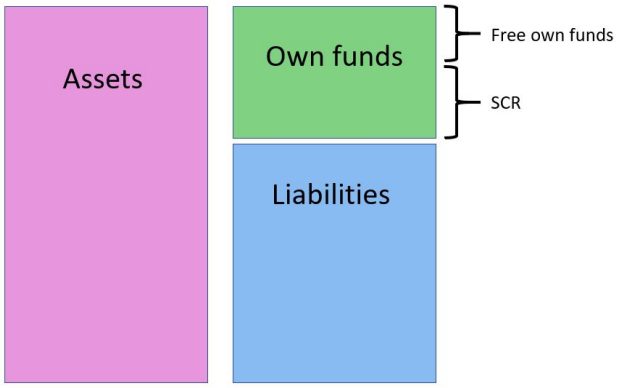

Figure 1.1: *Insurance balance sheet under Solvency II.*

Figure 1.1 presents a simplified illustration of the relation between assets and liabilities under Solvency II. Here, own funds refer to the net asset value (NAV) that remains when the market value of liabilities is deducted from the total market value of assets. Expressed in balance sheet terms, the regulations require that eligible own funds must be higher than the SCR. The insurers are responsible for calculating and meeting said requirements, and they are allowed to apply internal models for the computations.

Under Solvency II regulations, the SCR is based on VaR calibrated to a 99.5% confidence level over a 1-year time horizon.

The Standard Formula for SCR Calculation

The standard formula for SCR calculation is provided by the European insurance and occupational pensions authority (EIOPA), and is currently used by the majority of European insurers (Hooghwerff et al., 2017). It is a standardized calculation method based on a number of underlying assumptions, meaning it might not be appropriate for an insurance undertaking whose risk profile deviates significantly from the assumptions. As previously mentioned, internal models are allowed for SCR calculations in these cases.

When applying the SCR standard formula, each individual risk module is calibrated to the predefined 99.5% confidence level. Following this, the resulting VaR levels are aggregated using linear correlation techniques, and the overall SCR can be evaluated. The calculations are based on the assumption of a linear dependency structure between risk factors, with a modification to the correlation coefficients to account for potential tail dependencies and skewed distributions. For further information on the underlying assumptions of the standard formula, see EIOPA (2014).

The framework used in this thesis differs from that of the standard formula, as the VaR will be calculated over the entire NAV distribution rather than performing individual evaluations of each risk factor. As a result, potential aggregation errors are avoided.

1.1.3 Financial Risk

Insurers face various financial risks associated with assets backing liabilities, and identifying the main sources of risk is an essential part of ALM. In this section, the primary financial risks related to the assets and liabilities of an insurance undertaking will be briefly introduced. Risks related directly to a specific insurance product, such as surrender risk and mortality risk, will be overlooked as this is not considered to be within the scope of the thesis.

Interest Rate Risk

Interest rate risk represents the risk of losses resulting from movements in interest rates and their impact on future cash-flows. This is ultimately a function of the gains and losses on reinvestment and disinvestment of the actual cash flows that are realized in future.

Liquidity Risk

Liquidity risk is the exposure to the illiquidity of the assets and liabilities, i.e., the risk that a given financial asset cannot be traded quickly enough in the market without impacting the market price.

Market Risk

The risk from movements in equity and other non-fixed income assets on the balance sheet due to factors affecting the entire market. The market risk includes not just the exposure to losses in market value, but also the mismatch risk associated with backing insurance liabilities with non-fixed income assets such as equity.

Credit Risk

Credit risk is the exposure associated with a borrower's failure to meet a contractual obligation. This risk also includes decreases in market value of financial assets resulting from an increase in credit spread, in case the assets require liquidation before maturity. This ties credit risk to liquidity- and interest rate risk.

1.2 Objective

Aiming to reach an efficient ALM under Solvency II regulations, the objective of this thesis is to construct a suitable optimization framework that takes the complex interaction between assets and liabilities into account. An LSMC approach will be implemented to obtain approximations of future net asset values, and a proxy function will be constructed based on the results. If a close approximation is achieved, this method provides a time efficient alternative to traditional ALM calculations using full nested Monte Carlo simulations. The analysis is focused on the maximization of the risk adjusted net asset value, subject to some restrictions on risk and asset return. The effects of allocating capital into several asset classes with different risk attributes are studied, and an optimal allocation compatible with the SCR is obtained. For comparison, a similar study is conducted using a mean-variance optimization framework.

1.3 Thesis Outline

The disposition of the remaining part of the thesis is structured in the following way:

Chapter 2: Concepts & Definitions In this chapter, some useful financial and statistical definitions are presented. After this, a mean-variance optimization framework will be introduced, followed by a corresponding framework based on the risk adjusted net asset value.

Chapter 3: Theory Chapter 3 presents the theoretical background to the thesis. The LSMC method is introduced along with a suitable optimization method for the resulting proxy function, as well as some appropriate performance measures. The chapter proceeds with a description of the optimization algorithms used in the ALM optimization. It concludes with a summary of the mathematical simulation models, generating the risk factors underlying the least-squares Monte Carlo method.

Chapter 4: Methodology Here, the methodology used to derive the results is presented. Simulation schemes for the various risk factor models are defined, along with the implemented dependence modelling method. A liability framework based on a replicating portfolio approach is determined, and the entire ALM optimization process is summarized for the RANAV and MVO frameworks.

Chapter 5: Results The results obtained from implementing the methodology are presented in this chapter. After listing the parameters and restrictions used in the implementation, the performance and goodness of fit of the LSMC regression is tested and summarized. ALM optimization results are subsequently displayed and compared for the RANAV and MVO frameworks, and the effects of moving capital between different asset classes are studied.

Chapter 6: Conclusion & Discussion In the concluding chapter, the main findings of the ALM optimization are summarized and discussed. The performance of the implemented methods are reviewed, and the resulting limitations and advantages are listed. Possible future research topics are proposed, along with some potential extensions to the current framework.

Chapter 2

Concepts & Definitions

In this chapter, some financial and statistical concepts and definitions will be presented. The chapter begins with useful definitions of risk measures, followed by some descriptive statistics of financial time series. After this, a mean-variance optimization framework will be briefly introduced. Lastly, a corresponding framework based on the risk adjusted net asset value will be outlined.

2.1 Risk Measures

The choice of risk measure is of great significance when conducting most types of financial analysis, and the results may be considerably affected if an inappropriate measure is used. In the below paragraphs, a definition of general and coherent risk measures, adapted from Riccioletti (2016), will be stated.

Let $\mathbb{X}$ be the set of all risks, consisting of e.g. a firms loss at a specified point.

Definition A risk measure $\rho(X)$ is a mapping from $\mathbb{X}$ into $\mathbb{R}$.

A measure of risk $\rho(X)$ is thus a real number that allows us to express the riskiness of a portfolio. With a general definition for risk measure in place, we are ready to define the coherent risk measure.

Definition A risk measure $\rho(X)$ is coherent if it satisfies the following axioms:

A1. Sub-additivity: For all $X_1 \in \mathbb{X}$ and $X_2 \in \mathbb{X}$, we have

$$\rho(X_1 + X_2) \leq \rho(X_1) + \rho(X_2)$$

This axiom ensures that the risk of a portfolio is smaller or equal than the sum of the risk of each position due to diversification. In this sense, we can say that the sub-additivity property sets an upper bound to the risk of a portfolio.

A2. Translation Invariance: For all $X \in \mathbb{X}$ and $m \in \mathbb{R}$, we have

$$\rho(X + m) = \rho(X) + m$$

Thus, adding a risk-free amount to a portfolio results in an decrease in the risk of the position by exactly the same amount, implying that a risk less investment does not provide diversification.

A3. Positive Homogeneity: For all $X \in \mathbb{X}$ and $\tau > 0$, we have

$$\rho(\tau X) = \tau\rho(X)$$

This axiom implies that, for instance, when the exposure to a specific position doubles, then the risk measure related to that position doubles as well.

A4. Monotonicity: For all $X_1 \in \mathbb{X}$ and $X_2 \in \mathbb{X}$ with $X_1 \leq X_2$, we have

$$\rho(X_1) \geq \rho(X_2)$$

This property asserts that if in each possible outcome the position X_2 performs better than position X_1, then the risk associated with X_1 should be higher by comparison.

2.1.1 Standard Deviation

Beginning with the most elementary risk metric, standard deviation is a measure that quantifies the amount of variation or dispersion in a set of data values. The mathematical definition of standard deviation in the discrete case is as follows;

Define X as a discrete random variable that takes values from a finite data set $x_i,\ i = 1, ..., n$ with equal probability. Then X has the standard deviation:

$$\sigma = \sqrt{E[\ (X - E[X])^2\ ]} = \sqrt{\sum_{i=1}^{n}(x_i - E[X])^2}$$

where $E[X]$ denotes the expected value of X.

Standard deviation fulfills all of the above axioms except for the translation invariance. This is because the addition of a constant m does not change the standard deviation of X;

$$\rho(X + m) = \sqrt{E[\ (X + m - E[X + m])^2\ ]} = \sqrt{E[\ (X - E[X])^2\ ]} = \rho(X)$$

An additional note is that the variance, i.e. the squared standard deviation, is neither positive homogeneous nor sub-additive.

2.1.2 Value-at-Risk

Value-at-risk (VaR) has become the primary risk measure for determining capital charges against market risk. Informally, VaR can be described as the maximum loss in a specified period for some confidence level. Formally, VaR_α is the 1-α-percentile of the return distribution or, equivalently, the α-percentile of the loss distribution:

$$VaR_\alpha(l) = F_L^{-1}(\alpha) = inf\{l \in \mathbb{R} \mid F_L(l) \geq \alpha\}, \qquad \alpha \sim [0, 1]$$

where the loss distribution F_L is the distribution function of the random variable l. Figure 2.1 gives an intuitive picture of VaR for a confidence level of $1 - \alpha$.

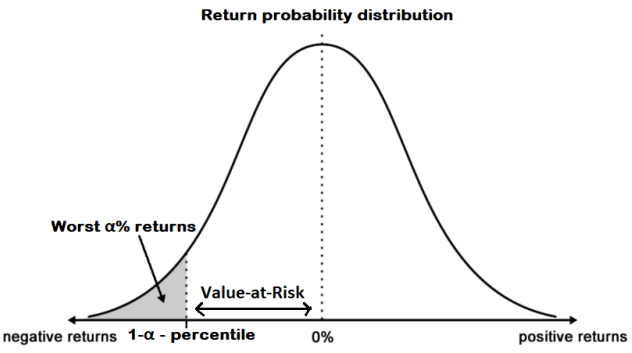

Figure 2.1: *Value-at-Risk of a demeaned return distribution.*

In terms of the SCR, where a 1-year $VaR_{99.5\%}$ is considered, this would correspond to the worst loss one would expect to occur in a single year over a 200-year time horizon. Alternatively, one could say that there is a 0.5% probability for a loss of $VaR_{99.5\%}$ over the next year.

A complication regarding VaR is that the property of sub-additivity is not satisfied. This is caused by the fact that VaR is not an expectation, and therefore the shape of the tail before and after the VaR probability does not necessarily have any bearing on the actual VaR. As a result, the aggregate VaR of a portfolio can be higher than the sum of VaR's of the individual assets in the portfolio, meaning that a diversification effect is not guaranteed. However, regarding asset returns that meet the stylized facts, VaR has been shown to be sub-additive in practice. Consequently, for a vast enough number of assets, VaR is considered a coherent risk measure. For further details, see for instance Daníelsson et al. (2005).

2.1.3 Conditional Value-at-Risk

Conditional Value-at-risk (CVaR), also known as expected shortfall, can be viewed as a coherent alternative to VaR. CVaR is defined as the weighted average of losses exceeding VaR, providing information on how much, on average, the worst case scenarios will cost for a given confidence level. This, along with the attractive mathematical properties a coherent risk measure holds, gives CVaR an advantage over VaR which only conveys how often the worst cases will occur.

Using above VaR-notations, the mathematical definition of CVaR is the following:

$$CVaR_\alpha(l) = E[\, l \mid l \geq VaR_\alpha]$$

2.2 Financial Time Series

When considering financial time series, in particular asset returns, there are a number of stylized facts concerning distributional properties to keep in mind. The facts deemed of most relevance to this thesis will be presented below for future reference.

2.2.1 Stylized Facts

The following stylized facts are a set of properties, common in financial time series across many instruments, markets and time periods. For affirmations, see for instance Cristelli (2014) and Cont (2001).

Heavy tails: The distribution of returns displays large fluctuations leading to heavy tails with finite tail index, brought on by extreme outcomes. The precise form of the tails is however difficult to determine.

Gain/loss asymmetry: Large drawdowns can be observed in financial time series, but not equally large upward movements. This is due to an asymmetry in the return probability distribution function; positive returns have less impact on the time series than negative returns of the same absolute magnitude. This leads to a skewness in the return distribution.

Volatility clustering: Periods of large fluctuations tend to be followed by other large fluctuation-periods regardless of the sign, which implies that high-volatility events tend to cluster in time.

Leverage effect: The volatility of an asset is in most measures negatively correlated with the returns of the asset. This implies that the volatility tends to rise in response to a lower return than expected, and vice versa.

2.3 Mean-Variance Optimization

The mean-variance optimization (MVO) framework is a component of Markowitz (1952) groundbreaking work "Modern Portfolio Theory". The fundamental goal of MVO is to maximize the ratio of expected portfolio return to standard deviation, by optimally allocating investments between different assets.

Traditional MVO concerns only the asset side of the balance sheet. However, since our application concerns ALM, it would lead to clear disadvantages to disregard the liability side of the balance sheet. This

will be more thoroughly discussed in section 2.4. The MVO framework outlined in this thesis will therefore consider the ratio of expected NAV to standard deviation, rather than expected asset return. For simplicity of notation, we will from now on refer to this as the MVO ratio. In basic mathematical terms, it could be defined as the following:

Suppose there are N risky assets, and let w_n be the proportion of capital invested into asset n, with $\sum_{i=1}^{N} w_i = 1$. We then get the following optimization problem, with $\mathbf{w}^{MVO}$ denoting the vector of optimal weights:

$$\mathbf{w}^{MVO} = arg \max_{w_i} \frac{E[NAV_p]}{\sigma_p} \tag{2.1}$$

Here, $E[NAV_p]$ and σ_p denote the expected NAV and standard deviation of the portfolio, respectively.

The Efficient Frontier

The efficient frontier is defined by all portfolios with the highest expected return for a given level of risk, or alternatively, the lowest risk for a given expected return. In short, this curve contains all efficient portfolios in a risk-return framework. Relating the prior case to the considered MVO ratio, this would be equivalent to maximizing equation 2.1 for a fixed σ_p.

2.3.1 Limitations of MVO

The MVO framework has since its publication in 1952 dominated the asset allocation process, but it has a number of well-known deficiencies to consider upon implementation.

Only the first two moments are considered; the expected return and the risk, which in this framework is quantified by the standard deviation. In light of this, a traditional assumption often made is that returns are independently and identically normal distributed, making statistical properties of asset returns more manageable. In addition to this, the expected return, standard deviation and correlations are all assumed to be known. This alone presents a considerable difficulty, since the estimation of these attributes is often far from trivial.

Recalling the previously mentioned stylized facts, it is evident that the first two moments do not suffice in order to define a realistic return distribution. The positive excess kurtosis, from the gain/loss asymmetry, as well as the heavy tails and volatility clustering present apparent issues in this regard.

Considering the specific case of ALM studied in this thesis, complex interactions between assets and liabilities are also to be taken into account, in addition to distributional properties. Traditional MVO concerns only the asset side of the balance sheet, without considering the implications on the net assets. Recall the discussion in section 1.1.1 on the inappropriateness of using an asset-only management for insurance portfolios. The relative risk associated with assets backing liabilities is completely ignored in this approach. Consequently, traditional MVO is deemed insufficient for ALM calculations.

For this reason, the MVO framework applied in this thesis will take the entire NAV into account rather than just the assets, replacing the expected asset return with the expected NAV. Because of the shortcomings of the MVO risk measure, however, the MVO framework will be implemented only as a complement to the main optimization framework. The intention is to compare the results between frameworks, which can provide useful insights on the impact of the considered risk measure.

2.4 RAROC & RANAV

The risk adjusted return on capital (RAROC) is, as the name implies, a risk adjusted profitability measure. Taking both risk management and performance evaluation into regard, RAROC enables a consistent comparison of risky financial returns for a range of different capital allocations.

The measure is formally defined as the ratio of expected return to economic capital. Economic capital is a fairly wide-ranging concept, determined by what quantity RAROC is intended to measure. However, a general definition of economic capital is that it represents the amount of capital needed to cover all financial requirements, in order to absorb significant losses from unexpected shocks in market values. A common approach to calculating the economic capital is by VaR, meaning the following equality can be stated:

$$RAROC = \frac{Expected\ return}{Economic\ capital} = \frac{Expected\ return}{VaR}$$

In this thesis, a similar risk adjusted profitability measure will be considered. At difference from RAROC, this measure will take the expected NAV into account, rather than the expected return. This enables us to directly study the impacts on the expected NAV distribution as capital is moved between different asset classes. A similar study using a NAV to SCR approach is seen in e.g. Lombardo and Bailly (2014).

This ratio will be referred to as the risk adjusted net asset value (RANAV) throughout the thesis, and is defined as the following:

$$RANAV = \frac{Expected\ net\ asset\ value}{VaR}$$

2.4.1 Optimizing with Respect to RANAV

A framework corresponding to the above defined MVO framework can be constructed by instead using RANAV as objective function. This approach would have similarities to the considered MVO framework, as expected NAV would be maximized with respect to some measure of risk. The difference lies in the considered risk measure, which in the RANAV framework consists of VaR rather than the MVO standard deviation. As previously mentioned, VaR has some significant advantages over standard deviation when representing portfolio risk. Most importantly, standard deviation does not sufficiently capture the total risk of returns. This is mainly due to the gain/loss asymmetry in financial time series - standard deviation assumes symmetric distributions, which expects the probability of returns being above or below the mean to be the same. VaR, on the other hand, captures the end tail of the distribution, providing additional information on the maximum loss. This makes VaR a risk measure in many senses preferable to standard deviation, even though estimation difficulties remain.

As to why the coherent CVaR is not the risk measure of choice, there are two simple reasons. Firstly, VaR has also been shown to be a coherent risk measure under conditions that are usually met when the stylized facts in section 2.2.1 apply. The second reason is regulatory - since the SCR is based on the 1-year 99.5% VaR, choosing the same risk metric makes calculations compatible.

In line with the notations used in section 2.3, an analogous optimization framework with respect to RANAV can be defined. For a given confidence level α, we get the following optimization problem:

$$\mathbf{w}^{RANAV} = arg\ \max_{w_i}\ \frac{E[NAV_p]}{VaR_\alpha(p)} \tag{2.2}$$

where $E[NAV_p]$ and $VaR_\alpha(p)$ denote the expected NAV and VaR of the portfolio, respectively, and w_i is the proportion of capital invested into asset i, with $\sum_{i=1}^{N} w_i = 1$.

Chapter 3

Theory

In this chapter, the theoretical background to the thesis is presented. The chapter begins with an introduction to the least-squares Monte Carlo method, where some underlying theory on nested simulation and least-squares regression is demonstrated. An optimization method for the regressed proxy function is then briefly introduced, followed by the performance measures used to evaluate the goodness of fit of the model. After this, the algorithms used in the ALM optimization are presented. The chapter concludes with a summary of the mathematical simulation models used to generate the risk factors underlying the least-squares Monte Carlo method.

Before diving into the theoretical concepts of this thesis, we will start by stating a general valuation framework. For the subsequent part, the reader is assumed to be familiar with basic probability theory and stochastic calculus.

Assume a complete probability space $(\Omega, \mathcal{F}, P)$. The state space Ω is the set of all possible outcomes ω of the stochastic economy, $\mathcal{F}$ denotes the σ-algebra on Ω, while P is the probability measure defined on $(\Omega, \mathcal{F})$. We define $(\mathcal{F}(t))_{t\geq 0}$ to be the filtration generated by the relevant price process in the economy, containing all information available up to time t. Let $(\mathcal{F}(t))$ be a sub-σ-algebra of $\mathcal{F}$, and assume that for all $s < t < \infty$, $\mathcal{F}(s) \subseteq \mathcal{F}(t) \subseteq \mathcal{F}(\infty) := \mathcal{F}$. Consistent with the no-arbitrage concept, assume the existence of a risk neutral probability measure Q, equivalent to P. The difference between the two probability measures will be discussed later on in this chapter. Lastly, let $\phi(\omega, t \geq 0, T)$ denote the path generated by a European option's pay-off up to maturity T.

3.1 Least-Squares Monte Carlo

Least-squares Monte Carlo (LSMC) is a simulation-based method, well-used in the field of mathematical finance. The method can be viewed as a two-step procedure. First, a nested Monte Carlo (MC) simulation consisting of outer and inner scenarios is performed. In the outer scenarios, realizations of all risk factors are generated up to a predefined time horizon. In the inner scenarios, each instrument is valuated conditional on the simulated risk factors. Next, the resulting values from the valuation scenarios are regressed in a least-squares sense. The objective of the method is to decrease the number of required scenarios in order to greatly reduce the computational burden, while maintaining a high accuracy.

One advantage with the LSMC technique is that it allows for an increasing complexity. The more realistic the model, the less likely it is that an analytical pricing formula exists. As a consequence, simulation based pricing algorithms such as LSMC are required. In the financial field, the method is often used to calculate the value of an option with multiple sources of uncertainty, or whose complicated features make an analytical solution impractical or even impossible. Many insurance liabilities fit into this category because of their complex and path dependent nature (Cathcart, 2012).

LSMC was first introduced by Longstaff and Schwartz (2001) as a scheme to estimate the price of an American option, performed by stepping backward in time. For a setting closer to the objective of this thesis, Bauer et al. (2010) employs LSMC to the calculation of the required risk capital, providing a mathematical framework for the calculation of the SCR. Two additional references of high relevance are Cathcart (2012)

and Bacinello et al. (2011), who valuate unit-linked insurance products with featured embedded guarantees using the LSMC method.

This sections defines the LSMC approach starting with a presentation of nested MC simulation, followed by a definition of linear least-squares regression. To conclude, suitable proxy functions will be proposed along with appropriate optimization schemes.

3.1.1 Step 1: Nested Monte Carlo Simulation

As previously mentioned, a nested MC simulation is performed as two types of consecutive scenarios:

- Outer scenarios, where realizations of all risk factors are generated under a real world measure P up to a certain horizon.
- Inner scenarios, branching out from the endpoints of the outer scenarios, where risk neutral simulations under Q are used to valuate each instrument conditional on the generated risk factors.

Before further defining the nested MC simulation, a clarification of the concepts of real world and risk neutral scenarios is in place.

Real world vs. risk neutral scenarios In general, there are two measures used in financial simulation. The risk neutral measure Q is used to recover the price of an instrument based on the assumption of no arbitrage. Under Q, risk is hedged and options can be priced using their expected discounted cash flows. This makes the pricing compatible with the pricing of other contracts in the market, meaning the prices are consistent.

Returning to our valuation framework, the no-arbitrage valuation theory dictates that the price $p(\omega, t, T)$ of the option is given by taking the expectation of the discounted pay-off $\phi(\omega, t, T)$ with respect to the risk neutral pricing measure Q:

$$p(\omega, t, T) = E^Q[\ e^{-\int_t^T r(s)ds}\phi(\omega, t, T)\ |\ \mathcal{F}(t)\ ] \tag{3.1}$$

where $r(t)$ denotes the risk free short rate at time t.

The real world measure P, on the other hand, is consistent with the risk preferences of the market, as investors expect higher returns when taking larger risks. All cash flow projections are modelled under the real world measure.

Summarizing, any attempt to project values for a risky portfolio under Q must be based on an appropriate real world model under P, in order to incorporate the current setting of the market.

In our context, we use each outer real world scenario to project the risk factors forward with the time horizon of one year. Using each outer scenario as starting point, a number of inner, risk free scenarios are then used to calculate the arbitrage free value of the portfolio. The portfolio will in our setting approximate net asset values, for which the liability side has a structure similar to that of a forward contract and a European put option. It will be properly defined in chapter 4, and we will until then refer to it as the NAV function for simplicity.

For a simple illustration, consider the following for n_{out} outer and n_{inn} inner simulations:

Let y_{ij} correspond to inner risk neutral simulation $i,\ i = 1, ..., n_{inn}$, with outer real world simulation $j,\ j = 1, ..., n_{out}$ as starting point, and let X_j be a vector containing all inner simulations y_{ij}. Let $NAV(X_j, t) := NAV[X_j]$ denote the NAV at time t. This value is calculated as the average of the discounted risk neutral values $NAV[y_{ij}]$ of all inner simulations according to real world simulation j, obtained from the pricing formula 3.1. Figure 3.1 shows an overview of this procedure.

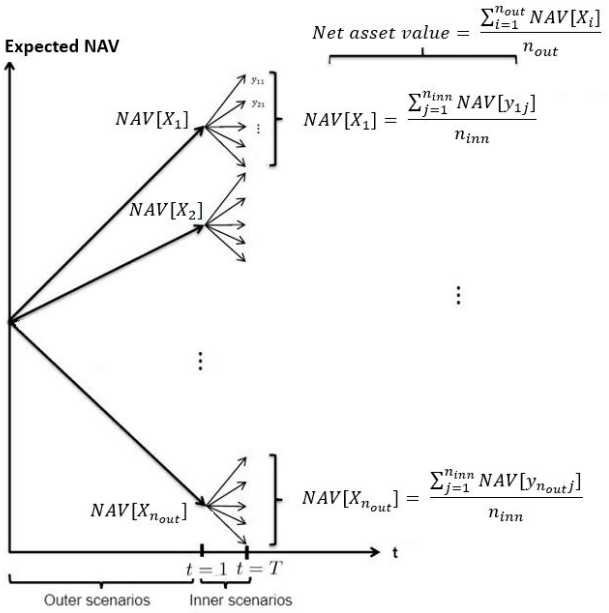

Figure 3.1: *NAV valuation from a nested Monte Carlo simulation.*

3.1.2 Step 2: Least-Squares Regression Procedure

Moving on to the second step of the LSMC method, a least-squares (LS) regression is performed over the NAVs at time t, $NAV[X_i]$, $i = 1, ..., n_{out}$, calculated as the average of all risk neutral values. Figure 3.2 gives an intuitive illustration of this process.

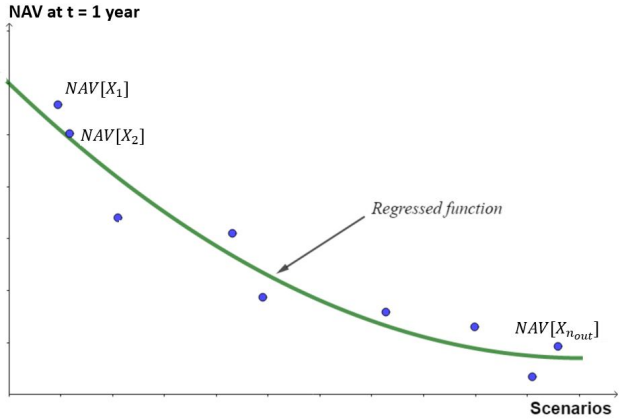

Figure 3.2: *Fitted LSMC regression of NAV.*

The idea underlying the LSMC method is that the NAV can be approximated by a proxy function obtained from the regression, jointly with the cross-sectional information provided by the nested simulation. This reduces the number of required inner scenarios, and consequently the computation time, while maintaining a high accuracy in the results. Before defining a suitable proxy function, an introduction to LS regression will be presented.

3.1.3 Linear Least-Squares Regression

The purpose of linear LS regression is to relate a number of explanatory variables to a response variable, in order to fit the observed data to a linear function by LS estimation. In the case considered in this thesis,

this corresponds to fitting the risk factors at year one to the resulting NAV at maturity.

For p explanatory variables with n observations, a linear model can be expressed on the following matrix form:

$$\mathbf{Y} = \mathbf{X}\beta + \epsilon$$

where;
$\mathbf{Y} \in \mathbb{R}^{n\times 1}$ is the vector of observations on the response variable
$\mathbf{X} \in \mathbb{R}^{n\times p+1}$ is the design matrix consisting of a column of ones, followed by the p column vectors of the observations on the explanatory variables
$\beta \in \mathbb{R}^{p+1\times 1}$ denotes the vector of parameters to be estimated
$\epsilon \in \mathbb{R}^{n\times 1}$ is a vector of random errors.

Assumptions: For an LS estimation to be viable, there are a few assumptions that should be checked in order to guarantee a reliable outcome. Focusing on a selected few, the following assumptions carry substantial benefits if satisfied. However, results may still be satisfactory even if all assumptions are not met (Osborne and Waters, 2002).

1. Linearity: The relationship between the response and explanatory variables is assumed to be linear.

2. Homoscedacity: The variance of the explanatory variable errors ϵ is assumed to be the same across all values of the explanatory variable.

3. Independence between errors: The errors of the explanatory variable are assumed to be independent.

4. No multicollinearity: There can be no redundancies in the information contained in the explanatory variables. This means that $\mathbf{X}$ must be of full column rank, i.e., there can be no linear dependencies among the columns of $\mathbf{X}$.

Least-Squares Estimation

As previously mentioned, β is a vector of unknown constants to be estimated from the data, in this context using LS estimation. An important note on LS estimates is that an assumption on normally distributed variables is not required. Even in the absence of normality, LS estimates have the lowest variance among all linear unbiased estimators, making it the best linear unbiased estimate (B.L.U.E).

Let Assumption 4 be fulfilled and $\mathbf{X}$ have full column rank. The LS estimation of β is obtained as:

$$\hat{\beta} = arg\ \min_{\beta} \ || \ \mathbf{Y} - \mathbf{X}\beta \ ||_2^2$$

with $||\mathbf{a}||_2^2 = \mathbf{a}'\mathbf{a}$ denoting the 2-norm of the vector $\mathbf{a}$, and $\mathbf{a}'$ being the conjugate transpose. The optimal $\hat{\beta}$ is thereby found by making $\mathbf{X}\beta$ the best possible approximation of $\mathbf{Y}$, in a LS sense. This is achieved by solving the normal equations, expressed in equation 3.2. Since the normal equations are consistent, they will always have a solution.

$$\mathbf{X}'\mathbf{X}\hat{\beta} = \mathbf{X}'\mathbf{Y} \quad \Longrightarrow \quad \hat{\beta} = (\mathbf{X}'\mathbf{X})^{-1}\mathbf{X}'\mathbf{Y} \tag{3.2}$$

3.1.4 Proxy Functions

The general idea of the LSMC method is that the net asset values $NAV[X_i],\ i = 1, ..., n$, can be approximated by a proxy function obtained from the LS regression, jointly with the cross-sectional information provided by the nested MC simulation. Once a suitable proxy function has been established, the simulation of inner scenarios is no longer necessary to obtain approximate NAVs, which greatly reduces the computational burden.

In order to set up a good proxy function, a choice of appropriate basis functions has to be made. The literature proposes various alternatives, and a common approach is to use the set of orthogonal Laguerre polynomials. This is the approach used in e.g. Longstaff and Schwartz (2001).

In this thesis, however, the regression basis functions will be a set of regular polynomial terms up to a pre-specified order for each of the risk factors and their cross terms. One motivation for this choice of basis function is that the regular polynomial approach is considered less complex and easy to visualize. In addition to this, the difference in performance between regular and Laguerre polynomials has in similar applications been shown to be very small in, for instance, Danielsson and Gistvik (2014) and Cathcart (2012).

Consider a NAV function with maturity T. At time t, let the approximate net asset value $NAV^{prox}(\mathbf{x}, t)$ be a function of the LS estimates β, the risk factors $\mathbf{x}$ and their respective cross terms. For a pre-specified polynomial order p, N risk factors and m cross terms this provides the following equation:

$$NAV^{prox}(\mathbf{x}, t) = f(\mathbf{x}, \beta, g(\cdot)) = \beta_0 + \sum_{i=1}^{N}\sum_{j=1}^{p} \beta_{(i-1)p+j} x_i^j + \sum_{i=1}^{m} \beta_{pN+i} g_i(x_1, ..., x_N) \tag{3.3}$$

where $g(\cdot)$ denotes a set of functions describing each of the cross terms. As an example, consider the following NAV proxy function of risk variables x_1 and x_2, with a polynomial degree of two:

$$NAV^{prox}(x_1, x_2, t) = \beta_0 + \underbrace{\beta_1 x_1 + \beta_2 x_1^2}_{\text{Risk } x_1 \text{ terms}} + \underbrace{\beta_3 x_2 + \beta_4 x_2^2}_{\text{Risk } x_2 \text{ terms}} + \underbrace{\beta_5 x_1 x_2}_{\text{Cross term}}$$

The values of the basis functions are independently and identically distributed across the different simulation paths. In a framework regarding the pricing of American options, weak assumptions on the existence of moments imply that the fitted values of the regression converges in mean square and in probability to the true option value (Longstaff and Schwartz, 2001). A similar convergence can be shown to hold for a liability function, assuming some very general conditions on the liability pay-offs are met (Koursaris, 2011). In practice, the rate of convergence depends on a number of different factors, such as the number of risk variables, the variability of the estimates β, as well as the smoothness and differentiability of the true NAV function.

3.1.5 Optimizing the Proxy Function

A drawback with the regular polynomial regression approach is the large number of terms in the basis function, rapidly increasing with the number of risk drivers and polynomial order. Each valuation has some associated sampling error. By choosing a too complex regression model, one can end up fitting to the sampling error as well as the underlying NAV, creating a problem of statistical over-fitting. In our particular LSMC setting, this can cause the proxy function to try to fit the outer scenario points too closely, even as sampling errors cause them they differ from the true NAV. As a consequence, some regions of the NAV proxy distribution might appear almost oscillatory, which is obviously not a correct representation of the true NAV distribution (Cathcart, 2012).

Thus, a method for selecting an adequate subset of the polynomial terms is required. This section will present two suitable methods for this purpose; least angle regression and the lasso method. Following this, a useful modification that allows us to combine the two methods and, as a result, reduce the computational burden, will be presented.

The Lasso

The lasso method is an attractive version of ordinary LS that constrains the sum of the absolute regression coefficients. This forces certain coefficients to be set to zero, effectively choosing a simpler model by excluding the coefficients at issue.

Keeping previous notations, assume that the explanatory variables $\mathbf{X}$ have been standardized to be zero-mean and unit length, and that the response $\mathbf{Y}$ is zero-mean. For n observations and N explanatory variables, we obtain the prediction vector:

$$\mathbf{X}\hat{\beta} = \sum_{i=1}^{N} x_i \hat{\beta}_i$$

yielding the following residual sum of squares:

$$SS_{res}(\hat{\beta}) = || \mathbf{Y} - \mathbf{X}\hat{\beta} ||^2 = \sum_{j=1}^{n} (y_j - x_j\hat{\beta}_j)^2$$

The lasso method selects the optimal parameters $\hat{\beta}^{lasso}$ by minimizing the residual sum of squares subject to a restriction t on the absolute norm of $\hat{\beta}$:

$$\hat{\beta}^{lasso} = arg \min_{\hat{\beta}} SS_{res}(\hat{\beta}), \quad \sum_{i=1}^{N} |\hat{\beta}_i| \leq t \tag{3.4}$$

This shrinkage technique tends to shrink the parameters toward zero, especially for small values of t. The method has been showed in e.g. Hastie et al. (2001) to improve prediction accuracy, in addition to offering the parsimonious benefits of a simpler model, as it trades off decreased variance for increased bias.

Least Angle Regression

The least angle regression (LARS) is closely related to the forward stagewise regression method, where the explanatory variable with the largest absolute correlation with the response is selected in each step. In contrast to the popular forward stepwise method, who is often accused of being overly greedy in the elimination of variables that might be of significance to the response, the forward stagewise is a more cautious method due to its considerably smaller step sizes. The LARS algorithm allows the implementation of the forward stagewise using rather large steps, accelerating the computations.

A full account of the LARS procedure can be found in Efron et al. (2003). To get an intuitive idea, a brief introduction will be presented here.

As in forward stepwise, all coefficients are initially set to zero, and the explanatory variable, call it x_1, with the highest correlation to the response $\mathbf{Y}$ is selected. Next, the largest step possible is taken in the direction of x_1 until another explanatory variable, x_2, has an equally large correlation with the current residual ϵ_1. While the forward stepwise would continue along x_1, LARS advances in an equiangular direction, i.e. the "least angle direction", between x_1 and x_2 until the next variable with the highest correlation is found. This process is repeated by each time proceeding equiangularly between the selected covariates, in each successive step adding one explanatory variable to the model.

In algebraic phrasing, the correlations between the explanatory variables and response depend only on the projection $\bar{\mathbf{Y}}$ of $\mathbf{Y}$ onto the linear space spanned by the covariates $\mathbf{X}$:

$$Cov(\mathbf{X}\hat{\beta}) = \mathbf{X}'(\mathbf{Y} - \mathbf{X}\hat{\beta}) = \mathbf{X}'(\bar{\mathbf{Y}} - \mathbf{X}\hat{\beta})$$

The start value of the algorithm is $\mathbf{X}\hat{\beta}^0 = 0$, as the response has been demeaned. Since the largest covariance is found between the variable x_1 and $\mathbf{Y}$, $\bar{\mathbf{Y}} - \mathbf{X}\hat{\beta}$ makes the smallest angle with x_1. This brings LARS to augment $\mathbf{X}\hat{\beta}^0$ in the direction of x_1, creating the subsequent estimate:

$$\mathbf{X}\hat{\beta}^1 = \mathbf{X}\hat{\beta}^0 + \hat{\gamma_1}x_1$$

where $\hat{\gamma_1}$ is chosen such that $\bar{\mathbf{Y}} - \mathbf{X}\hat{\beta}$ is equally correlated with x_1 and x_2. Consecutive LARS steps are then taken along equiangular vectors.

For a general definition, let $\mathcal{A}$ denote the active set with indices corresponding to the explanatory variables with the greatest absolute correlations. Let $\mathbf{X}\hat{\beta}^{\mathcal{A}}$ be the current LARS estimate. The subsequent step is then given by:

$$\mathbf{X}\hat{\beta}^{\mathcal{A}_+} = \mathbf{X}\hat{\beta}^{\mathcal{A}} + \hat{\gamma}u_{\mathcal{A}} \tag{3.5}$$

where $u_{\mathcal{A}}$ denotes the equiangular vector between the selected covariates, and $\hat{\gamma}$ is the smallest possible value such that some new variable joins the active set $\mathcal{A}$.

Modified Least Angle Regression using Lasso

This modification to LARS, proposed by Efron et al. (2003), produces lasso estimates while significantly reducing the computational burden. Due to the substantial benefits, this is the method chosen for the regression in this thesis.

In a LARS manner, the algorithm moves along the equiangular direction whose forward progress is determined by the currently most correlated variables. However, the lasso modification adds some restrictions on the equiangular strategy.

Suppose that we have just completed a LARS step, and that the corresponding LARS estimate $\hat{\beta}^{\mathcal{A}}$ is equivalent to a lasso solution $\hat{\beta}^{lasso}$. For notation's sake, we will denote this LARS/lasso estimate as $\hat{\beta}_j$ for an index j from the active set $\mathcal{A}$. The sign of any non-zero $\hat{\beta}_j$ can then be shown to always agree with the sign of the current estimate correlation:

$$sign\{\hat{\beta}_j\} = sign\{\ Cov(\ x_j'(\mathbf{Y} - \mathbf{X}\hat{\beta}))\} := s_j \tag{3.6}$$

Define $\omega_{\mathcal{A}}$ as a unit vector yielding equal angles in the equiangular vector $u_{\mathcal{A}}$, and let $\hat{d}$ be a vector containing $s_j\omega_{\mathcal{A}j}$ for $j \in \mathcal{A}$, and zero elsewhere. The LARS/lasso estimate can now be expressed in the following way:

$$\beta_j(\gamma) := \hat{\beta}_j + \gamma\hat{d}_j$$

As a result of the sign restriction 3.6, $\beta_j(\gamma)$ will change sign at $\gamma_j = -\frac{\hat{\beta}_j}{\hat{d}_j}$, meaning that the first sign change occurs at:

$$\tilde{\gamma} := \underset{\gamma_j > 0}{min}\ \gamma_j$$

Let $\hat{\gamma}$ be defined by the LARS estimate in 3.5. If $\tilde{\gamma} \leq \hat{\gamma}$, $\beta_j(\gamma)$ can not be a lasso solution for $\gamma > \tilde{\gamma}$. This is again due to the sign restriction 3.6, since $\tilde{\gamma} \leq \hat{\gamma}$ would imply that $\beta_j(\gamma)$ changed sign while s_j did not.

This leads us to the lasso modification of 3.5; If $\tilde{\gamma} \leq \hat{\gamma}$, stop the ongoing LARS step at $\gamma = \tilde{\gamma}$ and exclude index j from the calculation of the next equiangular direction:

$$\mathbf{X}\hat{\beta}^{\mathcal{A}_+} = \mathbf{X}\hat{\beta}^{\mathcal{A}} + \tilde{\gamma}u_{\mathcal{A}}, \quad \mathcal{A}_+ = \mathcal{A} - j$$

With this modification, assuming the calculations only involve a single index j at a time, the LARS algorithm yields all lasso solutions. For a complete description of the modified LARS/lasso procedure, see Efron et al. (2003). The software used in the practical application is part of the Scikit-learn machine learning package, developed by Pedregosa et al. (2011).

3.2 Performance measures

To evaluate whether the proxy function obtained from the LMSC regression is sufficient to explain the structure of the true NAV, some assessments of the goodness of fit are required. In this section, the performance measures applied for this purpose are presented.

3.2.1 Cross-validation

Cross-validation is a technique for assessing how well the regressed model generalizes to an independent data set. There are several cross-validation methods, and considering the setting of this thesis an appropriate method would be to compare with a benchmark. By regressing the proxy function using an independent set of simulations, the regressed function can then be applied to the simulations that generated the benchmark. The resulting regressed values can thereby be cross-validated against the benchmark to determine the goodness of fit of the regressed model.

In this thesis, the full nested MC simulation will provide the true NAV and set the benchmark. This means that the underlying simulation models are assumed to be correct, which is an obvious simplification. Model uncertainty testing will however be left out, as it is not considered to be within the scope of the thesis.

The cross-validation against the regressed NAV proxy function will be conducted using several performance measures, presented in the following paragraphs.

3.2.2 R-square

In statistics, one of the most commonly used performance measures is the R-square. The R-square is generally based on the assumption that the regression in question is linear. If this is the case, the sums of the squared errors always add up in a specific manner:

$$SS_{tot} = SS_{reg} + SS_{res}$$

For observations $y_i,\ i = 1, ..., n$ of the response $\mathbf{Y}$, with $\bar{y}$ being the mean of the observed data and $\hat{y}_i,\ i = 1, ..., n$ the regressed values, the above notations are defined as the following:

$SS_{tot} := \sum_{i=1}^{n}(y_i - \bar{y})^2$ denotes the total sum of squares,

$SS_{res} := \sum_{i=1}^{n}(y_i - \hat{y}_i)^2$ is the sum of squares of residuals,

$SS_{reg} := \sum_{i=1}^{n}(\hat{y}_i - \bar{y})^2$ denotes the regression sum of squares.

The R-square, also known as the coefficient of determination, determines what proportion of total variation is explained by the regressed model. In other words, R-square is a performance measure that explains how well the regressed function approximates the observed data. Using above notations, the R-square is defined as:

$$R^2 = 1 - \frac{SS_{res}}{SS_{tot}} \tag{3.7}$$

Since the sum of squares of residuals in theory should be less or equal to the total sum of squares, R-square is a number between zero and one. The smaller the sum of squares of residuals, the higher R-square and, consequently, the better the fit of the regressed function.

3.2.3 Adjusted R-square

A drawback with regular R-square is that it assumes that every independent variable in the model contributes to explaining the variation in the response. Adjusted R-square, on the other hand, penalizes the R-square value as more explanatory variables are included. As a result, adjusted R-square yields the proportion of total variation explained only by the variables that in reality affect the response. Using above R-square notations, the adjusted R-square is given by:

$$R^2_{adj} = 1 - (1 - R^2)\frac{n-1}{n-p-1} \tag{3.8}$$

where p is the total number of regressors.

3.2.4 Out of Sample R-square

In order to adapt the regular and adjusted R-square to a cross-validation framework, a slight adjustment is made. Definitions 3.7 and 3.8 still apply along with the sum of squares definitions of SS_{tot} and SS_{res}. The difference lies in the examined data set $\mathbf{Y}$. In this application we want to compare the benchmark, consisting of the full nested MC values, to the regressed values we obtain when applying the regressed proxy function to the outer simulations that generated the benchmark. The proxy function will in turn be regressed over a separate set of LSMC simulations.

Let equation 3.7 define the out of sample R-square, with;

$SS_{tot} := \sum_{i=1}^{n}(y_i - \bar{y})^2$ denoting the total sum of squares,

$SS_{res} := \sum_{i=1}^{n}(y_i - \hat{y}_i)^2$ denoting the sum of squares of residuals.

In this case, $y_i,\ i = 1, ..., n$ are the observed benchmark values of the full nested simulation, $\bar{y}$ is the benchmark mean, and $\hat{y}_i,\ i = 1, ..., n$ are the values obtained when running the simulations that generated the benchmark through the regressed proxy function.

The out of sample adjusted R-square is obtained by simply replacing R-square with the out of sample R-square, while the sample size n is taken from the benchmark.

3.2.5 Comparison of Moments

By comparing distributional properties, another kind of cross-validation can be applied between the benchmark and regressed NAV. In this setting, we will focus on the first four moments of the resulting distributions. Recalling the stylized facts in section 2.2.1, the considered moments are all central concerning financial time series.

Let X be a random variable that takes values from a finite data set $x_i,\ i = 1, ..., n$ with equal probability, and let:

$$E[X^k] = \frac{1}{n}\sum_{i=1}^{n} x_i^k$$

The four initial central moments of the probability density function of X are defined as:

1. Mean: $\mu := E[X]$
As the name implies, the mean determines the mean value of the probability distribution.

2. Variance: $\sigma^2 := E[\ (X-\mu)^2\ ] = E[X^2] - \mu^2$
Being the squared standard deviation, the variance quantifies the amount of dispersion in the distribution.

3. Skewness: $\gamma := \frac{E[\ (X-\mu)^3\ ]}{E[\ (X-\mu)^2\ ]^{3/2}} = \frac{E[X^3]-3\mu\sigma^2-\mu^3}{\sigma^3}$
The skewness is a measure of the asymmetry in the probability distribution. A negative skew implies that the left tail of the probability density function is longer or heavier than the right tail, and vice versa. A symmetrical distribution, e.g. the normal distribution, has zero skewness.

4. Kurtosis: $\beta := \frac{E[\ (X-\mu)^4\ ]}{E[\ (X-\mu)^2\ ]^2} = \frac{E[X^4]-4E[X^3]\mu+6E[X^2]\mu^2-3\mu^4}{\sigma^4}$
Kurtosis measures the "tailedness" of the distribution. A common notation is the excess kurtosis, which is simply the kurtosis subtracted by three. This associates the kurtosis to a normal distribution, which has an excess kurtosis of zero. Distributions with an excess kurtosis less than zero are called platykurtic, implying lighter tails and fewer and less extreme outliers than the normal distribution. In the opposite case, distributions with a kurtosis greater than zero are said to be leptokurtic.

In addition to the moments, the quantiles of the NAV distribution are of interest. The 0.5% quantile is of particular importance, since SCR calculations are central to this thesis. A comparison of relevant quantiles will therefore be added to the goodness of fit-analysis.

3.2.6 Time Performance

The remaining performance measure concerns the difference in computation time between the LSMC regression and the full nested MC simulation. Since the full nested method is very costly in terms of computational burden, the reduction in run time is a very important aspect to the LSMC method.

Using the full nested MC simulation as benchmark, the runtime required for each segment of the LSMC method will be measured, allowing us to evaluate the improvements in time efficiency.

3.3 Optimization Methods

Returning to the main objective of the thesis, a suitable multidimensional optimization algorithm is required to find the optimal amount of capital invested into each asset class. In this setting, it is essential that the selected optimization method does not require any gradient information. This is due to the disposition of the NAV proxy function, making it impossible to obtain partial derivatives. This will be returned to in chapter 4, after the liability function has been properly defined.

Two methods satisfying the above requirement are the Nelder-Mead and the Powell method, which will be presented in the remaining part of this section.

3.3.1 The Nelder-Mead Method

The Nelder-Mead method is an effective and computationally compact direct search method proposed by Nelder and Mead (1965). It is a simplex method, using a multidimensional triangular approach to find a local minimum of an objective function. This method uses only function values, and does not try to form any approximate gradients.

For an intuitive explanation of the algorithm, consider the two-dimensional case, where a simplex corresponds to a triangle. Let the objective function be denoted by f. The Nelder-Mead method applies a pattern search, where the objective function values $f(x_1, x_2)$ at the three vertices of a triangle are compared. The vertex where the objective function is largest is rejected, and the next iteration step replaces it with a new vertex. This process is repeated, generating a sequence of triangles for which the worst vertex is replaced in each step.

In the n-dimensional case, a simplex S is defined as the convex hull of $n+1$ vertices $x_0, ..., x_n \in \mathbb{R}^n$. A requirement is that the starting point of the algorithm has to be non-degenerate, i.e. the points $x_0, ..., x_n$ can not lie in the same hyperplane. The Nelder-Mead method then performs a sequence of transformations on the working simplex S, aimed at decreasing the objective function values at its vertices. The four possible transformations of the Nelder-Mead algorithm are reflection, shrinkage, expansion and contraction, allowing S to change not only in size, but also in shape. The four parameters controlling the simplex transformation are presented in equation 3.9, along with standard values suggested by Singer and Nelder (2009).

$$\begin{aligned} &Reflection: \ \alpha = 1 \\ &Contraction: \ \beta = 1/2 \\ &Expansion: \ \gamma = 2 \\ &Shrinkage: \ \delta = 1/2 \end{aligned} \tag{3.9}$$

The simplex transformation algorithm can be described with the following three steps:

- Order the worst, best and the second best vertex of S by the the values of the objective function:

$$f_w = min_j \ f_j, \ f_b = max_j \ f_j, \ f_s = max_{j \neq n} \ f_j$$

- Compute the centroid c of the best side, i.e. the side opposite the worst vertex x_w:

$$c = \frac{1}{n} \sum_{j \neq w} x_j$$

- Compute a new working simplex from the current S. This is achieved by replacing the the worst vertex x_w with a point with lower function values by using reflection, expansion or contraction with respect to the best vertex x_b. All test points lie on the line defined by x_w and c. If no better vertex is found among the test points, S is shrunk towards x_b and n new vertices are computed.

Using notations seen in Singer and Nelder (2009), a brief summary of the transformations is presented below.

Reflect: The reflection point x_r is obtained as: $x_r = c + \alpha(c - x_w)$. Set $f_r = f(x_r)$. If $f_w \leq f_r < f_s$, x_r replaces x_w.

Expand: If $f_r < f_w$, the expansion point x_e is computed as: $x_e = c + \gamma(x_r - c)$. Set $f_e = f(x_e)$. If $f_e < f_r$, x_e replaces x_w. Otherwise, x_w is replaced by x_r. This way, only the best of x_r and x_e, i.e. the point providing the lowest objective function value, is accepted as the new vertex.

Contract: If $f_r \geq f_s$, the contraction point x_c is obtained by using the better of the points x_w and x_r. If $f_w < f_r$, $x_c = c + \beta(x_r - c)$. Otherwise, $x_c = c + \beta(x_w - c)$. Set $f_c = f(x_c)$. If $f_c \leq f_r$ in the first case, or $f_c < f_w$ in the second, x_c replaces x_w.

Shrink: If none of the above transformations worked and x_w has not been replaced, a shrinkage is performed by computing n new vertices $x_j = x_l + \delta(x_j - x_l)$ and setting $f_j = f(x_j),\ j = 1, ..., n$.

This process is iterated until the simplex S becomes sufficiently small, or when the objective function values $f(x_0, ..., x_n)$ are close enough. For a more thorough account of the Nelder-Mead method, see for instance Singer and Nelder (2009).

A drawback with this method is that the objective function needs to be fairly unimodal to obtain a reliable result. In addition to this, not much is known in general about the convergence properties of the method. For objective functions with certain properties, Nelder-Mead fails to converge to a minimizing point. For instance, it has been shown by e.g. McKinnon (1999) that particularly smooth objective functions can cause the algorithm to converge to a non-stationary point.

On a positive note, however, the Nelder-Mead method is considerably faster than other similar methods. The method is known to give significant improvements in the first few iterations, and it has been shown to obtain a good reduction in the function value using a relatively small number of function evaluations (Singer and Nelder, 2009).

3.3.2 The Powell Method

In similarity to the Nelder-Mead method, the Powell algorithm (Powell, 1964) does not require any gradients of the objective function. This is a conjugate direction method, performing a sequential one-dimensional minimization routine.

Like all direction set methods, Powell's conjugate direction method consists of a procedure for updating the set of directions until a local minimum is found. What distinguishes the conjugate direction method is that the minimization is performed along a conjugate set of directions, yielding a more efficient algorithm. Since this is a central concept in the Powell method, a more detailed description of the conjugate direction set is in place. The following definition is adapted from Press et al. (2007).

Define a set of directions $\mathbf{u}=(u_1, ..., u_n)$, and let f be a differentiable function. If f is minimized along $\mathbf{u}$, the gradient Δf must be perpendicular to $\mathbf{u}$ at the line minimum. If this was not the case, it would imply that there is still a nonzero directional derivative along $\mathbf{u}$. Choose a point p as the origin of the coordinate system. f can then be approximated by its Taylor series expansion:

$$f(\mathbf{x}) = f(p) + \sum_i \frac{\delta f}{\delta x_i} x_i + \frac{1}{2} \sum_{i,j} \frac{\delta^2 f}{\delta x_i \delta x_j} x_i x_j + ... \approx f(p) - \mathbf{b}^t \mathbf{x} + \frac{1}{2} \mathbf{x}^t \mathbf{A} \mathbf{x}$$

where $\mathbf{b}=-\Delta f|_p$ and $\mathbf{A}$ is the Hessian matrix. Considering the approximation of the Taylor series, the gradient is obtained as $\Delta f = \mathbf{Ax}$ **-** $\mathbf{b}$. For an $\mathbf{x}$-value obtained by $\mathbf{Ax} = \mathbf{b}$ the gradient will vanish, implying that an extremum has been found. Moving in the direction of u, the gradient adjusts in the following way:

$$\delta(\Delta f) = \mathbf{Au}$$

Applying this to a minimization procedure, assume that a minimum has been found when moving in the direction of u. Let $\mathbf{v}$ denote a new direction set, and move f along $\mathbf{v}$. In order for the minimization along $\mathbf{u}$ to remain undisturbed by the motion along $\mathbf{v}$, the change in the gradient has to be perpendicular to $\mathbf{u}$:

$$\mathbf{u}^t \delta(\Delta f) = \mathbf{u}^t \mathbf{A} \mathbf{v} = 0$$

If this holds, $\mathbf{u}$ and $\mathbf{v}$ are said to be conjugate. An entire set of vectors is conjugate when this relation holds pairwise for all members of the set.

Powell's method finds a set of mutually conjugate directions applying a quadratic convergence, while it does not require any gradient information. By letting the initial set of directions equal the basis vectors, i.e. $\mathbf{u} = (u_1, ..., u_n) = (e_1, ..., e_n)$, a local minimum can be approximated by iterating the following stepwise procedure.

- Start the procedure by saving the start position as p_0. For $i = 1, ..., n$, move p_{i-1} along u_i to obtain the minimum p_i.
- Update the direction set $\mathbf{u}$ by setting $u_i = u_{i-1}$ for $i = 1, ..., n-1$, and set $u_n = p_n - p_0$.

- Lastly, move p_n to the minimum along direction u_{n-1}. Denote this point p_0, and repeat the above procedure until the objective function f stops decreasing.

Powell has showed that for k iterations this algorithm produces a set of directions whose last k members $(u_{n-k}, ..., u_n)$ are mutually conjugate. In line with this, setting the number of iterations equal to the dimension n the Powell method will exactly minimize a quadratic form. Using the fact that most functions are quite well approximated by a quadratic function near their minima, methods that converge to the minimum of a quadratic function will also find the the minimum of a general function.

However, there is an apparent drawback with this method that is worth a mention. In each step, u_n is discarded in favor of $p_n - p_0$. This is likely to produce a set of directions that "fold up" on each other and become linearly dependent (Press et al., 2007). Consequently, the direction set no longer spans the entire n-dimensional parameter space, and the algorithm only finds the local minimum over a subspace. Additionally, the Powell method, in similarity to the Nelder-Mead, relies on function evaluations rather than gradients. As a result, there is a risk of convergence to non-minimizing points, in particular for objective functions that are not fairly unimodal.

3.4 Simulation Models

In this section, the theory underlying the models simulating the risk factors will be presented. The risk factors should adequately explain the risk characteristics of the NAV, and they are chosen such that several of the financial risks associated with ALM introduced in section 1.1.3 are represented. The selected risk drivers are the following:

Equity: A stock process, denoted $\{S(t)\}_{t\geq 0}$, will be generated using a Bates model.

Risk free rate: The risk free short rate, $\{r(t)\}_{t\geq 0}$, will be simulated from a Hull-White model to price risk free treasury bonds.

Credit rate: A default intensity, $\{\lambda(t)\}_{t\geq 0}$, will be generated from a Cox-Ingersol-Ross++ model to price corporate bonds with credit risk.

In the remaining part of this chapter, some of the most relevant models in the literature will be presented for each risk factor.

3.4.1 Short Rate Models

In this section some popular short rate models relevant to this thesis will be introduced, along with a connection to bond-pricing.

The short rate $r(t)$ represents an instantaneous interest rate valid for an infinitesimally short period of time. In our context, the Hull-White short rate model will be used to generate a risk free rate, which will be used to price risk free treasury bonds. In addition to this, a Cox-Ingersol-Ross++ model will be used to model a default intensity. This will be used to obtain a short rate with credit risk, allowing us to price defaultable corporate bonds. The bonds will in turn be two of the risk factors driving the NAV function, which will be properly defined in chapter 4.

Before presenting the models, some useful definitions stated in Björk (2009) will be presented for later reference.

Definition The money account process representing a risk free investment has the following dynamics:

$$dB(t) = r(t)B(t)dt, \quad B(0) = 1 \tag{3.10}$$

yielding the solution:

$$B(t) = e^{\int_0^t r(s)ds} \tag{3.11}$$

This is interpreted as the dynamics of a bank account, with the risk free short rate of interest $r(t)$.

Definition A zero coupon bond (ZCB) with maturity T is a contract which guarantees the holder 1 unit of currency to be paid out at maturity. The price $p(t,T)$ at time t is given by the risk neutral valuation formula:

$$p(t,T) = E^Q[\ e^{-\int_t^T r(s)ds} \mid \mathcal{F}(t)\ ] = E^Q[\ \frac{B(t)}{B(T)} \mid \mathcal{F}(t)\ ] \tag{3.12}$$

Note that this expression is present in the pricing formula 3.1, where the ZCB price is applied as a discount factor to the option pay-off. In this setting, we assume a perfect and arbitrage-free capital market, meaning that the risk neutral probability measure Q takes the money account $B(t)$ as numeraire.

Affine Models

As a starting point, a general approach to short rate modelling will be specified. The short rate is modelled under risk neutral probability measure Q as the solution of a stochastic differential equation (SDE) of the following form:

$$dr(t) = \mu(t,r(t))dt + \sigma(t,r(t))dW^Q(t) \tag{3.13}$$

where $W^Q(t)$ denotes a standard Brownian motion under Q, $\mu(t,r(t))$ is referred to as the drift term under Q, and $\sigma(t,r(t))$ denotes the diffusion of the process.

The particular class of short rate models considered in this thesis admits a special characteristic referred to as an affine term structure (ATS). For one-factor models this property ensures that a closed form expression for bond prices exists, as log bond prices are linear functions of the short rate:

$$p(t,T) = e^{A(t,T)-B(t,T)r(t)} \tag{3.14}$$

An affine function $f^{aff}(x)$ can be defined as a linear function plus a constant; $f^{aff}(x) = ax+c,\ a,c \in \mathbb{R}$. In order to hold an ATS, the drift and diffusion of the model must be of affine form, with possibly time dependent coefficients:

$$\begin{cases} \mu(t,r(t)) &= \alpha(t)r(t) + \beta(t) \\ \sigma(t,r(t)) &= \sqrt{\gamma(t)r(t) + \delta(t)} \end{cases} \tag{3.15}$$

Should this condition hold, the model is said to hold an ATS of the form 3.14, where A and B satisfies the following systems:

$$\begin{cases} \frac{\delta}{\delta t}B(t,T) + \alpha(t)B(t,T) - \frac{1}{2}\gamma(t)B^2(t,T) &= -1 \\ B(T,T) &= 0 \end{cases} \tag{3.16}$$

$$\begin{cases} \frac{\delta}{\delta t}A(t,T) &= \beta(t)B(t,T) - \frac{1}{2}\delta(t)B^2(t,T) \\ A(T,T) &= 0 \end{cases} \tag{3.17}$$

The Vasiček Model

One of the most common one-factor ATS short rate models is the Vasiček model, introduced by Vasiček (1977). This model was the first to capture mean reversion, meaning that short rates cannot rise indefinitely under Q, but instead show a tendency to revert to a long run value. Another property of the Vasiček model is the theoretical possibility for the short rate to become negative, which was viewed as a drawback during pre-crisis times when negative rates were highly uncommon. The model has also been met with some critique regarding its poor fit to the current term structure of interest rates.

The risk neutral Q-dynamics of the Vasiček model are given by:

$$dr(t) = (b - ar(t))dt + \sigma dW^Q(t) \tag{3.18}$$

where a, b and σ are held constant. Matching the coefficients of the Q-dynamics with 3.15, and solving the systems 3.16 and 3.17 yields the following ATS structure:

$$\begin{aligned} B(t,T) &= \frac{1}{a}(1-e^{-a(T-t)}) \ , \\ A(t,T) &= \frac{(B(t,T)-(T-t))(ab-\frac{1}{2}\sigma^2)}{a^2} - \frac{\sigma^2 B^2(t,T)}{4a} \end{aligned} \tag{3.19}$$

With the ATS structure known, the bond price can easily be obtained using equation 3.14.

The Hull-White Model

To address the issue of the Vasiček model's bad term structure fit, Hull and White (1993) developed an extension of the model. The Hull-White model is calibrated to fit the currently-observed structure of the forward rate, by allowing the forward yield curve to be incorporated into the model. Along with this improvement, there is the continued allowance of negative values, which can be seen as either a drawback or an advantage in a short rate model. Negative rates has been widely observed in the market after the 2008 financial crisis, which advocates the use of a model with a positive probability of reaching negative values. Due to its benefits, Hull-White is the model of choice for generating the risk free rate in this thesis.

The Q-dynamics of the one-factor Hull-White model are presented below:

$$dr(t) = (\theta(t) - ar(t))dt + \sigma dW^Q(t) \tag{3.20}$$

Comparing 3.20 to the Vasiček dynamics in 3.18, it can be noted that the only difference between the two ATS models lies in the drift term. In the Hull-White framework, the constant drift b is replaced by a time-varying deterministic parameter $\theta(t)$, which is calibrated to fit the observed initial term structure of the forward rate:

$$\theta(t) = \frac{\delta}{\delta t}f(0,t) + af(0,t) + \frac{\sigma^2}{2a}(1-e^{-2at}) \tag{3.21}$$

Here, $f(0,t) = -\frac{\delta}{\delta t} log\ p(0,T)$ denotes the instantaneous forward rate at time 0 for a maturity t. With the model dynamics known, the ATS can once again be obtained. Affine B remains the same as in 3.19, as $\theta(t)$ is not part of its structure. For a $\theta(t)$ chosen according to 3.21, Björk (2009) states the following bond pricing formula:

$$p(t,T) = \frac{p(0,T)}{p(0,t)} exp(B(t,T)f(0,t) - \frac{\sigma^2}{4a}B^2(t,T)(1-e^{-2at}) - B(t,T)r(t)) \tag{3.22}$$

The CIR++ Model

The last one-factor short rate model presented in this thesis is the Cox-Ingersoll-Ross++ (CIR++) model, introduced by Cox et al. (1985).

The dynamics of the CIR++ model under risk neutral measure Q are the following:

$$\begin{cases} dx(t) = \kappa(\theta - x(t))dt + \sigma\sqrt{x(t)}dW^Q(t), \\ \lambda(t) = x(t) + \psi(t) \end{cases} \tag{3.23}$$

where κ, θ and σ are positive constants. This model is yet another extension of the Vasiček model, bestowing it with the before-mentioned mean reversion property. An advantage of the CIR++ model is, however, that the process $x(t)$ generates positive values as long as the Feller condition $2\kappa\theta \geq \sigma^2$ holds. This property makes the CIR++ model suitable for modelling e.g. volatilities and default intensities, i.e. the probability of default for a certain time period, conditional on no earlier default. By a proper choice of $\psi(t)$ another advantage can be added; similarly to the Hull-White model, $\psi(t)$ can be calibrated to fit the initial term structure.

In our context, the CIR++ model will be implemented to generate a default intensity process $\lambda(t)$, which will serve to price corporate bonds with credit risk. This makes the choice of $\psi(t)$ slightly more complicated, since a default intensity term structure corresponding to ZCB prices is hard to come by. For the application in this thesis, $\psi(t)$ will be calibrated to a global corporate average cumulative default rate in order to produce default intensities of a realistic magnitude.

Before moving on to the pricing of the bond, a suitable recovery rate must be established. Below, three common recovery structures are listed along with a brief explanation. For a more thorough presentation, see e.g. Duffie and Singleton (1999).

Recovery of treasury Here, the bond is assumed to pay a fraction δ of the face value at maturity. This is equivalent to immediately upon default being paid the same fraction of the value of a risk-free bond with the same maturity as the corporate bond, and reinvesting this amount into the risk-free bond.

Recovery of face value Under this recovery structure, the bond pays a fraction δ of its face value immediately upon default.

Recovery of market value In this model, a recovery payment corresponding to a fraction δ of the pre-default market value of the bond is made immediately upon default.

Recovery rates are in reality a complex matter involving substantial negotiation between parties. All of the above models are thereby simplified (Backman, 2015). In this thesis, the recovery of face value will be applied, meaning the holder will receive a fraction δ of the bond's face value in case of default. The defaults, in turn, will occur at the end of the simulation horizon, with a probability given by the aforementioned cumulative default rate. This simplification was only incorporated to solve an issue that arose at a late stage, at which point a more complex and realistic approach could not be applied due to time shortage.

Let $p^{CR}(t,T)$ denote a bond with credit risk. As the CIR++ model is in the class of ATS models, the bond price can again be written on the affine form. Given that default has not occurred at time t, the price is given by the following expression:

$$\begin{aligned} p^{CR}(t,T) &= E^Q[e^{-\int_t^T r(s)+\lambda(s)ds} \mid \mathcal{F}(t)\ ] \\ &= p(t,T)E^Q[e^{-\int_t^T \lambda(s)ds} \mid \mathcal{F}(t)\ ] \\ &= p(t,T)e^{A(t,T)-B(t,T)\lambda(t)} \end{aligned} \tag{3.24}$$

where $r(t)$ and $p(t,T)$ denotes the risk free rate and ZCB, respectively. In the CIR case, affine A and B would be given by:

$$\begin{aligned} A(t,T) &= log\left(\frac{g(0,T)\bar{A}(0,t)exp(-B(0,t)x_0)}{g(0,t)\bar{A}(0,T)exp(-B(0,T)x_0)}\bar{A}(t,T)e^{B(t,T)\psi(t)}\right), \\ \bar{A}(t,T) &= \left(\frac{2\gamma e^{(\gamma+\kappa)(T-t)/2}}{(\gamma+\kappa)(e^{\gamma(T-t)}-1)+2\gamma}\right)^{2\kappa\theta/\sigma^2}, \\ B(t,T) &= \frac{2(e^{\gamma(T-t)}-1)}{(\gamma+\kappa)(e^{\gamma(T-t)}-1)+2\gamma} \end{aligned}$$

Here, $g(0,t)$ denotes the probability that a default has not yet occured at time t. Letting $\tau > t$ denote the time of default, $g(0,t)$ is given by the following expression:

$$g(0,t) = Pr(t<\tau) = E^Q[\ e^{-\int_0^t \lambda(u)du} \mid \mathcal{F}(0)\ ]$$

3.4.2 Equity models

When generating the remaining risk driver, equity, it is essential to select a model that captures relevant stylized facts concerning asset returns, presented in section 2.2.1. In this section, some widely used equity models will be introduced. Starting from the basic Black-Scholes model, the model complexity will increase gradually until reaching the model of choice for this thesis; the Bates model.

The Black-Scholes Model

The Black-Scholes (B-S) model was first introduced by Black and Scholes (1973), and quickly gained popularity on account of its closed form solutions to European-style option pricing.

The dynamics consists of a geometric Brownian motion:

$$dS(t) = \mu S(t)dt + \sigma S(t)dW^P(t) \tag{3.25}$$

where the drift μ and diffusion σ are constant by assumption, and $W^P(t)$ denotes a standard Brownian motion under real world measure P. Under Q-dynamics, theory dictates that the drift of the stock process should equal the risk free rate to ensure absence of arbitrage.

There are, however, well-known deficiencies to consider when applying the B-S model. To mention a few, the assumption of a deterministic diffusion that remains constant makes it impossible to capture the volatility clustering of asset returns. The heavy tails often displayed in financial time series represent another stylized fact the model fails to capture, along with the gain/loss asymmetry.

The Heston Model

The Heston model was developed by Heston (1993) as an extension of the B-S model, with the intent of capturing the volatility clustering observed in asset returns more realistically by introducing stochastic volatility. To achieve this, the volatility of the equity model is modelled as a separate CIR process. This makes it possible to introduce a linear correlation between asset returns and variance. Consequently, this allows for the modelling of statistical dependencies between the underlying asset and its volatility, which is another prominent feature of financial markets.

The P-dynamics of the Heston model are defined as the following:

$$\begin{cases} dS(t) = \mu S(t)dt + \sqrt{V(t)}S(t)dW_s^P(t) \\ dV(t) = \kappa(\theta - V(t))dt + \sigma\sqrt{V(t)}dW_v^P(t) \\ dW_s^P(t)dW_v^P(t) = \rho\ dt \end{cases} \tag{3.26}$$

where $V(t)$ denotes the variance at time t, μ is the drift of the stock process, while $W_s^P(t)$ and $W_v^P(t)$ are two Brownian motions with correlation ρ. Regarding the parameters of the volatility process; θ denotes the long-term variance, σ the diffusion, and κ the mean-reversion speed.

The Merton Jump Diffusion Model

Another approach with the attempt to better capture the properties of asset return series was developed by Merton (1976). The Merton jump diffusion (MJD) model tackles the issue by introducing random shocks affecting the asset value, enabled by adding a compound Poisson jump process to the original B-S model displayed in 3.25. This yields the following P-dynamics:

$$dS(t) = \mu S(t)dt + \sigma S(t)dW^P(t) + S(t_-)dJ(t) \tag{3.27}$$

where $S(t_-) := \lim_{v \to t} S(v)$ denotes the left limit of $S(t)$, meaning that if a jump occurs the value of $S(t)$ is taken just before the jump. The compounded jump process $J(t)$ is defined as follows:

$$J(t) = e^{\sum_{i=1}^{N(t)} Y_i}$$

$J(t)$ contains two sources of randomness, which are assumed to be independent. Firstly, we have the Poisson process $N(t)$ with intensity λ_J controlling the timing of the random jumps. The magnitude of the jump is the second randomization. In the MJD model, the asset return's jump size is assumed to follow a log normal distribution with mean μ_J and standard deviation σ_J.

To account for the additional jump process, the drift under risk neutral Q-dynamics needs adjustment;

$$\mu = r - \lambda_J(E[J(t)] - 1) = r - \lambda_J(e^{\frac{\sigma_J^2}{2} + \mu_J} - 1)$$

where r denotes the risk free rate. In total, this extends the original B-S model by the three extra parameters λ_J, μ_J and σ_J, controlling the resulting skewness and excess kurtosis of the process distribution.

The Bates Model

The fourth and last equity model presented in this thesis was introduced by Bates (1996). The Bates model consists of a combination of the previously mentioned Heston and MJD model, including both stochastic volatility and a compounded jump process to the dynamics. Several empirical results (see, for instance, Benzoni et al. (2002) and Bakshi et al. (1997)) indicate that both of these components are critical ingredients for a realistic return dynamics. Based on these arguments, the Bates model will be the model used in this thesis to generate a stock price process.

The dynamics under P are given by simply adding the MJD jump component from 3.27 to the Heston model:

$$\begin{cases} dS(t) = \mu S(t)dt + \sqrt{V(t)}S(t)dW_s^P(t) + S(t_-)dJ(t) \\ dV(t) = \kappa(\theta - V(t))dt + \sigma\sqrt{V(t)}dW_v^P(t) \\ dW_s^P(t)dW_v^P(t) = \rho dt \end{cases} \tag{3.28}$$

where the parameters are defined as those in 3.27 and 3.26.

3.5 Dependence Modelling

An important aspect when considering multiple separate simulation processes is the dependency structure between them.

As an example, assume a rise in the risk free rate occurs. Borrowing becomes more expensive, which might slow down the growth rate of a firm by e.g. curtailing expansion plans and new ventures. Consequently, the stock price of the firm declines, implying a negative correlation. Alternatively, a higher interest rate suggests that it might be profitable to take capital out of markets and invest into the firm. In this case, stock prices will fall until the rate of return matches the other financial instruments on a risk-adjusted basis.

Continuing in line with the above example, say a significant drop in a firm's stock price has occurred. Consequently, it is rather likely that the event triggering the fall of the stock price also increases the probability of default of the firm, which in turn leads to a drop in the firm's bond price.

As the example implies, it is reasonable to assume that a significant correlation exists between the concerned risk factors. To obtain an accurate simulation across various asset classes, the underlying dependency structure must be captured. In the setting of this thesis, this will be accomplished by introducing a correlation in the driving Brownian motions of the respective models.

This section begins with an introduction to the basic Pearson correlation, followed by a presentation of the sample dependency method implemented in this thesis.

3.5.1 The Pearson Correlation Coefficient

When assessing linear correlation, the most widely applied measure in statistics is the Pearson correlation coefficient. For a mathematical definition, let X_1 and X_2 denote two random variables. The Pearson correlation ρ_{X_1,X_2} between X_1 and X_2 is given by the following formula:

$$\rho_{X_1,X_2} = \frac{\sigma_{X_1,X_2}}{\sigma_{X_1}\sigma_{X_2}}$$

where σ_{X_1,X_2} denotes the covariance between X_1 and X_2, and σ_{X_i} stands for the standard deviation of X_i, $i = 1, 2$. The covariance between two random variables is always less or equal than the product of the respective standard deviations, implying that $\rho_{X_1,X_2} \in [-1, 1]$. Recalling the risk metric definitions in section 2.1, another important property of the Pearson correlation coefficient is that it is translation invariant under separate changes in both location and scale. For constants a, b, c, d with $b, d > 0$, this means that the correlation between $a + bX_1$ and $c + dX_2$ still equals ρ_{X_1,X_2}.

For simplicity of notation, the Pearson correlation will throughout the thesis be referred to as only the correlation.

3.5.2 Sample Dependency

In this thesis, the dependency structure between the various risk factors will be captured by introducing a correlation in the driving Brownian motions of the respective models. A suitable dependence modelling framework is therefore required, and it will in our case consist of a straightforward Cholesky decomposition approach.

Consider a random vector $\mathbf{Y}$ with unit variance. Then, the correlation matrix of $\mathbf{Y}$ equals the covariance matrix, which by definition is given by:

$$\mathbf{R} = E[\ \mathbf{Y}\mathbf{Y}'\ ]$$

Let $\mathbf{Z}$ denote a vector with uncorrelated random variables with zero mean and unit variance. Hence, the correlation matrix of $\mathbf{Z}$ is given by the identity matrix $\mathbf{I}$. To generate samples with correlation $\mathbf{R}$ the Cholesky decomposition is required. Being a correlation matrix, $\mathbf{R}$ is symmetric and positive definite, meaning that the Cholesky decomposition is possible to obtain as:

$$\mathbf{R} = \mathbf{L}\mathbf{L}'$$

where $\mathbf{L}$ is a lower triangular matrix. Set $\mathbf{X} = \mathbf{L}\mathbf{Z}$. The correlation matrix of $\mathbf{X}$ is then given by:

$$E[\ \mathbf{X}\mathbf{X}'\ ] = E[\ (\mathbf{L}\mathbf{Z})(\mathbf{L}\mathbf{Z})'\ ] = \underbrace{E[\ \mathbf{L}\mathbf{Z}\mathbf{Z}'\mathbf{L}'\ ] = \mathbf{L}E[\ \mathbf{Z}\mathbf{Z}'\ ]\mathbf{L}'}_{E[\cdot] \text{ is a linear operator}} = \mathbf{L}\mathbf{I}\mathbf{L}' = \mathbf{L}\mathbf{L}' = \mathbf{R}$$

Thus, the vector $\mathbf{X}$ contains samples with the desired correlation $\mathbf{R}$.

3.6 Financial Instruments

A key part of the thesis lies in the definition of a suitable ALM framework, which includes the construction of a replicating portfolio for the liability side of the balance sheet. As the structure of the liability function resembles that of a class of variable annuities, the replication will set out to mirror its pay-off structure. In order to accomplish this, a set of basic financial derivative instruments is required.

In this section, the pay-off structures of some well-known vanilla instruments will be defined, to later be utilized in the portfolio replication procedure. The section concludes with a brief presentation of the variable annuity.

3.6.1 The Forward Contract

The forward is among the most straightforward of financial contracts, consisting of a non-standardized agreement between two parties to buy or sell an asset at a specified future time, for a strike agreed upon today. For a long position, with maturity T and strike K, the pay-off $\phi^F(T)$ at maturity is the following:

$$\phi^F(T, K) = A(T) - K$$

where $A(T)$ denotes the spot price of the underlying asset at maturity.

3.6.2 The European Option

A European option is basically a forward contract with a built-in optionality; the holder of the contract has the possibility to choose whether or not to exercise the option. This means that the pay-off for a long position will remain greater or equal to zero, since any reasonable holder would not exercise an option that generates a loss. There are two types of European options; the call option and the put option, giving the holder the right to purchase or sell the underlying security, respectively. The pay-offs for a long position are given by:

$$\textit{Call option} : \phi^C(T, K) = (A(T) - K)^+$$
$$\textit{Put option} : \phi^P(T, K) = (K - A(T))^+$$

where $(x)^+ := max(x, 0)$.

3.6.3 The Variable Annuity

A variable annuity (VA) is in general defined as a unit-linked insurance contract which offers guarantee benefits for the holder. Being unit-linked, the value of the VA is directly linked to the value of the underlying asset. Thereof, the VA provides a series of payments which depend on the performance of the underlying investment for a fixed period. While the contract allows the holder to benefit from an upswing in the value of the underlying instrument, the embedded guarantee reserve partially or totally protects the holder from drops in the underlying value.

A VA has a more complex structure than the vanilla instruments, and the pay-off function may differ significantly from contract to contract. To get an intuitive idea of the VA contract, a general VA can be said to have two phases; the accumulation phase and the payout phase. During the accumulation phase, one or more purchase payments are added to the contract, and the earnings accumulate on a tax-deferred basis. This is because a VA can be purchased by making either a single or a series of purchase payments. The benefits of tax deferral are often long-range, meaning that this contract is primarily designed for long-term investments such as retirement. When the payout phase begins, regular payments are paid out from the insurance company during a fixed period.

The pay-off structure of a simplified VA will be defined in section 4.3.1.

Chapter 4

Methodology

This chapter will treat the methodology used to derive the results in chapter 5. The chapter begins by presenting the simulation schemes used for the various risk factor models, followed by an account of the method used for the dependence modelling. After this, the liability function will be defined along with the implemented replicating portfolio approach. To conclude, the entire process of the ALM optimization framework using the LMSC approach will be summarized.

4.1 Model Simulation Schemes

As all simulation models considered in this thesis are defined in continuous time, suitable simulation methods must be derived to allow for a discrete time step simulation. For a simple enough model structure, as for e.g. the Hull-White model, discretization schemes are not necessary as an analytic expression of the solution to the governing dynamics is available. Regarding models with more complex dynamics, e.g. square root processes such as Bates and CIR++, an exact simulation method might not be practical or even exist. In these cases, the need for an appropriate discretization scheme arises.

This section will present the simulation schemes used in this thesis for each of the selected simulation models. As both CIR++ and Bates contain an underlying CIR process, the same discretization scheme will be applied to both models. The method of choice is in this case the quadratic exponential scheme, which will first be applied to the underlying CIR process before being adapted to the respective simulation model.

4.1.1 Exact Simulation

For models with a simple enough structure, or, alternatively, a known closed form distribution, an exact simulation scheme can be derived. In this section, such schemes will be derived for the Hull-White and CIR model.

The Hull-White Model

As previously mentioned, the straightforward dynamics of the Hull-White model makes it possible to derive an analytic expression of the solution to the model dynamics. This enables us to access an exact and unbiased simulation algorithm free from approximation errors.

Let $r(t)$ hold the Hull-White dynamics expressed in 3.20. An analytical solution for every $0 \leq s \leq t$ can be expressed in terms of a Vasiček process complemented by an independent deterministic function:

$$\begin{aligned} r(t) = &\underbrace{r(s)e^{-a(t-s)} + \sigma \int_s^t e^{-a(t-u)} dW^Q(u)}_{\text{Vasiček process}} \\ &+ \underbrace{f(0,t) - e^{-a(t-s)} f(0,s) + \frac{\sigma^2}{2a^2}((1-e^{-at})^2 - e^{-a(t-s)}(1-e^{-as})^2)}_{\text{Deterministic terms}} \end{aligned} \tag{4.1}$$

A derivation of the above analytical solution is found in appendix A. Consequently, $r(t)$ conditional on the filtration $\mathcal{F}(s)$ is normally distributed with the following moments:

$$\begin{aligned} E^Q[r(t) \mid \mathcal{F}(s)\ ] &= r(s)e^{-a(t-s)} + f(0,t) + \frac{\sigma^2}{2a^2}(1-e^{-at})^2 \\ &- e^{-a(t-s)}(f(0,s) + \frac{\sigma^2}{2a^2}(1-e^{-as})^2) \\ Var^Q[r(t) \mid \mathcal{F}(s)\ ] &= \frac{\sigma^2}{2a^2}(1-e^{-2a(t-s)}) \end{aligned} \tag{4.2}$$

By using 4.1 and 4.2, it is possible to construct a simple yet effective simulation algorithm for the short rate $r(t)$ using the following recursive approach:

- For n time steps with a fixed step space Δ, define:

$$y(t) = r(t\Delta) - f(0,t\Delta) - \frac{\sigma^2}{2a^2}(1-e^{-at\Delta})^2$$

- Taking the analytical solution 4.1 into regard, an autoregressive recursive relation can be derived for $y(t)$:

$$\begin{aligned} &y(0) = 0 \\ &... \\ &y(t) = \alpha(\Delta)y(t) + e(t), \quad t = 1, ..., n, \\ &\alpha(\Delta) = e^{-a\Delta} \end{aligned}$$

  where the errors $e(t),\ t = 1, ..., n$ are independent and identically normal distributed:

$$e(t) \in N(\ 0, \frac{\sigma^2}{2a^2}(1-e^{-2a\Delta}))$$

- To simulate the short rate $r(t)$, the following sequence is implemented:

$$\begin{aligned} &r(0) = r_0 \\ &... \\ &r(t\Delta) = y(t) + f(0,t\Delta) + \frac{\sigma^2}{2a^2}(1-e^{-at\Delta})^2, \quad t = 1, ..., n \end{aligned}$$

Algorithm 1 displays a pseudo code overview of the Hull-White short rate simulation method used in this thesis.

Algorithm 1 Simulation scheme for the Hull-White model.

Data: a, $\sigma, r_0, \Delta, \{f(0,t_i)\}_{i=1}^n$
Result: $\{\mathrm{r}(\mathrm{t}_i)\}_{i=1}^n$

$\mathrm{r}(\mathrm{t}_0) = r_0$
$y(0) = 0$
for $i \longleftarrow 1$ *to* n **do**
  $s_e^2 = \frac{\sigma^2}{2a}(1-e^{-2a\Delta})$
  Draw Z $\sim \mathcal{N}(0,1)$
  $e(t) \longleftarrow Zs_e$
  $y(t) \longleftarrow e^{-a\Delta}y(t-1) + e(t)$
  $r(t_i) \longleftarrow y(t) + f(0,t_i) + \frac{\sigma^2}{2a^2}(1-e^{-at_i})^2$
end

The CIR Model

Although the CIR process, defined as the first line of 3.23, is a rather complex square root process, the distribution of future values $x(t)$ is known in closed form. As stated by Brigo and Mercurio (2012), the CIR process follows a non-central chi-square distribution with $d = 4\kappa\theta/\sigma^2$ degrees of freedom. For $t < T$, the distribution has a non-centrality parameter $\eta(t,T) = x(t)4\kappa e^{-\kappa(T-t)}/\sigma^2(1-e^{-\kappa(T-t)}$, yielding the following cumulative distribution function:

$$F(z;d;\eta) = e^{-\eta/2}\sum_{i=0}^{\infty}\frac{(\eta/2)^i}{i!2^{d/2+i}\Gamma(d/2+i)}\int_0^z y^{d/2+i-1}e^{-z/2}dy$$

where $\Gamma(\cdot)$ denotes the gamma function. A non-central chi-squared distribution can be viewed as a normal chi-squared distribution with a Poisson-distributed degrees of freedom. Using this relation, Andersen et al. (2010) has proposed the following simulation algorithm:

- For a time step Δ, draw a Poisson random variable N with mean $E[N] = 1/2x(t)\eta(t,t+\Delta t)$.
- Given N, draw a regular chi-square random variable $\mathcal{X}^2_\nu$ with $\nu = d + 2N$ degrees of freedom.
- Simulate the CIR process $x(t)$ by setting:

$$x(t+\Delta) = \mathcal{X}^2_\nu\frac{e^{-\kappa\Delta}}{\eta(t,t+\Delta t)}$$

This exact simulation has the advantage that the simulations are entirely bias-free as the sampling is from the original distribution. Due to the significant computational burden of this method, however, it is often numerically advantageous to use a discretization scheme if a large number of samples is required.

4.1.2 The Quadratic Exponential Scheme

The quadratic exponential (QE) scheme is a moment matching discretization scheme specifically developed for square-root processes. Although biased, results has proven to be highly accurate in, for instance, Pelsser and van Haastrecht (2008). Additionally, the application of the QE scheme greatly reduces the computational burden by comparison to the exact scheme defined in the previous subsection. In the remaining part of this section, the QE scheme will be derived for the CIR process, and later on adapted to the Bates and CIR++ models.

The CIR Model

The QE scheme, proposed by Andersen et al. (2010), is based on the concept that the density function of the CIR process $x(t+\Delta t)$ conditional on $x(t)$ can be well approximated using a moment matching technique. The main idea is thus to find distributions that behave similarly to the chi-square defined in the previous subsection.

If $x(t)$ is sufficiently large, the following quadratic representation has been shown to approximate the conditional distribution of $x(t+\Delta t)|x(t)$ sufficiently well:

$$x(t+\Delta) = a(b+Z)^2 \tag{4.3}$$

where Z is a standard normal random variable, while a and b are determined by moment matching. For a small $x(t)$, the moment-matching exercise fails to work and a switching rule based on the asymptotic density of the CIR process is introduced:

$$x(t+\Delta) = \begin{cases} 0, & U \le p \\ \beta^{-1}\ log\ \frac{1-p}{1-U}, & U > p \end{cases} \tag{4.4}$$

where U is a standard uniform random variable, while p and β are non-negative constants. By using moment-matching techniques, the conditional mean m and variance s^2 of the CIR process are established:

$$
\begin{aligned}
m &= E[x(t+\Delta)|x(t)] = \theta + (x(t)-\theta)e^{-\kappa\Delta} \\
s^2 &= Var[x(t+\Delta)|x(t)] = \frac{x(t)\sigma^2 e^{-\kappa\Delta}}{\kappa}(1-e^{-\kappa\Delta}) + \frac{\theta\sigma^2}{2\kappa}(1-e^{-\kappa\Delta})^2
\end{aligned} \tag{4.5}
$$

Set $\psi_s := s^2/m^2$, and let the constants a, b, p and β be determined as the following:

$$
\begin{aligned}
a &= \frac{m}{1+b^2}, \quad b^2 = 2\psi_s^{-1} - 1 + \sqrt{2\psi_s^{-1}(2\psi_s^{-1}-1)}, \\
p &= \frac{\psi_s - 1}{\psi_s + 1}, \quad \beta = \frac{2}{m(\psi_s+1)}
\end{aligned} \tag{4.6}
$$

Introduce a critical level $\psi_c \in [1,2]$. According to Andersen et al. the choice of ψ_c has little effect on the quality of the overall simulation scheme, so it is arbitrarily set to $\psi_c = 1.5$. The switching rule determines which equation is applied in the simulation process; if $\psi_s \leq \psi_c$ equation 4.3 is implemented, otherwise equation 4.4 is used. To conclude, the QE discretization algorithm for a CIR process is summarized for a simulation step from $x(t)$ to $x(t+\Delta)$ below:

- Given $x(t)$, compute m and s^2 from equation 4.5, and set $\psi_s = s^2/m^2$.
- Draw a standard uniform random variable U.
- If $\psi_s \leq \psi_c$:
  - Draw a standard normal random variable Z.
  - Set $x(t+\Delta) = a(b+Z)^2$, with a, b given by equation 4.6.
- If $\psi_s > \psi_c$:
  - Set $x(t+\Delta) = \begin{cases} 0, & U \leq p \\ \beta^{-1}\ log\ \frac{1-p}{1-U}, & U > p \end{cases}$, with p, β defined in equation 4.6.

The CIR++ Model

The only difference between the CIR and the CIR++ process is the addition of the deterministic function $\psi(t)$, to obtain a default intensity process $\lambda(t)$. Thus, the QE discretization scheme above is easily adapted to the CIR++ case by in each time step including $\psi(t)$. Algorithm 2 shows an overview of the procedure.

Algorithm 2 QE discretization scheme for the CIR++ model.

Data: $\kappa, \theta, \sigma, x_0, \Delta, \{\psi(0,t_i)\}_{i=1}^n$
Result: $\{\lambda(t_i)\}_{i=1}^n$
$\lambda(t_0) = x_0 + \psi(t_0)$
for $i \longleftarrow 1$ *to* n **do**
  $m = \theta + (x(t_{i-1}) - \theta)e^{-\kappa\Delta}$
  $s^2 = \frac{x(t_{i-1})\sigma^2 e^{-\kappa\Delta}}{\kappa}(1 - e^{-\kappa\Delta}) + \frac{\theta\sigma^2}{2\kappa}(1 - e^{-\kappa\Delta})^2$
  $\psi_s = s^2/m^2$
  Draw U $\sim \mathcal{U}(0,1)$
  if $\psi_s \leq \psi_c$ **then**
    $b^2 = 2\psi_s^{-1} - 1 + \sqrt{2\psi_s^{-1}(2\psi_s^{-1} - 1)}$
    $a = \frac{m}{1+b^2}$
    Draw Z $\sim \mathcal{N}(0,1)$
    $\lambda(t_i) \longleftarrow a(b + Z)^2 + \psi(t_i)$
  else
    $p = \frac{\psi_s - 1}{\psi_s + 1}$
    $\beta = \frac{2}{m(\psi_s+1)}$
    if $0 \leq U \leq p$ **then**
      $\lambda(t_i) \longleftarrow 0 + \psi(t_i)$
    else
      $\lambda(t_i) \longleftarrow \beta^{-1}\ log\ \frac{1-p}{1-U} + \psi(t_i)$
    end
  end
end

The Bates Model

Recalling the definition of the Bates model in section 3.4.2, the volatility of the Bates process is modelled as a separate CIR process. In addition to this, a compound Poisson process is added to introduce random jumps in the process.

We start our expansion of the QE discretization scheme to fit the Bates process by considering only the addition of stochastic volatility, and add the Poisson jump process at a later stage. In other words, we begin by finding a suitable discretization for the Heston model.

Using the notations from the Heston dynamics given by equation 3.26, the explicit solution to the stock process can be expressed as:

$$S(t+\Delta) = S(t) exp\left(\int_t^{t+\Delta} (\mu - \frac{1}{2}V(u))du + \int_t^{t+\Delta} \sqrt{V(u)} dW_s^p(u)\right)$$

Applying Ito's lemma along with a Cholesky decomposition, the log stock price can be written as (Pelsser and van Haastrecht, 2008):

$$\begin{aligned} log\ S(t+\Delta) &= log\ S(t) + \mu\Delta - \frac{1}{2}\int_t^{t+\Delta} V(u)du \\ &+ \rho\int_t^{t+\Delta} \sqrt{V(u)} dW_v^p(u) + \sqrt{1-\rho^2}\int_t^{t+\Delta} \sqrt{V(u)} dW^p(u) \end{aligned} \tag{4.7}$$

where $W^p(u)$ is a Brownian motion independent of $W_v^p(u)$. Looking at the stochastic volatility dynamics of the Heston model, the explicit solution to the CIR process is given by:

$$V(t+\Delta) = V(t) + \int_t^{t+\Delta} \kappa(\theta - V(u))du + \sigma \int_t^{t+\Delta} \sqrt{V(u)}dW_v^p(u)$$
$$\iff \int_t^{t+\Delta} \sqrt{V(u)}dW_v^p(u) = \sigma^{-1}\left(V(t+\Delta) - V(t) - \kappa\theta\Delta + \kappa\int_t^{t+\Delta} V(u)du\right)$$

Substituting the above integral into the solution of the log stock process 4.7, Broadie and Kaya (2006) has shown that the solution can be altered into:

$$log\ S(t+\Delta) = log\ S(t) + \left(\frac{\kappa\rho}{\sigma} - \frac{1}{2}\right)\int_t^{t+\Delta} V(u)du$$
$$+ \frac{\rho}{\sigma}(V(t+\Delta) - V(t) - \kappa\theta\Delta) + \mu\Delta + \sqrt{1-\rho^2}\int_t^{t+\Delta}\sqrt{V(u)}dW^p(u)$$

At this point, a drift interpolation method can be applied to approximate the integrated volatility process:

$$\int_t^{t+\Delta} V(u)du \approx (\gamma_1 V(t+\Delta+t) + \gamma_2 V(t))\Delta$$

In this case, Pelsser and van Haastrecht propose the predictor-corrector setting using $\gamma_1 = \gamma_2 = 0.5$. Substituting the integrated volatility processes by their approximations, the asset sampling scheme for the Heston model can be expressed as follows:

$$\begin{aligned} log\ S(t+\Delta) &= log\ S(t) + \left(\mu - \frac{\rho\kappa\theta}{\sigma}\right)\Delta + \frac{\rho}{\sigma}(V(t+\Delta) - V(t)) \\ &+ \left(\frac{\rho\kappa}{\sigma} - \frac{1}{2}\right)(\gamma_1 V(t+\Delta) - \gamma_2 V(t))\Delta + \sqrt{1-\rho^2}Z\sqrt{(\gamma_1 V(t+\Delta) - \gamma_2 V(t))\Delta} \\ &= log\ S(t) + K_0 + K_1 V(t) + K_2 V(t+\Delta) + \sqrt{K_3 V(t) + K_4 V(t+\Delta)}Z \end{aligned} \tag{4.8}$$

where Z is a standard normal random variable, and with:

$$\begin{aligned} K_0 &= \Delta\left(\mu - \frac{\rho\kappa\theta}{\sigma}\right), \quad K_1 = \gamma_1\Delta\left(\frac{\rho\kappa}{\sigma} - \frac{1}{2}\right) - \frac{\rho}{\sigma}, \\ K_2 &= \gamma_2\Delta\left(\frac{\rho\kappa}{\sigma} - \frac{1}{2}\right) + \frac{\rho}{\sigma}, \quad K_3 = \gamma_1\Delta(1-\rho^2), \\ K_4 &= \gamma_2\Delta(1-\rho^2) \end{aligned} \tag{4.9}$$

Once a discrete asset sampling scheme is in place, it can be used in conjunction to the QE scheme for the volatility process by simulating $V(t+\Delta)$ according to the above CIR process QE discretization algorithm.

What remains now is to add the compounded Poisson process to incorporate discontinuous jumps to the stochastic volatility model. This is by comparison rather trivial, as this process is completely independent of the volatility process. Recall from section 3.4.2 that the number of jumps is controlled by a Poisson process $N(t)$ with intensity λ_J, while the magnitude of the jump is assumed to follow a log normal distribution with mean μ_J and standard deviation σ_J. Hence, by drawing a random variable $Y = N(t+\Delta) - N(t)$ from the Poisson process $Poi(\lambda_J\Delta)$, the stochastic jump parameter J can be determined using the following algorithm:

- Draw $Y \sim Poi(\lambda_J\Delta)$. This determines if any jump occurs in time step Δ.
- If $Y = 0$:
  - Set the jump parameter $J = 0$, meaning no jump occurs.
- If $Y \neq 0$:
  - Draw a standard normal random variable Z.
  - Set $J = \mu_J Y + \sigma_J\sqrt{Y}Z$

By adding the jump process J to the Heston sampling scheme 4.10, the full Bates asset sampling scheme can be expressed as follows:

$$log\ S(t+\Delta) = log\ S(t) + K_0 + K_1 V(t) + K_2 V(t+\Delta) + \sqrt{K_3 V(t) + K_4 V(t+\Delta)} Z + J \tag{4.10}$$

where $K_i,\ i = 0, ..., 4$ are defined in 4.9, and J is given by the above algorithm. For a pseudo code overview of the QE discretization scheme applied to the Bates model, see algorithm 3.

Algorithm 3 QE discretization scheme for the Bates model.

Data: $\mu, \kappa, \theta, \sigma, \mu_J, \sigma_j, \lambda, \rho, x_0, v_0, \Delta$
Result: $\{\mathrm{S}(\mathrm{t}_i)\}_{i=1}^{n}$

$X(t_0) = x_0$
$V(t_0) = v_0$
$\gamma_1 = \gamma_2 = 1/2$
$K_0 = \Delta\left(\mu - \frac{\rho\kappa\theta}{\sigma}\right)$
$K_1 = \gamma_1\Delta\left(\frac{\rho\kappa}{\sigma} - \frac{1}{2}\right) - \frac{\rho}{\sigma}$
$K_2 = \gamma_2\Delta\left(\frac{\rho\kappa}{\sigma} - \frac{1}{2}\right) + \frac{\rho}{\sigma}$
$K_3 = \gamma_1\Delta(1-\rho^2)$
$K_4 = \gamma_2\Delta(1-\rho^2)$
for $i \longleftarrow 1\ to\ n$ **do**
  $m = \theta + (V(t_{i-1}) - \theta)e^{-\kappa\Delta}$
  $s^2 = \frac{V(t_{i-1})\sigma^2 e^{-\kappa\Delta}}{\kappa}(1 - e^{-\kappa\Delta}) + \frac{\theta\sigma^2}{2\kappa}(1 - e^{-\kappa\Delta})^2$
  $\psi_s = s^2/m^2$
  Draw $\mathrm{U} \sim \mathcal{U}(0,1)$
  if $\psi_s \leq \psi_c$ **then**
    $b^2 = 2\psi_s^{-1} - 1 + \sqrt{2\psi_s^{-1}(2\psi_s^{-1} - 1)}$
    $a = \frac{m}{1+b^2}$
    Draw $\mathrm{Z}_1 \sim \mathcal{N}(0,1)$
    $\mathrm{V}(\mathrm{t}_i) \longleftarrow a(b + Z_1)^2$
  else
    $p = \frac{\psi_s - 1}{\psi_s + 1}$
    $\beta = \frac{2}{m(\psi_s+1)}$
    if $0 \leq U \leq p$ **then**
      $V(t_i) \longleftarrow 0$
    else
      $V(t_i) \longleftarrow \beta^{-1}\ log\ \frac{1-p}{1-U}$
    end
    Draw $Y \sim Poi(\lambda_J\Delta)$
    if $Y = 0$ **then**
      $J \longleftarrow 0$
    else
      Draw $Z_2 \sim \mathcal{N}(0,1)$
      $J \longleftarrow \mu_J Y + \sigma_J\sqrt{Y} Z_2$
    end
    Draw $Z_3 \sim \mathcal{N}(0,1)$
    $X(t_i) \longleftarrow X(t_i) + K_0 + K_1 V(t_{i-1}) + K_2 V(t_i) + \sqrt{K_3 V(t_{i-1}) + K_4 V(t_i)} Z_3 + J$
    $S(t_i) \longleftarrow exp(X(t_i))$
  end
end

4.2 Generating Correlated Samples

As previously mentioned, a straightforward Cholesky decomposition approach will be implemented to introduce a dependency structure between the risk factors.

An important note is that there can be no correlation between the risk free rate $r(t)$ and the default intensity $\lambda(t)$. Recall the CIR++ pricing formula for a bond with credit risk, expressed in equation 3.24. The Hull-White-generated risk free rate is present in this formula, as the bond price is discounted using the risk free ZCB. If a correlation between $r(t)$ and $\lambda(t)$ is present, this would because of the square root term in the CIR++ diffusion lead to a loss of the affine properties of the model. Consequently, there would no longer be a closed form pricing formula to the defaultable corporate bond.

However, there are no such issues regarding the correlation between the stock process $S(t)$ and the default intensity, nor between $S(t)$ and the risk free rate. This implies that the resulting correlation matrix $\mathbf{R}$ used in the sampling will be of the following form:

$$\mathbf{R} = \begin{bmatrix} 1 & \rho_{s,r} & \rho_{s,\lambda} \\ \rho_{r,s} & 1 & 0 \\ \rho_{\lambda,s} & 0 & 1 \end{bmatrix} \tag{4.11}$$

where $\rho_{s,r}$ denotes the correlation between stocks and risk free rate, and $\rho_{s,\lambda}$ the correlation between stocks and default intensity.

4.2.1 The Cholesky Decomposition Approach

In the setting of this thesis, the dependency structure will be applied by introducing a correlation in the driving Brownian motions of the respective models. Using the Cholesky decomposition approach described in section 3.5.2, the sampling process for n samples and three risk factors is described in the following steps;

- Compute $\mathbf{L} \in \mathbb{R}^{3\times 3}$ by setting $\mathbf{R} = \mathbf{LL}$'.
- Let $\mathbf{Z} \in \mathbb{R}^{n\times 3}$ be a matrix of uncorrelated standard normal samples.
- Obtain the matrix of correlated samples $\mathbf{X} \in \mathbb{R}^{n\times 3}$ by setting $\mathbf{X} = \mathbf{LZ}$.

4.3 The Liability Framework

As mentioned in chapter 1, the ALM framework has its main focus on the financial risk exposure associated with asset-backed liabilities. This means a suitable insurance liability framework, with an appropriate pay-off structure, must be established. In this thesis, the implementation will consist of a replicating portfolio approach using basic financial instruments.

The type of insurance products considered here have a unit-linked performance structure, meaning they are linked to the value of an underlying investment, while including an embedded guarantee reserve. In recent years, this type of insurance product has gained considerable popularity among policyholders (Cathcart, 2012). The liabilities are thereby based on the replicated cash flow of a class of VA's that hold the desired unit-linked pay-off structure, since they make an appropriate basis for insurance liability calculations.

In the below section, a suitable portfolio replication scheme will be proposed for the considered class of VA's. Following this, the replicating portfolio will be adapted to represent a simplified liability function, and a proper definition of the liability framework applied in this thesis will be presented.

4.3.1 Replicating Portfolio of Variable Annuities

Recalling the introduction in section 3.6.3, the VA is a contract that depends on the underlying instruments value process. Moreover, the VA provides protection against losses of a certain magnitude by introducing a guarantee reserve to the contract.

The definition of a replicating portfolio is based on the no-arbitrage principle; if the cash flow of a portfolio equals that of another asset or, alternatively, liability, their values must also be equal to eliminate the possibility of arbitrage. The intention behind a portfolio replicating a class of VA's is to quantify the risk

exposure of the liabilities underlying an insurance product. This is achieved by considering the liabilities in terms of a replicating portfolio of basic financial instruments, mirroring a simplified relationship between liabilities and the underlying assets. Once set up, the replicating portfolio can be used to predict the behaviour and change in market value of the liabilities, across a range of economic scenarios. Consequently, this portfolio can be applied to make NAV calculations more efficient, by significantly reducing the computational burden. A similar replicating portfolio approach regarding unit-linked insurance products containing embedded guarantees can be seen in e.g. Cathcart (2012).

The potential of the portfolio replication approach is recognized by an increasing number of insurers; according to a CRO Forum study, 31% of insures were using replicating portfolios for NAV calculations by 2008 (Hermans and Waaijer, 2013).

When implementing a portfolio replication scheme, the first step is to determine what financial instruments the portfolio should consist of. To keep the complexity down, vanilla instruments with straightforward pay-off structures are chosen, such as the forward contract and European option defined in section 3.6.

Next, the cash flow pattern of the VA must be examined in relation to the underlying instrument. As previously mentioned, a VA has a complex structure which may differ significantly from contract to contract. As a concrete example, consider a VA on the Euro Stoxx 50 index. Figure 4.1 displays the cash flow of the considered VA at year 6.

Figure 4.1: *Cash flow of variable annuity in thousands of Euros with underlying Euro Stoxx 50 index at year 6. Plot from Hermans and Waaijer (2013).*

The above plot reveals a distinct pattern in the cash flow. After a certain value has been reached, the VA has an apparent positive correlation to the underlying index, portraying an embedded guarantee and unit-linked value progression.

At this point, we can start doing some preliminary work on the liability function definition, by replicating a simplified pay-off structure of a single pay-out VA. To put this into context, consider the 6-year VA in figure 4.1, and set the level at which the VA starts showing a positive correlation to the underlying index equal to K'. To replicate the pay-off of this contract, we start with a closer inspection of the cash flow in the above figure. Up until the the Euro stoxx 50 index reaches K', the cash flow appears to have a constant lower bound. We denote this constant annuity level K, representing a guaranteed payout. After reaching K', the relation between the VA and the index appears linear. An outline to the replicated pay-off $\phi^{VA}(T,K)$ at maturity $T = 6$ could be expressed in the following way:

$$\phi^{VA}(T,K) = \begin{cases} K, & A(T) \leq K' \\ A(T), & A(T) > K' \end{cases} \tag{4.12}$$

where $A(T)$ denotes the spot price of the underlying asset at maturity. From the plot of the VA cash flow it is evident that $K' < K$. If K' is increased until equalling K, however, this would shift the level at which the linear relation starts forward. By setting $K' = K$, we can thus create a lower bound for the VA cash flow at the guaranteed payout level. As a result, the lower bound can be replicated by using a forward contract and a European put option. The pay-off expressed in 4.12 can now be represented as the following:

$$\phi^{VA}(T,K) = A(T) + (K - A(T))^{+} = \phi^{F}(T,0) + \phi^{P}(T,K) \tag{4.13}$$

where $\phi^F(T,0)$ denotes the pay-off of a forward contract with strike 0, and $\phi^P(T,K)$ is the pay-off of a European put option with strike K, with both contracts having a maturity T. By setting the guaranteed payout $K = 5000$, and maturity $T = 6$ years, the discounted pay-off is re-scaled to match the cash flow in figure 4.1. Figure 4.2 gives an overview of the replicated VA pay-off 4.13 and relates it to the actual cash flow.

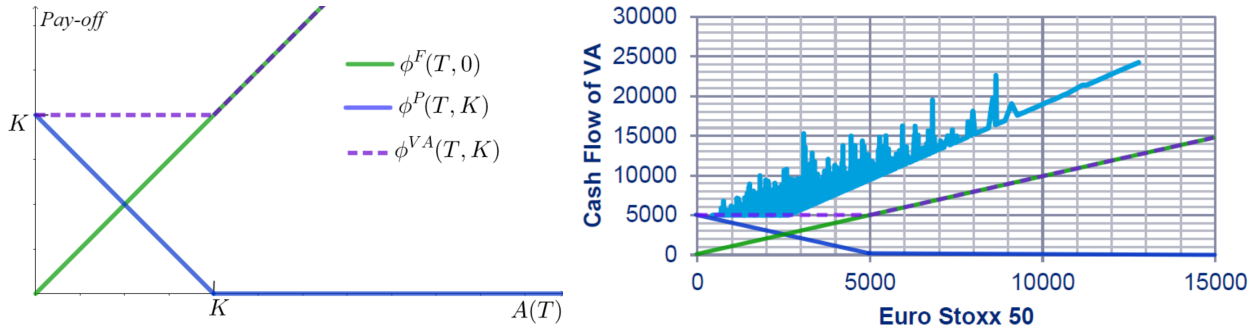

(a) (b)

Figure 4.2: *(a) Replication of variable annuity pay-off using a European put option and a forward contract. (b) Discounted pay-off from figure (a) in relation to 6-year variable annuity cash flow.*

4.3.2 The Liability Function

In NAV calculations, the difficulty often lies in the evaluation of the liability side of the balance sheet. Assets can usually be valued by benchmarking against observable market prices. Liabilities related to contractual obligations, however, are not traded on the financial markets and must therefore be valued using other methods.

In this thesis, the replicating portfolio approach outlined in the above section will be used to valuate the liabilities. The simulations of the future cash flow should according to the no-arbitrage principle yield the same approximate liability value as the replicating portfolio. Consequently, a simplified liability function that still captures complex interactions between assets and liabilities can be derived and implemented in the valuation process.

Nevertheless, it is important to keep in mind that the real world liability value is a function of a far vaster number of variables. Liabilities could be affected by e.g. thousands of different bonds and equity holdings on the asset side, health and longevity prospects of the holders, and many other factors for which risk quantification is considerably harder to determine. The often long-term nature of insurance products, in addition to their exposure to multiple risk-drivers, increases the difficulty of replicating even the simplest liability structures (Cathcart, 2012). In this thesis, the before-mentioned replicating portfolio is assumed to be the true liability function. The valuation is thus made more manageable by introducing a smaller dimensionality to the risks. Further simplifications to the liability structure include that only one cash flow at maturity is considered, and that no premiums or fees are taken into regard.

We begin by defining the asset side of the balance sheet. In our application, the asset side consists of a portfolio containing assets from three dependent asset classes; equity, treasury bonds and corporate bonds. Let the total asset market value at time t be denoted by $A(t)$. Taking the three asset classes into regard, we define our asset value as the following:

$$\begin{aligned} &A(t) = w_S S(t) + w_{RF} RF(t) + w_{CR} CR(t), \\ &w_S + w_{RF} + w_{CR} = 1, \ w_k > 0, \ k = S, RF, CR \end{aligned} \tag{4.14}$$

where;

$S(t)$ denotes the stock process value generated by the Bates model,

$RF(t)$ is the value of a risk free treasury bond, generated by the Hull-White model,

$CR(t)$ denotes the value of a corporate bond with credit risk, generated by the CIR++ model,

$w_k,\ k = S, RF, CR$ stands for the proportion of capital invested into asset class k. In this context, all asset class weights are held positive and sum up to one.

Before properly defining the liability side, let us state the fundamental identity of accounting:

$$NAV(t) = A(t) - L(t)$$

where $NAV(t)$ stands for the total NAV, while $A(t)$ and $L(t)$ denotes the asset and liability market value at time t, respectively. The liabilities will be based on the VA replicating portfolio derived in section 4.3.1, with pay-off given by equation 4.13. However, the liability function can not be set to exactly equal the pay-off of the considered replicating portfolio. In this case, the resulting NAV at maturity T would become unreasonable:

$$NAV(T) = A(T) - L(T) = A(T) - (A(T) + (K - A(T))^+) = -(K - A(T))^+ \tag{4.15}$$

Figure 4.3a displays the resulting pay-off of equation 4.15 related to the underlying asset value. As the NAV at time T would be either zero or negative, the replicated VA pay-off 4.13 is clearly unsuitable as liability function. To remedy this, we introduce a scaling factor $\alpha \in (0, 1)$. By doing so, we obtain a liability value that grows proportionally to the backing asset value while maintaining a positive guarantee reserve of αK:

$$L(T) = \alpha(A(T) - (K - A(T))^+) \tag{4.16}$$

Using liability function 4.16, the resulting NAV would be of the following form:

$$NAV(T) = A(T) - L(T) = A(T)(1 - \alpha) - \alpha(K - A(T))^+ \tag{4.17}$$

Figure 4.3b illustrates the pay-off structure of the NAV expressed in 4.17. Because of the reasonable magnitudes of the resulting liability- and net asset values, 4.16 will be the liability function applied in this thesis.

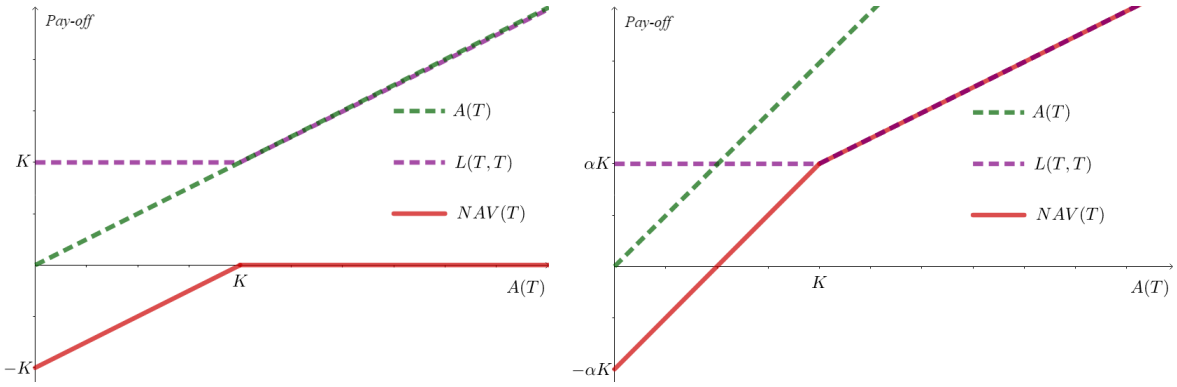

(a) (b)

Figure 4.3: *NAV at maturity for liability function (a)* $L(T) = A(T) + (K - A(T))^+$ *(b)* $L(T) = \alpha(A(T) + (K - A(T))^+)$

In our application, we are interested in the NAV at a time t prior to maturity, since our intention is to allocate for a maximal RANAV at this point. Discounting expression 4.17, the NAV at time $t < T$ is given by:

$$\begin{aligned} NAV(t) &= E^Q[A(t) - L(t) \mid \mathcal{F}(t)\ ] \\ &= E^Q[e^{-\int_t^T r(s)ds}(A(T)(1-\alpha) - \alpha(K - A(T))^+) \mid \mathcal{F}(t)\ ] \\ &= P(t,T)E^Q\underbrace{[A(T)(1-\alpha) - \alpha(K - A(T))^+ \mid \mathcal{F}(t)\ ]}_{\text{Unknown at time t}} \end{aligned} \tag{4.18}$$

where $p(t,T)$ denotes the risk free ZCB. Thus, the unknown section of 4.18 requires estimation, which will be accomplished using a LSMC regressed NAV proxy function. This will be returned to in the subsequent section, where the ALM optimization framework is outlined.

4.4 The ALM Optimization Framework

The final step of the methodology is to determine a suitable ALM optimization framework under Solvency II regulations. In this section, the liability function defined in section 4.3.2 will be be implemented to obtain a framework that takes the complex interaction between assets and liabilities into account. Letting the SCR define the riskiness of the NAV, the objective of this framework is the maximization of the RANAV, obtained by selecting the optimal amount of capital invested into each asset class.

Let us start by recalling the definition of RANAV from section 2.4. RANAV is formulated as the ratio of expected NAV to VaR, making it a suitable objective function in this context. Redefining the optimization problem 2.2 to match the ALM structure in question, an optimization framework adapted to this thesis can be outlined.

Let the asset and liability structures be defined as in section 4.3.2, and let $\mathbf{w}$ denote a vector of weights, containing the proportion of capital invested into each asset class.

$$\begin{aligned}&\mathbf{w} = [\ w_S,\ w_{RF},\ w_{CR}\ ],\\ &w_S + w_{RF} + w_{CR} = 1,\ w_k > 0,\ k = S, RF, CR\end{aligned}$$

Let $VaR_{99.5\%}(NAV(t))$ denote the VaR of the NAV at time t, calibrated to a 99.5% confidence level to match the SCR. A lower risk ratio constraint $RANAV^{min}$ is introduced to ensure solvency. An additional constraint A^{min} on a minimum return on assets is also added, allowing the insurer to be competitive compared to e.g. cash investments and minimum rates offered by other insurers. To reach the minimum return, a lower limit w_S^{min} to the proportion of capital invested into equity will be set.

Consequently, the vector of risk adjusted weights $\mathbf{w}^{RANAV}$ optimizing the ratio of expected NAV to VaR is found by solving the following maximization problem:

$$\begin{aligned}&\mathbf{w}^{RANAV} = arg\ \max_{\mathbf{w}} \frac{E^Q[NAV(t) \mid \mathcal{F}(t)\ ]}{VaR_{99.5\%}(NAV(t))}\ ,\\ &RANAV > RANAV^{min},\\ &A(T) \geq A^{min},\\ &w_S \geq w_S^{min}\end{aligned} \tag{4.19}$$

A stochastic simulation approach can be implemented to estimate the expected NAV. The overall VaR is thereafter easily obtained from the quantiles of the resulting NAV distribution. Ergo, this is where the LSMC method comes into play. After projecting all risk drivers one year into the future for a given set of asset class weights, the LSMC method regresses over the NAV at maturity T, averaged over all inner scenarios. The resulting proxy function provides us with approximations of the expected NAV for a broad range of economic scenarios. Recalling the NAV equation expressed in 4.18, the resulting NAV function would be of the following form:

$$\begin{aligned}&NAV(t) = P(t,T)E^Q[A(T)(1-\alpha) - \alpha(K - A(T))^+ \mid \mathcal{F}(t)\ ]\\ &= P(t,T)NAV^{prox}(T)\end{aligned}$$

where $NAV^{prox}(T)$ is approximated using the LSMC method. The resulting polynomial proxy function, of the type described in equation 3.3, would be a function of the LARS/lasso estimates β^{LSMC}, the three risk factors, and their respective cross-terms $g(\cdot)$. For a polynomial order of two, assuming the full set of polynomial terms is used, the NAV proxy function would have the following appearance:

$$\begin{aligned}&NAV^{prox}(T) = f(S(t), RF(t), CR(t), \beta^{LSMC}, g(\cdot))\\ &= \beta_0 + \beta_1 S(t) + \beta_2 RF(t) + \beta_3 CR(t) + \beta_4 S(t)^2 + \beta_5 S(t)RF(t)\\ &+ \beta_6 S(t)CR(t) + \beta_7 RF(t)^2 + \beta_8 RF(t)CR(t) + \beta_9 CR(t)^2\end{aligned} \tag{4.20}$$

With all definitions in place, optimization problem 4.19 can now be stated in a more detailed fashion:

$$\mathbf{w}^{RANAV} = arg\ \max_{\mathbf{w}}\ \frac{NAV(t)}{VaR_{99.5\%}(NAV(t))} \tag{4.21}$$

where;

$NAV(t) = P(t,T)NAV^{prox}(T)$,

$NAV^{prox}(T) = f(S(t), RF(t), CR(t), \beta, g(\cdot))$

subject to;

$w_S + w_{RF} + w_{CR} = 1,\ w_k > 0,\ k = S, RF, CR,$

$RANAV > RANAV^{min}$,

$A(T) \geq A^{min}$

$w_S \geq w_S^{min}$

Recall from expression 4.14 that the asset value can only be determined for a predefined set of weights, granting the asset class allocation a direct impact on the asset value, and, consequently, liability value. This basic property has a large impact on the entire optimization framework - since the weights can not be extracted implicitly from the polynomial proxy function $NAV^{prox}(T)$, the regression must be re-performed each time a change in the underlying weights occurs. This emphasizes the advantage of using the LSMC method to calculate the NAV; having to re-valuate the NAV several times for different allocations is not an issue due to the time efficient LSMC regression. However, an optimization algorithm that operates only through function evaluations is required since partial derivatives can not be obtained. This makes the Nelder-Mead and Powell methods, presented in section 3.3, suitable choices. Since optimization methods which do not rely on gradients are often deemed less reliable, both methods will be implemented and compared. Note that the considered methods are minimization algorithms, meaning they will be implemented to find the local minimum of the negative RANAV.

For comparison, a similar optimization will be performed using the MVO framework described in section 2.3, with corresponding restrictions. Instead of optimizing the ratio of NAV to VaR, the expected NAV will be optimized subject to its standard deviation. Letting $\sigma_{NAV(t)}$ denote the standard deviation of the NAV, the optimal MVO weights are found by solving the following maximization problem:

$$\mathbf{w}^{MVO} = arg\ \max_{\mathbf{w}}\ \frac{NAV(t)}{\sigma_{NAV(t)}} \tag{4.22}$$

where;

$NAV(t) = P(t,T)NAV^{prox}(T)$,

$NAV^{prox}(T) = f(S(t), RF(t), CR(t), \beta, g(\cdot))$

subject to;

$w_S + w_{RF} + w_{CR} = 1,\ w_k > 0,\ k = S, RF, CR,$

$MVO > MVO^{min}$,

$A(T) \geq A^{min}$,

$w_S \geq w_S^{min}$.

4.5 Methodology Review

To summarize, the entire process of the ALM optimization framework using the LMSC approach will be briefly reviewed below. For a maturity T, the following steps are implemented:

Step 1: Using the nested Monte Carlo method, simulate n_{out}^{FN} outer scenarios of the risk factors up to the one-year outer time horizon. Set asset class values, all rescaled to have a starting value equalling 100, using the values at $t = 1$ year of the resulting processes:

$S^{FN}(1)$: Stock process value.

$RF^{FN}(1) = p(1, T^B)$: Price of a risk free treasury bond with maturity $T^B > T$.

$CR^{FN}(1) = p^{CR}(1, T^B)$: Price of a corporate bond with credit risk, with maturity $T^B > T$.

For each outer end point, simulate the same amount n_{out}^{FN} of inner risk neutral scenarios up to maturity T. Obtain corresponding asset class values $S^{FN}(T), RF^{FN}(T), CR^{FN}(T)$ and denote this the full nested set of simulations.

Step 2: For a given set of weights, set asset value $A^{FN}(T) = w_S S^{FN}(T) + w_{RF} RF^{FN}(T) + w_{CR} CR^{FN}(T)$. Obtain benchmark net asset value $NAV^{FN}(1) = P(1, T)(A(T)(1 - \alpha) - \alpha(K - A(T))^+)$ as the mean of all NAV's obtained from the full nested inner scenarios. These are considered to be the true NAVs used for later evaluation.

Step 3: Simulate n_{out}^{LSMC} new outer scenarios. Starting from each of the endpoints, simulate a far smaller amount n_{inn} of inner scenarios. Denote this the LSMC set of scenarios, and compute the corresponding asset class values $S^{LSMC}(t), RF^{LSMC}(t), CR^{LSMC}(t)$ for $t = 1, T$.

Step 4: For each set of weights, obtain net asset value $NAV^{LSMC}(T)$ at maturity as the mean of the NAVs obtained from the inner scenarios of the LSMC set. Via the LARS/lasso algorithm, fit a NAV proxy function $NAV^{prox}(T)$ to $NAV^{LSMC}(T)$ using outer risk factor values at time $t = 1$ from the LSMC set, $S^{LSMC}(1), RF^{LSMC}(1), CR^{LSMC}(1)$, as explanatory variables. Obtain parameter estimates β^{LSMC}.

Step 5: Once a NAV proxy function $NAV^{prox}(T)$ is found for a given set of weights, the input LSMC risk variables are replaced by the outer full nested scenarios, while the estimates β^{LSMC} remain the same. The regression is thereof only performed over the LSMC set, and the resulting parameters can be reused for new simulations without the need for re-estimation. After discounting to $t = 1$ year, the VaR can be calculated from the resulting NAV distribution, and thus the RANAV can be computed for this specific set of weights. At this point, the accuracy of the proxy function can be evaluated using cross-validation against the benchmark full nested value $NAV^{FN}(1)$.

Step 6: Using the Powell or Nelder-Mead optimization methods, step 4 and 5 are iterated for different sets of asset class weights until the increase in RANAV is sufficiently small. Ultimately, the set of optimal weights is obtained, and further evaluations as well as comparison to MVO framework is possible.

Chapter 5

Results

In this chapter, the results obtained from implementing the previous chapter's methodology for the RANAV and MVO frameworks are presented.

The chapter begins with a presentation of the parameters used in the underlying simulation models, along with the restrictions imposed in the ALM optimization framework. It proceeds with a goodness of fit analysis covering several allocations, where the accuracy and performance of the LSMC regression is examined. Following this, the ALM optimization results are presented and compared for the RANAV and MVO frameworks, and the effects of moving capital between different asset classes are studied.

5.1 Calibration & Model Parameters

This section presents the parameters used in the simulation models to generate the risk factors, along with some relevant comments. It concludes with a specification of the NAV function parameters, along with the implemented restrictions on risk and asset return.

5.1.1 Risk Free Rate

The risk free rate was generated using a Hull-White model, with the parameters used in both inner and outer scenarios presented in table 5.1.

a	σ
0.2	0.01

Table 5.1: *Parameters of Hull-White model.*

The parameters were selected to ensure a process with a slow and stable growth, providing reasonable short rate values.

To generate a risk free rate that evolves around a suitable yield curve, the time dependent parameter $\theta(t)$ was calibrated to fit a forward yield curve $f(0,t)$ composed of Swedish annual forward rates as of 28-02-2018, provided by EIOPA. For consistency, the initial value r_0 of the outer simulation was set to match the spot rate of the yield curve.

5.1.2 Credit Rate

The default intensity process, serving to price corporate bonds with credit risk, was generated by a CIR++ model. The parameters used in all scenarios are presented in table 5.2.

θ	σ	κ	δ
0.025	0.25	1.2	0.65

Table 5.2: *Parameters of CIR++ model.*

The deterministic function $\psi(t)$ was calibrated to a global corporate average cumulative default rate for an A-rated issuer, obtained from a study by Standard & Poor's Global Fixed Income Research (S&P, 2016). The initial value x_0 of the CIR process was set to the one-year default rate. Along with an appropriate choice of parameters, this calibration ensures that the CIR++ model provides default intensities of a realistic magnitude. The recovery rate δ was set to 0.65, meaning 65% of the bond's face value is paid out upon default.

5.1.3 Equity

The stock process was in this thesis generated using Bates model. Table 5.3 displays the model parameters for outer and inner scenarios.

Probability measure	μ	θ	σ	κ	μ_J	σ_J	λ_J	ρ
P	0.0676	0.07	0.02	0.1	-0.1	0.2	0.2	-0.5
Q	0.0176	0.07	0.02	0.1	-0.1	0.2	0.2	-0.5

Table 5.3: *Parameters of the Bates model under real world measure P and risk neutral measure Q.*

As opposed to the B-S model, Bates model is incomplete, meaning there is not just one unique Martingale measure under risk neutral dynamics. This allows us to select parameters for the volatility and jump process more freely. In this application, however, all parameters except for the drift will be set to equal values under both measures for simplicity.

Since the inner scenarios are generated under the risk neutral probability measure Q, the drift should equal the risk free rate to ensure that no arbitrage occurs. The correct drift would therefore be the Hull-White simulated risk free short rate. However, using the short rate process as input to the Bates model would increase the complexity of the dependency structure. An approximate rate is given by the forward yield curve, around which the risk free short rate evolves. The drift was therefore set to equal the forward rate at the end of the three-year inner simulation horizon, i.e. $f(0,3)$, after subtracting the expected value of the jump process. The outer scenarios, generated under P, has a risk premium of 5% added to the drift.

Some additional stylized facts from section 2.2.1 were taken into account when choosing the remaining parameters. To account for the gain/loss asymmetry, the jump sizes were set to have negative mean $\mu_J = -0.1$ corresponding to a 10% fall in the stock price. Furthermore, the correlation ρ between the stock process and the underlying volatility was kept negative to capture the leverage effect.

5.1.4 Dependence

The correlation matrix used for the dependence modelling was in this application determined in the following way:

The correlation $\rho_{s,r}$ between the stock process and the risk free rate was estimated using historical data. The stock process was represented by the OMXS30 index, and the risk free rate by the three month STIBOR rate. The latter is not an entirely correct representation, as it is in fact the instantaneous short rate we obtain from the Hull-White simulation. However, since the instantaneous short rate can not be observed on the market, the three month STIBOR rate will serve as an approximation.

As mentioned in section 4.2, there can be no correlation between the risk free short rate and the default intensity in order to preserve the affine properties of the CIR++ model.

Regarding the correlation $\rho_{s,\lambda}$ between the stock process and the default intensity, estimation using real data is problematic as reliable data on suitable default intensities is hard to come by. As discussed in section 3.5, a weak negative correlation between the two processes is not unlikely. The correlation coefficient between the stock process and the default intensity was therefore set to -0.04.

The resulting correlation matrix is presented below.

$$\mathbf{R} = \begin{bmatrix} 1 & \rho_{s,r} & \rho_{s,\lambda} \\ \rho_{r,s} & 1 & \rho_{r,\lambda} \\ \rho_{\lambda,s} & \rho_{\lambda,r} & 1 \end{bmatrix} = \begin{bmatrix} 1 & -0.046 & -0.040 \\ -0.046 & 1 & 0 \\ -0.040 & 0 & 1 \end{bmatrix}$$

5.1.5 The ALM Optimization Framework

The parameters used in the RANAV and MVO frameworks are presented in table 5.4, along with the imposed risk constraints and asset return requirements.

Framework	α	K	$RANAV^{min}$	MVO^{min}	A^{min}	w_S^{min}
RANAV	0.95	95	1.05	-	103.45	0.1
MVO	0.95	95	-	3.8	103.45	0.1

Table 5.4: *Constraints and parameters of the RANAV and MVO frameworks.*

As previously mentioned, all asset class values are rescaled to have a starting value of 100. Recalling the definition of the liability function in section 4.3, it partly consists of a European put option with strike K. Since this represents a guarantee reserve, we want the probability of K being greater than the asset value at maturity to be small. This probability obviously varies when the asset class allocation is altered. In particular, the more capital invested into equity, the larger this probability becomes due to the significantly larger amount of scenarios with asset values under K. As algorithms are forced to include at least 10% equity, a strike $K = 95$ was found to provide a reasonable probability of the expected asset value reaching below it; for an allocation consisting of 10% equity and 45% treasury bonds, this probability equals 0.58%.

Regarding the choice of scaling factor α, it was set arbitrarily to generate liability values that grow reasonably in relation to the backing assets.

The minimum expected asset value at maturity is set to 103.4, ensuring the insurer earns a minimum return on assets of at least 3.4%. A^{min} was set to an amount that is 0.05% higher than the required return, to account for expected approximation errors. The approximation errors motivating the adjustments to the ALM restrictions will be presented in section 5.2.

In the RANAV optimization framework, the VaR is calibrated to a 99.5% confidence level over a one-year time horizon to match the SCR. Recall that Solvency II regulations require that eligible own funds must be higher than the SCR. Since own funds refer to the expected NAV in this application, this means that a lower restriction on RANAV of 1 must be introduced to ensure solvency. $RANAV^{min}$ was set slightly higher to account for approximation errors.

The corresponding lower risk ratio restriction MVO^{min} for the MVO framework was set to 3.8. The derivation of MVO^{min} is returned to in section 5.3.2.

5.2 Goodness of Fit & Performance

Before moving on to analyze the optimization results, an examination of the accuracy and performance of the LSMC regressed NAV proxy function is conducted.

The simulations are generated at a monthly frequency following the summarized steps of the methodology review in section 4.5. The time horizon is one year for the outer simulations, and three years for the inner simulations, equaling a total maturity of four years. The treasury- and corporate bonds all have maturities of five years. As previously mentioned, a full nested MC simulation is set as benchmark. Keeping the notations used in the methodology review, we denote this the full nested set, which will consist of 10 000 outer and 10 000 inner scenarios per outer. An increase to the number of outer simulations is far less computationally costly than an increase to the inner simulations. This argument is applied to the LSMC set, increasing the number of outer simulations while considerably decreasing the number of inner simulations, to obtain a better precision in the resulting proxy function. The LSMC set thereby consists of 50 000 outer scenarios and 16 inner scenarios per outer.

In this section, the goodness of fit of the NAV proxy function, discounted to time $t = 1$ year, is evaluated through cross-validation with the benchmark NAV. The LSMC regression is as previously mentioned performed over an independent LSMC set using the LARS/lasso algorithm, thus reducing the risk of over-fitting. The maximum order of the polynomial basis functions comprising the liability proxy function is set to two. In addition to keeping the complexity of the model down by reducing the number of terms, it has been found in e.g. Danielsson and Gistvik (2014) that a maximum polynomial order greater than two does not lead to any significant increase in the goodness of fit. Some preliminary testing confirmed that this was the case in our application as well.

By regressing over an independent set of simulations, the regression only needs to be performed once for a given set of weights to obtain a proxy function that works for any set of outer scenarios. Consequently, no inner scenarios are required in future NAV calculations and a significant amount of computation time is saved. However, note that this only applies to the considered set of asset class weights. If a change in the underlying weights occurs, the expected NAV changes, and the regression would obviously have to be redone.

The cross-validation is conducted by running the asset values at year one from the full nested set as input to the NAV proxy function regressed over an independent LSMC set. Comparing the resulting LSMC approximations to the benchmark makes it possible to evaluate how well the LSMC model predicts the full nested NAV.

Since the distributional properties of the asset classes vary greatly, one can expect the performance of the proxy function to be affected when changing the asset allocation. The goodness of fit is therefore examined for four different asset class allocations.

5.2.1 Out of Sample R-square

Beginning with a commonly used measure, the out of sample R-square is examined for the following asset class allocations; an equal weight allocation, an allocation consisting mainly of equity, and the optimal RANAV and MVO allocations. The latter will be obtained by using the Nelder-Mead method to maximize the RANAV and MVO ratio, respectively, which will be examined more thoroughly in section 5.3. Keeping the notations from chapter 4, the vector of asset class weights is defined as $\mathbf{w} = [\ w_S,\ w_{RF},\ w_{CR}\ ]$, where S, RF and CR denotes equity, risk free treasury bonds and corporate bonds with credit risk, respectively. For simplicity of notation, we refer to the asset class allocations as the following;

$\mathbf{w}^{equal} = [\ 1/3,\ 1/3,\ 1/3\ ]$

$\mathbf{w}^{S} = [\ 0.9,\ 0.05,\ 0.05\ ]$

$\mathbf{w}^{opt}_{RANAV} = [\ 0.1,\ 0.33445,\ 0.56555\ ]$

$\mathbf{w}^{opt}_{MVO} = [\ 0.1,\ 0.496437,\ 0.403563\ ]$

where $\mathbf{w}^{opt}_{RANAV}$ and $\mathbf{w}^{opt}_{MVO}$ maximize the RANAV and MVO ratio, respectively.

After regressing over the LSMC set using the LARS/lasso method for each allocation, the resulting proxy function is run using the risk factors at year one from the full nested set as inputs. The same procedure is implemented using an ordinary LS regression, to discern whether the LARS/lasso method contributes to an increased fit. Below, the out of sample R-square and adjusted R-square from cross-validating the resulting LSMC approximations against the benchmark full nested values for the different allocations are presented.

	LARS/lasso		**LS**	
Allocation	R^2	R^2_{adj}	R^2	R^2_{adj}
$\mathbf{w}^{equal}$	0.936273	0.936216	0.936260	0.936196
$\mathbf{w}^{S}$	0.957344	0.957302	0.957336	0.957293
$\mathbf{w}^{opt}_{RANAV}$	0.995753	0.995749	0.995504	0.995499
$\mathbf{w}^{opt}_{MVO}$	0.997469	0.997466	0.997400	0.997398

Table 5.5: *Out of sample R-square and adjusted R-square of NAV proxy function using lasso/LARS method and ordinary LS for allocations* $\boldsymbol{w}^{equal}$, $\boldsymbol{w}^{S}$, $\boldsymbol{w}^{opt}_{RANAV}$ *and* $\boldsymbol{w}^{opt}_{MVO}$.

Comparing the out of sample R-square of the LARS/lasso with that of the LS method, a small improvement is distinguishable in all examined allocations. Not only is the R-square higher - the difference between R-square and adjusted R-square is smaller for the LARS/lasso method. This implies that the LARS/lasso includes a smaller number of regression parameters, thereby decreasing the risk of over-fitting.

Table 5.5 also reveals that the R-square is the highest for the optimal MVO allocation, $\mathbf{w}_{MVO}^{opt}$. Considering that this allocation contains the highest proportion of risk free treasury bonds this is not surprising, as the significantly lower variance decreases the dispersion in the expected NAV. It may however seem counter intuitive that the R-square of the equal weight allocation is lower than that of the allocation consisting mainly of equity. A look at table 5.7, containing the first four moments of the different allocations, provides a possible explanation. The NAV proxy function fails to capture the last two moments, skewness and kurtosis, as well as the first two. In table 5.6, which provides us with each asset class' distributional properties, the extreme kurtosis and significant negative skew of the defaultable corporate bonds is evident. In combination with a high amount of equity, which increases the dispersion of the NAV, the LSMC regression struggles to capture the more extreme outcomes, leading to a lowered R-square.

Summarizing, the R-square might be deemed sufficiently high for the optimal allocations, but it is certainly not for the remaining allocations. As the NAV proxy function corresponding to the optimal RANAV allocation is the most central to this thesis, however, the focus of the goodness of fit analysis will concern $\mathbf{w}_{RANAV}^{opt}$. For a visual representation, figure 5.1 displays a goodness of fit plot of the optimal RANAV allocation for a sample of 100 scenarios. Nevertheless, the insufficient fit of the regression negatively affects the reliability of the optimization. In light of this, benchmark evaluations will be performed alongside the optimizations, allowing us to better discern how close regressed optima is to that of the benchmark.

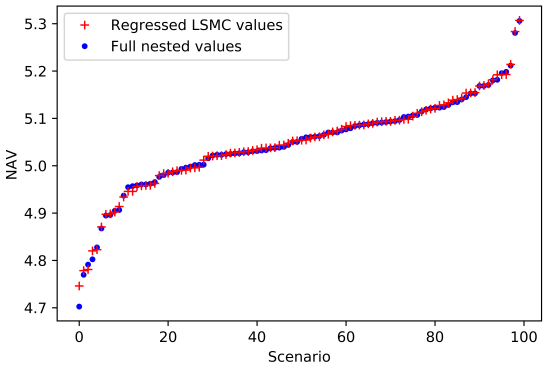

Figure 5.1: *Goodness of fit plot of full nested and LSMC regressed NAV at $t = 1$ for allocation $\boldsymbol{w}_{RANAV}^{opt}$.*

5.2.2 Comparison of Moments

In order to determine how well the distributional properties of the regressed values match those of the benchmark, a comparison of the first four moments defined in section 3.2.5 as well as some relevant quantiles will be conducted below. As RANAV and minimum asset return are central to this thesis, a comparison of the resulting NAV, VaR and expected return on assets concludes the cross-validation.

Asset class	**Mean**	**Variance**	**Skewness**	**Excess kurtosis**
Equity, S	105.534500	1598.002045	0.708123	1.479908
Treasury bonds, RF	102.062082	0.085399	0.009039	-0.001814
Corporate bonds, CR	104.525113	5.073425	-9.270162	138.090079

Table 5.6: *First four moments of benchmark asset distributions at $t = 4$ of equity, treasury bonds and corporate bonds.*

For future reference, we begin by presenting some distributional properties of each asset class at maturity,

displayed in table 5.6. The resulting distributions are obtained from the full nested simulation set, meaning they represent the true distributions. As expected, equity has the highest expected return of 5.53%, and by far the highest volatility. The corporate bonds display a significant negative skew and a large kurtosis, which is a result from the drop in value of the defaulted bonds. The distribution of the treasury bonds is the most well behaved, with low volatility and hardly any skewness or kurtosis. However, the above table also reveals that the expected treasury bond return at maturity is below the minimum requirements of 3.4%.

As the properties of the asset class distributions vary considerably, it is reasonable to expect the distributional properties of the NAV to differ when altering the allocation.

Allocation	Set	**Mean**	**Variance**	**Skewness**	**Excess kurtosis**
$\mathbf{w}^{equal}$	Full nested	3.536791	2.610976	-1.923162	6.013459
	LSMC	3.525004	2.461658	-1.413166	2.788938
$\mathbf{w}^{S}$	Full nested	-3.406486	44.610362	-1.494703	3.261290
	LSMC	-3.447321	42.984088	-1.296984	2.371751
$\mathbf{w}^{opt}_{RANAV}$	Full nested	5.045446	0.010974	0.035823	1.110832
	LSMC	5.045113	0.010998	0.063277	0.901939
$\mathbf{w}^{opt}_{MVO}$	Full nested	5.037032	0.010878	0.009711	1.128461
	LSMC	5.036594	0.010943	0.033612	0.857902

Table 5.7: *First four moments of full nested and LSMC regressed NAV at $t = 1$ for allocations $\boldsymbol{w}^{equal}$, $\boldsymbol{w}^{S}$, $\boldsymbol{w}^{opt}_{RANAV}$ and $\boldsymbol{w}^{opt}_{MVO}$.*

Table 5.7 displays the resulting distributional properties of the full nested and LSMC regressed NAV at year one. As anticipated, the moments vary considerably with the asset class allocation. An attribute all four allocations have in common is that the mean appears to be captured well by the LSMC regression, implying that a fairly unbiased estimation is achieved. While the variance has also been caught relatively well by the regression, the skewness and, especially, the kurtosis of the resulting distributions do not show the same goodness of fit.

The above table also reveals that allocations $\mathbf{w}^{equal}$ and $\mathbf{w}^{S}$ display a significant negative skew and excess kurtosis. This is a result of the liability structure; recall that the liabilities have an embedded guarantee reserve, including a European put option with strike K to the liability pay-off. Due to the large variance of the equity and proportion of defaulted corporate bonds, the kurtosis of $\mathbf{w}^{equal}$ and $\mathbf{w}^{S}$ increases dramatically. For the same reasons, the considered allocations have a significant amount of scenarios where asset values reach below K. This results in a positive skew in the liabilities, and, consequently, a negative skew in the NAV.

Another interesting note is that the last two moments of $\mathbf{w}^{equal}$ and $\mathbf{w}^{S}$ differ considerably from those of the optimal allocations. The resulting distribution moves from being strongly leptokurtic with a significant negative skew, into being a mildly leptokurtic distribution with a slight positive skew. In terms of Solvency II, these are both desirable properties as a light left tail results in a lower SCR.

The excess kurtosis and skewness present in all allocations constitute an additional issue for the MVO framework. As standard deviation assumes a symmetric distribution, taking no regard to whether the amount of NAVs below the distribution mean are equal to the amount above the mean, the full risk picture is not sufficiently captured for distributions with the above attributes. This will be further discussed in section 5.3.2.

Focusing the analysis on the optimal RANAV allocation, the LSMC regression slightly overestimates the skewness of the NAV distribution, implying a heavier right tail than the benchmark distribution. The kurtosis is underestimated, suggesting that the LSMC regressed distribution has fewer and/or less extreme outliers than the benchmark distribution. This implies that the regressed proxy function has trouble capturing the more extreme events at the tails of the NAV distribution.

Since SCR calculations are central to this thesis, the quantiles of the resulting NAV distributions are of great interest. Table 5.8 presents some relevant quantiles of the benchmark and LSMC regressed NAV.

Allocation	Set	**0.005**	**0.05**	**0.5**	**0.95**	**0.995**
$\mathbf{w}^{equal}$	Full nested	-3.273686	0.393934	3.952520	5.245957	5.815524
	LSMC	-2.348754	0.400864	3.880855	5.369623	5.554825
$\mathbf{w}^{S}$	Full nested	-29.103769	-16.539552	-1.827195	4.211162	6.364193
	LSMC	-27.373745	-16.358984	-2.104963	4.581191	5.719524
$\mathbf{w}^{opt}_{RANAV}$	Full nested	4.758580	4.873187	5.047697	5.213161	5.349610
	LSMC	4.767021	4.872588	5.046771	5.212280	5.344216
$\mathbf{w}^{opt}_{MVO}$	Full nested	4.745170	4.863368	5.039311	5.200555	5.335719
	LSMC	4.757464	4.861083	5.038277	5.201147	5.332387

Table 5.8: *Quantiles of full nested and LSMC regressed NAV at $t = 1$ for allocations $\boldsymbol{w}^{equal}$, $\boldsymbol{w}^{S}$, $\boldsymbol{w}^{opt}_{RANAV}$ and $\boldsymbol{w}^{opt}_{MVO}$.*

The increased fit of the LSMC regression in the optimal allocations is distinguishable in table 5.8 - the difference between the quantiles of the full nested benchmark and the regressed NAV is noticeably smaller for $\mathbf{w}^{opt}_{RANAV}$ and $\mathbf{w}^{opt}_{MVO}$. Again, the increased goodness of fit is largely explained by considerably less extreme results; the range between the 0.5% and 99.5% quantiles is significantly smaller for the optimal allocation.

As the SCR calculations concern the lowest 0.5% of the NAV distribution, this quantile is of particular interest. Consulting the above table, it appears the 0.5% quantile is systematically overestimated in all examined allocations. Additionally, the approximation error in this quantile appears to be larger than that of the remaining quantiles. A look at the goodness of fit-plot in figure 5.1 appears to confirm this suspicion. A reasonable motivation is the vastly underestimated kurtosis, which in combination with the overestimated skewness results in less extreme results in the lower end-tail of the approximated NAV distribution compared to that of the benchmark distribution.

To conclude the cross-validation, a comparison of the most central quantities of each framework is in place. As optimizations will be performed only in regard to the NAV proxy function, it is essential that the approximations are close to the benchmark values.

Allocation	Set	**NAV**	**VaR**	**RANAV**	**Asset return (%)**
$\mathbf{w}^{equal}$	Full nested	3.536791	6.810477	0.519316	4.040565
	LSMC	3.525004	5.873758	0.600127	4.226519
$\mathbf{w}^{S}$	Full nested	-3.406485	25.697283	-0.132562	5.310410
	LSMC	-3.447320	23.926424	-0.144080	5.814496
$\mathbf{w}^{opt}_{RANAV}$	Full nested	5.045446	0.286866	17.588139	3.802291
	LSMC	5.045113	0.278092	18.141908	3.849079

Table 5.9: *Expected NAV, $VaR_{99.5\%}$, RANAV at $t = 1$ and expected asset return at $t = 4$ of full nested and LSMC regressed set for allocations $\boldsymbol{w}^{equal}$, $\boldsymbol{w}^{S}$ and $\boldsymbol{w}^{opt}_{RANAV}$.*

Beginning with the RANAV optimization framework, table 5.9 displays the benchmark and LSMC approximations of the expected NAV, VaR, RANAV at year one and return on assets at maturity. In accordance with table 5.7, the LSMC regressed NAV proxy function approximates the expected NAV well.

However, as a result to the poor goodness of fit of the 0.5% quantile, the VaR is systematically underestimated for all allocations. Consequently, the absolute RANAV approximation becomes higher than that of the benchmark. To account for this approximation error, a small marginal will be added to the lower restriction on RANAV. Around the optimal allocation, the approximate RANAV is circa 97% as large as the benchmark RANAV. In order to account for variations between LSMC sets, the lower restriction is raised slightly and $RANAV^{min}$ is set to equal 1.05. This extra margin is added to match the restriction to the benchmark NAV around the optimal allocation, as this is the area of main interest.

A slight overestimation of the expected return on assets at maturity is another re-occurrence among all investigated allocations. Following above procedure, a small margin corresponding to the approximation error of the optimal allocation will be added to the restriction on return on assets, to ensure that the benchmark returns meet the requirements.

Allocation	Set	**NAV**	**Std**	**MVO ratio**	**Asset return (%)**
$\mathbf{w}^{equal}$	Full nested	3.536791	1.615851	2.188810	4.040565
	LSMC	3.525004	1.568967	2.246703	4.226519
$\mathbf{w}^{S}$	Full nested	-3.406485	6.679099	-0.510022	5.310410
	LSMC	-3.447320	6.556225	-0.525809	5.814496
$\mathbf{w}^{opt}_{MVO}$	Full nested	5.037032	0.104298	48.294453	3.403311
	LSMC	5.036594	0.104607	48.147545	3.450014

Table 5.10: *Expected NAV, standard deviation and MVO ratio at $t = 1$ and expected asset return at $t = 4$ of full nested and LSMC regressed set for allocations $\boldsymbol{w}^{equal}$, $\boldsymbol{w}^{S}$ and $\boldsymbol{w}^{opt}_{MVO}$.*

Regarding the MVO framework, the standard deviation appears to be slightly underestimated for allocations $\mathbf{w}^{equal}$ and $\mathbf{w}^{S}$. In the optimal allocation, the standard deviation is marginally overestimated. The approximation error in $\mathbf{w}^{opt}_{MVO}$ is however very slight, due to the small magnitude of the allocation's standard deviation. As a consequence, the absolute approximate MVO ratio becomes somewhat lower than the benchmark for the optimal allocation, and vice versa for the remaining allocations.

5.2.3 Time Performance

Lastly, the runtime of the full nested MC simulation is compared to that of the LSMC regression. As the ALM optimization workflow involves an optimization of the asset class weights, it consists of two segments; the nested MC simulation and the allocation optimization.

In this subsection, the averaged computation time of the different segments of the RANAV optimization framework are presented along with some relevant comments. The computation time required in the MVO framework was essentially the same, and will therefore be left out. To conclude, the total runtime of the full nested MC simulation is compared to that of the LSMC regression to evaluate the improvement in time efficiency.

The time performance is measured on a Lenovo Yoga laptop with an Intel Core i5-8250U, 1.60 GHz CPU and 8 Gb of RAM, using Windows 10. The process is run in Python 3.6.

Segment 1: Nested MC Simulation

As stated in the beginning of this section, the full nested set of MC simulations consists of 10 000 outer and 10 000 inner scenarios per outer, while the LSMC set consists of 50 000 outer and 16 inner scenarios per outer. Table 5.11 displays the averaged computation time for both sets.

Set	Runtime (s)
Full nested	42 236
LSMC	1 271

Table 5.11: *Runtime for simulation of full nested MC set vs. LSMC regression set.*

Segment 2: Optimizing the Asset Class Weights

Once the scenarios have been simulated and asset class values are obtained, the optimization algorithms are ready to run. As previously mentioned, the regression must be re-performed each time a change to the asset class allocation occurs, since the weights can not be explicitly extracted from the proxy function. This, in turn, means that the selected optimizing methods can not rely on gradients, which affects their performance. As a result, the starting point of the optimization algorithms is of importance, and one extra optimization is added to the ALM optimization workflow to find suitable starting values. This will be further discussed in section 5.3.

Table 5.12 displays the averaged computation time of the Nelder-Mead and Powell optimization methods over an LSMC regression set.

Method	Runtime (s)
Nelder-Mead	253
Powell	410

Table 5.12: *Runtime of one optimization using the Nelder-Mead and Powell methods over an LSMC regression set.*

Evaluation & Total Runtime

To conclude, the total runtime of the full nested MC simulation will be compared to that of the LSMC regression, in order to evaluate the difference in time efficiency.

An important note is that the computation time of the allocation optimization in the full nested set is left out. Since this optimization would not be in regard to any proxy function, it would allow for a more reliable optimizing method using gradients. Again, this will be further discussed in section 5.3. As finding a suitable optimizer for the full nested set is not considered to be within the scope of this thesis, this will be excluded from the analysis.

Before compiling the total runtime, an additional note on the advantages of using the LSMC regressed proxy function for function evaluation is made. The significant increase in time efficiency enables us to use a larger number of function evaluations, which facilitates the study of the effects from moving capital between asset classes. Table 5.13 displays the averaged computation time for one RANAV evaluation in the full nested set, as well as in an LSMC regression set.

Set	Runtime (s)
Full nested	740
LSMC	3.6

Table 5.13: *Runtime for RANAV evaluation on full nested MC set vs. LSMC regression set.*

To conclude, the runtime for both segments of the ALM optimization workflow is summated and presented in table 5.14. As the time efficiency of the Nelder-Mead was found to be superior to that of the Powell method, this is the optimization method represented in the below table.

Set	Nested simulation	Optimization	Total runtime (s)
Full nested	42 236	-	42 236
LSMC	1 271	253 + 253	1 777

Table 5.14: *Runtime for each segment and total runtime using Nelder-Mead method for full nested MC set vs. LSMC regression set.*

It is evident that, even without taking the full nested optimization into account, a considerable improvement in time efficiency is achieved; RANAV optimization using the LSMC regressed NAV proxy function is almost 24 times less time consuming than the full nested MC method. Additionally, once a proxy function is in place, function evaluation is rendered over 200 times faster than a full nested evaluation.

5.3 ALM Optimization Results

In this section, the effects of moving capital between the different asset classes are studied, and optimal allocations maximizing the RANAV are found. Results from the ALM optimization using the Nelder-Mead and Powell methods are presented and analyzed, and ultimately evaluated against the full nested benchmark. The section concludes with a similar analysis of the MVO framework.

5.3.1 Optimal RANAV Allocation

Let us begin by recalling the optimization framework in section 4.4. The aim is to maximize the RANAV, i.e. the ratio of expected NAV to SCR, by selecting the optimal amount of capital invested into each asset class.

The parameters are those presented in table 5.4, meaning the strike K equals 95 to account for the lower restriction on equity of 10%. This restriction is, in turn, imposed to ensure that the insurer is competitive compared to cash investments. For the same reason, a minimum return on assets of 3.4% is required, which is easily reached while maintaining a relatively high amount of risk free treasury bonds if the lower restriction on equity is kept. A lower restriction of 1 is introduced on the RANAV to ensure solvency under Solvency II regulations. Lastly, all asset class weights are assumed to be strictly positive and sum up to one.

LSMC Results

Iterating step four and five of the methodology review in section 4.5, the LSMC regression is performed over different asset class allocations until the increase in RANAV is sufficiently small. This is accomplished by minimizing the negative RANAV using either the Nelder-Mead or the Powell method, described in section 3.3. Both of the considered methods rely only on function values as gradients are impossible to obtain, meaning that there is a risk that the algorithms fail to converge to a minimizing point. Consequently, the starting point of the optimization algorithms becomes important. This is remedied by adding one preliminary optimization to the LSMC workflow, initiated at an equal weight allocation, in order to find suitable starting values.

After running the preliminary optimization, it became clear that the algorithms are not likely to place any more capital than required into equity. By placing too much capital into treasury bonds, however, the minimum return on assets might not be met. As the algorithms must be initiated within the restrictions in order for the optimizations to work, the following was therefore deemed as a suitable starting point for the algorithms:

$$\mathbf{w}^0 = [\ 0.1,\ 0.35,\ 0.55\ ] \tag{5.1}$$

Set	Method	w_S^{opt}	w_{RF}^{opt}	w_{CR}^{opt}	Runtime (s)	RANAV	Asset return (%)
1	**Nelder-Mead**	0.1	0.334450	0.565550	262	18.141087	3.848901
	Powell	0.1	0.334228	0.565772	431	18.141087	3.849448
2	**Nelder-Mead**	0.1	0.288158	0.611842	206	18.168987	3.966486
	Powell	0.1	0.288157	0.611843	397	18.168988	3.966489
3	**Nelder-Mead**	0.1	0.292585	0.607415	256	18.171248	3.960083
	Powell	0.1	0.292552	0.607448	401	18.171249	3.960167

Table 5.15: *Optimal asset class weights and approximate RANAV obtained using Nelder-Mead and Powell methods in three LSMC sets, with $\boldsymbol{w}^0$ given by 5.1.*

Table 5.15 displays three sets of optimal asset class weights obtained through the Nelder-Mead and Powell methods. Each optimization is run on a new independent LSMC set of simulations, meaning that some variation in the optimal allocation is expected.

The preliminary optimizations, started at $\mathbf{w}^{equal}$, yielded optimal allocations fairly close to those seen in table 5.15. The accuracy was not as precise, however, and the resulting RANAV slightly lower than that in the above table. This motivates the usage of a preliminary optimization to determine a more suitable starting point.

Comparing the performance of the two optimization methods, it is clear that they yield very similar results. This increases the reliability of the optimizations, as both algorithms evidently converge to the same optima. While the Powell method provides marginally higher RANAV in most examined cases, the time efficiency of the Nelder-Mead proves to be far superior by comparison. For this reason, the Nelder-Mead is deemed to be the preferred optimization method, and optimal allocations are set with regard to its results.

For a more extensive analysis, seven more Nelder-Mead optimizations were implemented over seven additional LSMC sets. The complete list of optimization results is found in appendix B. To get an apprehension of the dispersion of the optimization results, table 5.16 present the results averaged over all LSMC sets, along with the most extreme weights.

Asset class	Min	Mean	Max
w_S^{opt}	0.1	0.1	0.1
w_{RF}^{opt}	0.264663	0.318103	0.378711
w_{CR}^{opt}	0.521289	0.581898	0.635337

Table 5.16: *Minimum, mean and maximum of optimal asset class weights obtained using Nelder-Mead method in ten LSMC sets, with* $\boldsymbol{w}^0$ *given by 5.1.*

The above table shows considerable variation in the optimal allocations. Nevertheless, they have one quite expected common property; no more than the required amount is invested into equity. Considering the significantly higher volatility of the equity asset class, the small gain in NAV is not sufficient to make up for the substantial increase in VaR as more capital is invested into equity. It is therefore not surprising that the optimization algorithms always set w_S^{opt} to be as small as possible.

Regarding the remaining asset class weights, they appear to vary within an interval of circa 11% between the different LSMC sets. This is likely a result of the poor lower tail fit of the regression, making it harder for the regression to correctly capture the VaR. This will be investigated more thoroughly in the benchmark evaluation further on in this section.

Optimizing and averaging over several LSMC sets would certainly increase the accuracy. This would however decrease the time efficiency, as each optimization is performed over an independent LSMC set. Nevertheless, the required runtime would still be considerably smaller than that of a full nested simulation. As an example, consider an optimal allocation averaged over three separate LSMC sets. With the three LSMC simulations and Nelder-Mead optimizations, only performing a preliminary optimization on the first set, the required runtime would on average equal 4825 s. Thus, this method would still be almost nine times less time consuming than a full nested simulation.

In this thesis, however, the concluding optimization will only be performed over one LSMC set as time performance is of the essence. Hence, at random, set 1 from table 5.15 is selected and the optimal allocation is set as the result obtained via the Nelder-Mead algorithm:

$$\mathbf{w}_{RANAV}^{opt} = [\ 0.1,\ 0.33445,\ 0.56555\ ] \tag{5.2}$$

An advantage of the LSMC regression is that it provides a time efficient tool to analyze the sensitivity of the NAV to changes in asset allocation. By keeping one asset class weight fixed, the effects on RANAV can be studied while the remaining weights are moved within an interval of interest.

We start by examining the impact on RANAV of moving capital from corporate to treasury bonds. Keeping the proportion of capital invested into equity fixed at the optimal amount w_S^{opt}, given by 5.2, allows us to include the optimal allocation to the examination. As all optimal allocations agree on including exactly 10% equity, we are able to include evaluations from several LSMC sets to the analysis. Consequently, the impact on RANAV across independent LSMC sets can be compared. Figure 5.2a displays the approximate NAV and 99.5% VaR at year one, while figure 5.2b shows the resulting approximate RANAV, for ten evaluations on LSMC sets 1 - 3 moving w_{RF} equidistantly in the interval [0.01, 0.899].

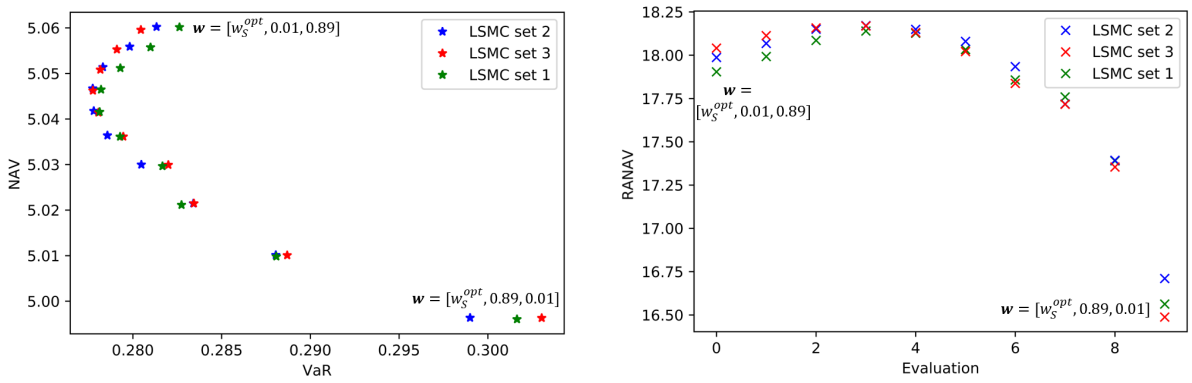

(a) (b)

Figure 5.2: *Ten equidistant evaluations in LSMC set 1 - 3 of approximate (a) NAV and* $VaR_{99.5\%}$ *(b) RANAV, with* $w_S^{opt} = 0.1$ *and* $w_{RF} \in [\ 0.01,\ 0.899\ ]$.

The above figure displays a curved relation between expected NAV and VaR. As capital is moved from corporate to treasury bonds, the NAV appears to decrease. This is not unexpected, as the lower expected return of the treasury bonds result in a lower NAV. However, one would perhaps expect the VaR to decrease as more capital is moved to treasury bonds. It can be added that optimizations performed with no lower restrictions on w_S showed this exact relation; both NAV and VaR decreases as w_{RF} grows, resulting in an optimal allocation consisting solely of treasury bonds. Figure 5.2a shows that this is only the case until the amount of treasury bonds reaches circa 40%. At this point, the VaR starts to increase as w_{RF} grows.

There are two explanations for this development. As 10% of capital is invested into equity, this significantly increases the VaR of the portfolio. The decreasing effect on VaR of moving capital from corporate to treasury bonds is therefore no longer as influential on the overall VaR. The second reason is the effect on the expected NAV of the liabilities, again caused by the embedded guarantee reserve in the shape of an European put option with strike K. By moving capital from corporate to treasury bonds the expected asset return at maturity is lowered, while, due to the previous reason, the dispersion of the results is not heavily affected. As a result, the number of scenarios with asset values reaching below the strike K grows, increasing the value of the "put option" section of the liabilities. This leads to a higher 99.5% quantile of the liabilities and, consequently, 0.05% quantile of the NAV, thereof increasing the VaR.

The approximation errors discovered in the goodness of fit examination are apparent when comparing the evaluations over the different LSMC sets. The regressions appear to agree well on the NAV, but there are obvious difficulties in the approximation of the VaR. Consequently, the optimal amount of treasury and corporate bonds vary within the sets. However, the above figure does offer an explanation to these variations. The VaR in LSMC set 1 has higher values than for the remaining sets, up until w_{RF} equals circa 40%. This causes a delay in the turning point where VaR starts to increase with the amount invested into treasury bonds. As a result, a considerably higher amount of treasury bonds is included to the optimal allocation in LSMC set 1. Again, this will be returned to in the benchmark evaluation.

For a fuller picture, the effects of moving capital from equity to corporate bonds is added to the analysis. As the optimal amount of treasury bonds varies between the LSMC sets, only set 1 will be included in this analysis. Figure 5.3 displays approximate NAV and VaR evaluations on LSMC set 1 while keeping either w_{RF} or w_S fixed at the optimal amount given by 5.2.

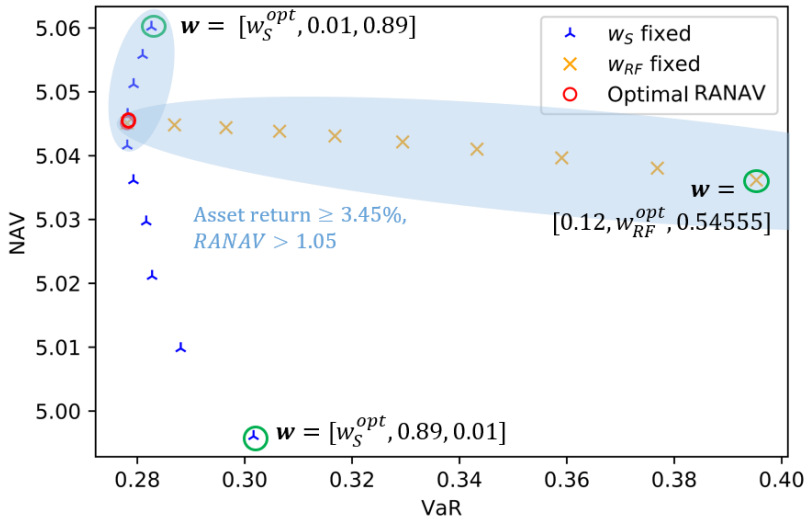

Figure 5.3: *Equidistant evaluations in LSMC set 1 of approximate NAV and* $VaR_{99.5\%}$*, with* $w_S^{opt} = 0.1$ *and* $w_{RF} \in [\ 0.01,\ 0.899\ ]$ *(blue), and* $w_{RF}^{opt} = 0.33445$ *and* $w_S \in [\ 0.1,\ 0.12\ ]$ *(yellow).*

Asset class allocations start reaching below the minimum return on assets if the amount of treasury bonds constitutes more than approximately 50% of the portfolio, given that the portfolio consists of 10% equity. The lower restriction on RANAV, however, is not reached until a significant additional amount of equity is included to the allocation. If the amount of treasury and corporate bonds is kept at the optimal amount given by 5.2, $RANAV^{min}$ is in LSMC set 1 reached for $w_S = 0.276$ and $w_S = 0.284$, respectively.

All allocations within the allowed restrictions are inside the blue fields, to better discern which allocations are viable options. The above plot clarifies that the optimal allocation contains an as small amount of equity as possible, and that it is within all required constraints.

Benchmark Evaluation

Having investigated the impacts on RANAV when moving from low to high risk assets, and found optimal asset class allocations on the LSMC sets, it is of great importance to see how well the LSMC regressed results agree with the full nested benchmark. This part of the analysis is of particular interest, as the goodness of fit was found to be unsatisfactory in some of the examined allocations.

As no approximations and, consequently, no proxy function is required, the benchmark NAV at maturity is directly given by expression 4.17. This allows for the implicit extraction of the assets class weights, meaning partial derivatives are obtainable. A more reliable optimization method utilizing the resulting gradients is therefore possible to implement. As previously mentioned, however, finding a suitable optimizer for the full nested set is not considered to be within the scope of this thesis. Since the Nelder-Mead and Powell algorithms optimize using function evaluations, these methods would be far too time consuming to implement on the full nested set. Instead, a number of RANAV evaluations will be performed on an increasingly small interval to find an approximate benchmark optima, to which the LSMC optima's can be compared.

By fixing the amount of capital invested into equity and treasury bonds at the optimal amount, the effects of moving capital between asset classes can once again be studied. This time, however, evaluations using the same weights will be performed on the full nested set, allowing for a comparison between the results of the LSMC regression and the benchmark.

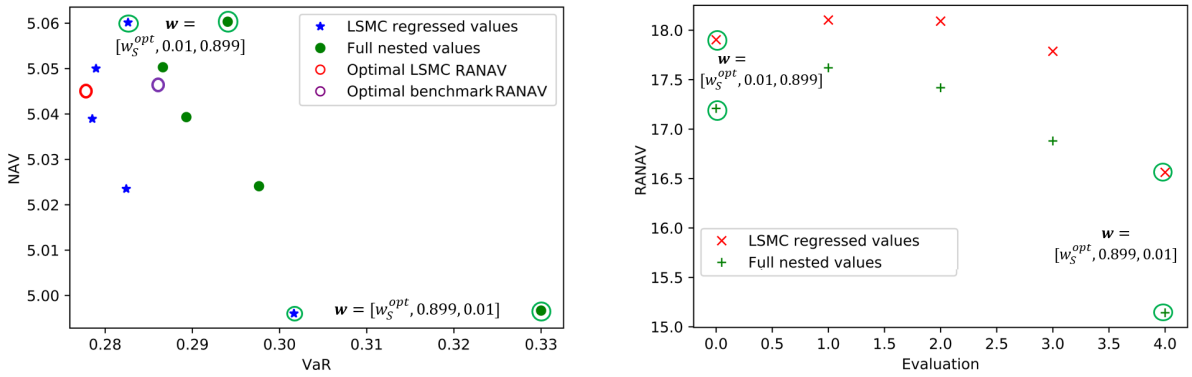

(a) (b)

Figure 5.4: *Five equidistant evaluations in LSMC set 1 vs. full nested set of (a) NAV and* $VaR_{99.5\%}$ *(b) RANAV, with* $w_S^{opt} = 0.1$ *and* $w_{RF} \in [\ 0.01,\ 0.899\ ]$.

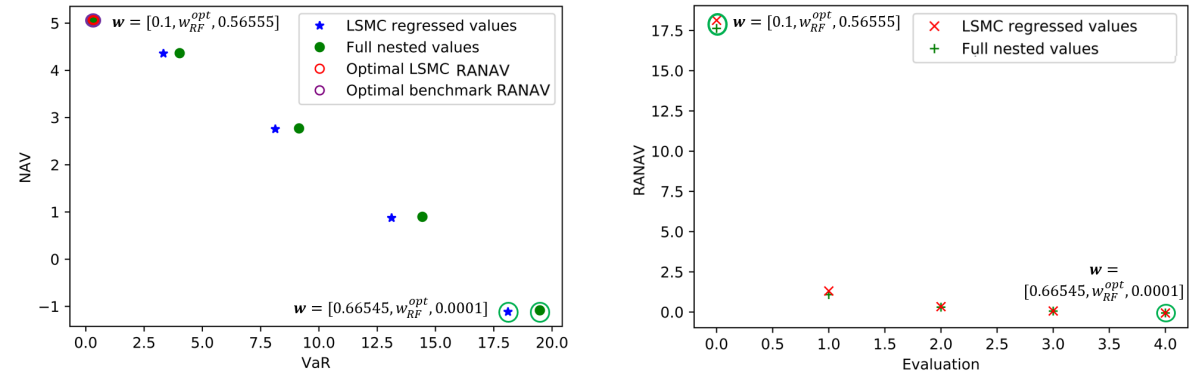

(a) (b)

Figure 5.5: *Five equidistant evaluations in LSMC set 1 vs. full nested set of (a) NAV and* $VaR_{99.5\%}$ *(b) RANAV, with* $w_{RF}^{opt} = 0.33445$ *and* $w_S \in [\ 0.1,\ 0.66545\ ]$.

As previously concluded, the NAV appears to be captured well by the LSMC regression, while there are obvious difficulties in the VaR-approximation. The explanation lies in the poor lower tail fit of the LSMC regression discussed in section 5.2, which increases the difficulty of approximating the 0.5% quantile of the NAV distribution.

Looking at figure 5.5, we can start by establishing that in both the full nested and the LSMC regressed case an as small amount as possible is placed in equity for a maximized RANAV. It is therefore reasonable to assume that the full nested optimal allocation also consists of 10% equity.

When attempting to find an optimal amount of capital to invest in the remaining asset classes, however, figure 5.4 indicates that the full nested benchmark and LSMC regression might not agree completely. To get closer to the assumed benchmark optima, evaluations where conducted on an increasingly small interval while keeping w_S fixed at 10%. Eventually, it was found that an allocation consisting of approximately 29.5% treasury bonds and 60.5% corporate bonds yields the highest benchmark RANAV, while still fulfilling the minimum return on assets requirements of 3.4%. A plot of the benchmark evaluations as w_{RF} is moved in the interval $[\ 0.29,\ 0.315\ ]$ is found in appendix D.

For a more thorough comparison between benchmark and LSMC regressed optimas, the averaged results from all Nelder-Mead optimizations, displayed in table 5.16, are re-examined. We denote the vector con-

taining the averaged optimal LSMC regressed weights $\mathbf{w}^{opt}_{average}$, while the vector containing the assumed full nested benchmark optima is denoted $\mathbf{w}^{opt}_{FN}$:

$$\mathbf{w}^{opt}_{average} = [\ 0.1,\ 0.318103,\ 0.581898\ ] \tag{5.3}$$

$$\mathbf{w}^{opt}_{FN} = [\ 0.1,\ 0.295,\ 0.605\ ] \tag{5.4}$$

Table 5.17 presents the expected RANAV and return on assets calculated over the full nested NAV distribution for allocations $\mathbf{w}^{opt}_{average}$ and $\mathbf{w}^{opt}_{FN}$.

Allocation	NAV	VaR	RANAV	Asset return (%)
$\mathbf{w}^{opt}_{average}$	5.046240	0.286507	17.612998	3.892735
$\mathbf{w}^{opt}_{FN}$	5.047351	0.286133	17.639876	3.899458

Table 5.17: *Expected benchmark NAV, $VaR_{99.5\%}$, RANAV at $t = 1$ and asset return at $t = 4$ for allocations $\boldsymbol{w}^{opt}_{average}$ and $\boldsymbol{w}^{opt}_{FN}$.*

Going by the averaged optimal LSMC allocation $\mathbf{w}^{opt}_{average}$, it appears to be fairly close to the benchmark optima. However, the optimizations over the LSMC regression sets appear to select an amount of treasury bonds higher by in average 1.3% in order to maximize the RANAV. Because of the significant variation in the optimal LSMC allocations, however, a far larger number of optimizations would be required in order to determine whether this is a systematic error.

The reason for this dispersion among the results is, once again, the VaR approximation error. Figure 5.4 shows that the VaR is systematically underestimated, and that the error is growing slightly with the amount invested into treasury bonds. As a result, the turning point where VaR starts increasing with w_{RF} is marginally shifted for the LSMC regression. In LSMC set 1, and most of the other considered LSMC sets, this lead to a small delay in the turning point. Consequently, the optimal amount of treasury bonds on average becomes slightly larger for the LSMC regression than for the benchmark.

5.3.2 Optimal MVO Allocation

As previously mentioned, the allocation yielding the maximal RANAV will be compared to an allocation that is optimal from an MVO point of view. Recalling the optimization framework outlined in section 4.4, the ALM optimization in regard to the mean-variance criteria will be conducted in a manner similar to the above RANAV optimization procedure. The difference lies in the risk measure; in the MVO framework the MVO ratio of expected NAV to standard deviation is maximized instead of NAV to VaR.

Since the focus of this thesis lies in the RANAV optimization framework, the MVO results will be presented in a more abbreviated manner. The analysis will instead be concentrated on comparisons between the resulting optimal MVO and RANAV allocations.

Before moving on to the optimization, the limitations of the MVO framework discussed in section 2.3 deserve a mention. The most apparent drawback is that standard deviation assumes a bell-shaped distribution, meaning the probability of NAV being above and below the mean is assumed to be the same.

Figure 5.6 displays the full nested NAV distribution at maturity for an equal weight asset allocation against a normal distribution, with the mean and standard deviation of the benchmark NAV. The attributes presented in table 5.7 in the goodness of fit analysis are apparent; the actual NAV distribution displays a considerably higher kurtosis than a normal distribution, resulting in a higher peak and heavier tails. The significant skew to the right is also visible in the below plot.

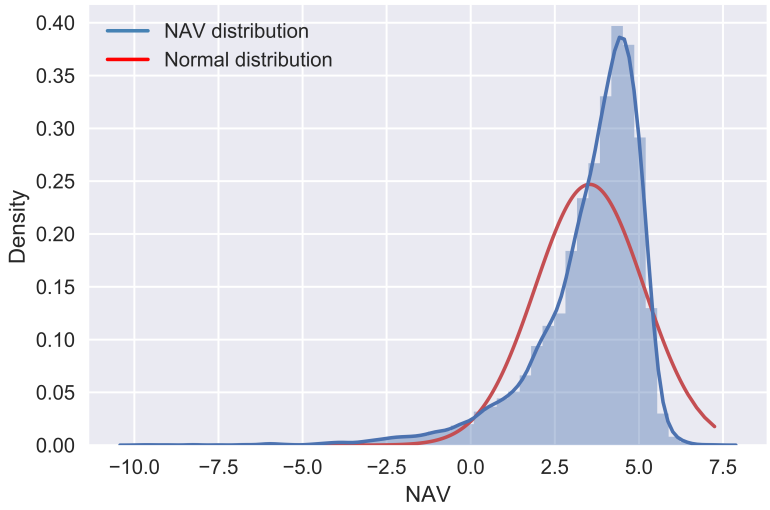

Figure 5.6: *Benchmark NAV distribution and normal distribution, with mean and standard deviation of benchmark NAV, for allocation* $\boldsymbol{w}^{equal}$.

This emphasizes the advantages of using VaR as risk measure rather than standard deviation. Since standard deviation only takes the first two moments into account, it fails to capture distributional properties that may significantly affect the expected risk. Figure 5.6 makes it evident that the lowest 0.5% quantile is far greater than that of a symmetric distribution, increasing the SCR considerably by comparison. In short, the full risk picture is not sufficiently captured in the MVO framework, which is important to keep in mind when analyzing the results.

The next step is to establish the restrictions of the MVO framework. Regarding the lower bound on the amount of equity and approximate minimum asset return, they are kept at the initial 10% and 3.45%, respectively. Regarding the restriction on risk, however, a lower limit MVO^{min} to the MVO ratio, corresponding to the lower RANAV restriction, is required. To find an approximation of this limit, a straightforward approach using the LSMC sets is applied.

From the restricted RANAV analysis, we know that the lower RANAV restriction in LSMC set 1 is reached for the following allocations:

$$\mathbf{w} = [\ 0.276,\ 0.33445,\ 0.38955\ ] \tag{5.5}$$

$$\mathbf{w} = [\ 0.284,\ 0.150450,\ 0.56555\ ] \tag{5.6}$$

The MVO ratio equals 3.7817 and 3.7838 for allocation 5.5 and 5.6, respectively. To account for variations between LSMC sets, the lower limit on the MVO ratio MVO^{min} is set to 3.8. Table 5.10 reveals that the optimal MVO ratio is underestimated by circa 0.3% by the LSMC regression, which is deemed small enough to be neglected when determining a lower restriction.

LSMC Results

As the Nelder-Mead was found superior in time efficiency, this is the only optimization method presented in the MVO framework. The preliminary optimization indicated that the MVO ratio was maximized for an allocation consisting of approximately 50% treasury bonds, which included no more than the mandatory 10% of equity. To ensure that the starting point was within the minimum return on assets requirement for all LSMC sets, however, the initial amount of treasury bonds was set to 47%.

The starting point of the Nelder-Mead algorithm was thereby set to:

$$\mathbf{w}^0 = [\ 0.1,\ 0.47,\ 0.43\ ] \tag{5.7}$$

Set	w_S^{opt}	w_{RF}^{opt}	w_{CR}^{opt}	Runtime (s)	MVO ratio	Asset return (%)
1	0.1	0.496437	0.403563	221	48.147545	3.450014
2	0.1	0.497904	0.402096	247	48.336535	3.450031
3	0.1	0.499822	0.400178	208	48.454359	3.450022

Table 5.18: *Optimal asset class weights and approximate MVO ratio obtained using Nelder-Mead method in three LSMC sets, with $\boldsymbol{w}^0$ given by 5.7.*

Beyond the mandatory 10% of equity, the optimal allocations in the above table have another attribute in common - the expected asset return is just above the minimum requirement of 3.45%. This suggests that the optimal allocation would contain a larger portion of risk free treasury bonds if no minimum asset return requirement was considered. To test this hypothesis, a second optimization with no asset return restriction is performed over the three LSMC sets. The table containing the results is found in appendix C. The unrestricted optimization confirmed the deduction; the optimal unconstrained allocation consists of circa 66% treasury bonds, resulting in an expected asset return that falls below the minimum requirement.

From the goodness of fit analysis conducted in section 5.2, it was concluded that the LSMC regression caught the variance far better than the VaR. It is therefore reasonable to expect the optimal MVO allocations to be more consistent by comparison. In the optimization with the minimum asset return requirement, however, we have a particular situation - the optima is determined by the restrictions rather than the objective function, making it hard to assess the performance of the optimization algorithm. When removing the asset return requirement, a larger variation is visible among the optimal allocations. Nevertheless, a far larger number of MVO and RANAV optimizations would be required to determine whether the accuracy of the optimal LSMC allocations is greater in the MVO framework. As this thesis has its main focus on the RANAV framework, further MVO ratio optimizations are left out.

For a deeper understanding of the effects on the MVO ratio as capital is moved from treasury to corporate bonds, we once again fix the amount invested into equity to the optimal amount. Selecting LSMC set 1, the optimal MVO allocation is thereby set as the following:

$$\mathbf{w}_{MVO}^{opt} = [\ 0.1,\ 0.496437,\ 0.403563\ ] \tag{5.8}$$

It could be of interest to include the optimal allocation with no restriction on asset return to the analysis. We denote this allocation $\mathbf{w}_{MVOunrestr}^{opt}$, which is in LSMC set 1 given by:

$$\mathbf{w}_{MVOunrestr}^{opt} = [\ 0.1,\ 0.664990,\ 0.235010\ ] \tag{5.9}$$

All allocations within the allowed restrictions are once again marked by the blue field. The below plots appear to agree that the optimal amount of treasury bonds will always be as high as the minimum return requirement allows.

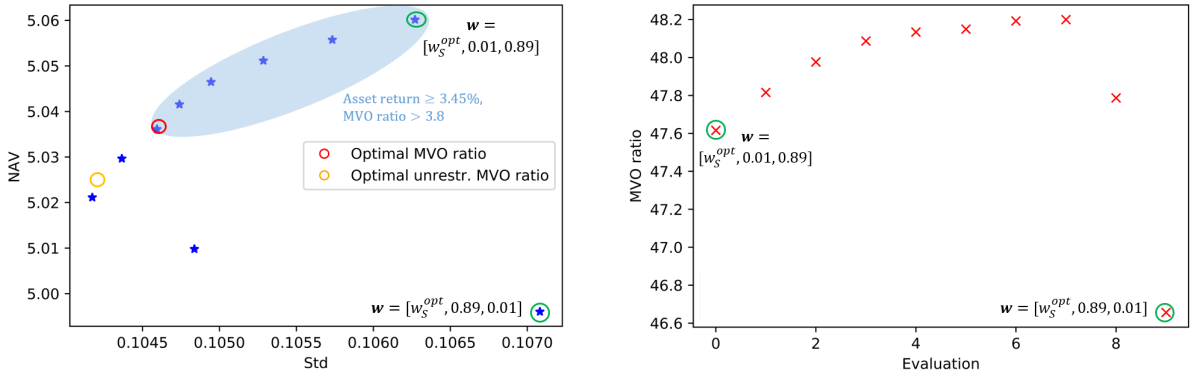

(a) (b)

Figure 5.7: *Ten equidistant evaluations in LSMC set 1 of approximate (a) NAV and standard deviation (b) MVO ratio, with* $w_S^{opt} = 0.1$ *and* $w_{RF} \in [\ 0.01,\ 0.899\ ]$.

A relation similar to the Markowitz efficient frontier is visible in figure 5.7a, where all efficient allocations in the considered NAV to standard deviation framework are contained. This plot has certain resemblances with the curved NAV to VaR relation displayed in figure 5.2; at a certain point, the risk starts to increase with the amount invested into treasury bonds. The explanation to this remains the same as in the RANAV framework, discussed in section 5.3.1. The difference between the two frameworks lies in the turning point, where the risk begins to increase with w_{RF}. For the RANAV framework, where VaR is considered instead of standard deviation, this turning point appears as circa 40% of the allocation consists of treasury bonds, instead of the approximate 70% of the MVO framework. This emphasizes the difference between the two risk measures; by taking the kurtosis and skewness of the NAV distribution into account, VaR provides additional information on the expected maximum loss. The standard deviation, on the other hand, only provides the overall dispersion of the distribution. For comparison, the benchmark RANAV of the optimal MVO allocation 5.8 is presented in table 5.19 along with that of the optimal RANAV allocation, given by equation 5.2.

Allocation	NAV	VaR	RANAV	Asset return (%)
$\mathbf{w}_{RANAV}^{opt}$	5.045446	0.286866	17.588139	3.802291
$\mathbf{w}_{MVO}^{opt}$	5.037031	0.291861	17.258275	3.403312

Table 5.19: *Expected benchmark NAV,* $VaR_{99.5\%}$*, RANAV at* $t = 1$ *and asset return at* $t = 4$ *for allocations* $\boldsymbol{w}_{RANAV}^{opt}$ *and* $\boldsymbol{w}_{MVO}^{opt}$.

The optimal RANAV allocation is selected due to its lower excess kurtosis and higher positive skewness, displayed in table 5.7, which decreases the overall SCR. In the MVO framework, these properties are disregarded in favour for the standard deviation, which is lower for an allocation consisting of a significantly higher amount of treasury bonds. As a result, $\mathbf{w}_{MVO}^{opt}$ provides a portfolio with a lower NAV and higher SCR than that of $\mathbf{w}_{RANAV}^{opt}$, while just barely fulfilling the minimum return on assets requirements.

Figure 5.8 displays a visual representation of the expected NAV and VaR of the optimal RANAV and MVO allocations.

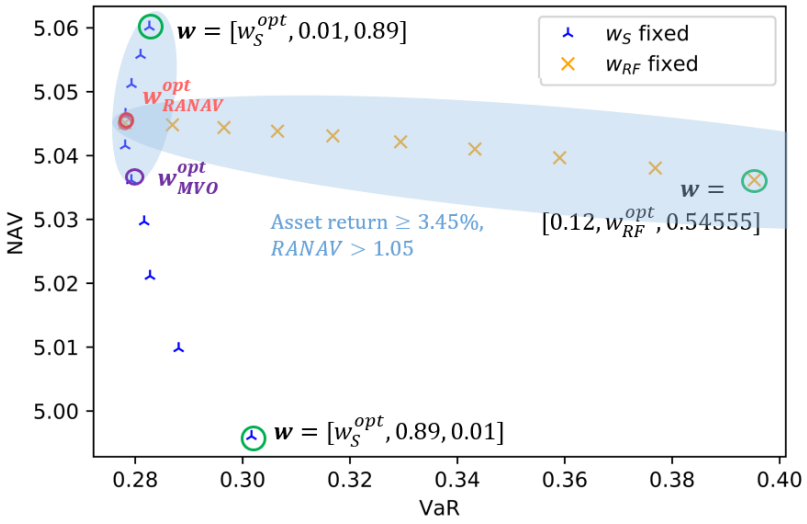

Figure 5.8: *Optimal RANAV and MVO allocations. Equidistant evaluations of approximate NAV and* $VaR_{99.5\%}$ *performed in LSMC set 1, with* $w_S^{opt} = 0.1$ *and* $w_{RF} \in [\ 0.01,\ 0.89\ ]$ *(blue), and* $w_{RF}^{opt} = 0.33445$ *and* $w_S \in [\ 0.1,\ 0.12\ ]$ *(yellow).*

Benchmark Evaluation

To conclude the analysis of the MVO framework, the LSMC regressed results are compared to those of the full nested benchmark. Following the procedure implemented in RANAV optimization framework, a number of evaluations will be conducted on LSMC set 1 as well as the full nested set.

We set the optimal allocation to equal equation 5.8. Figures 5.9 and 5.10 present RANAV evaluations as the optimal amount of equity and treasury bonds are kept fixed, respectively.

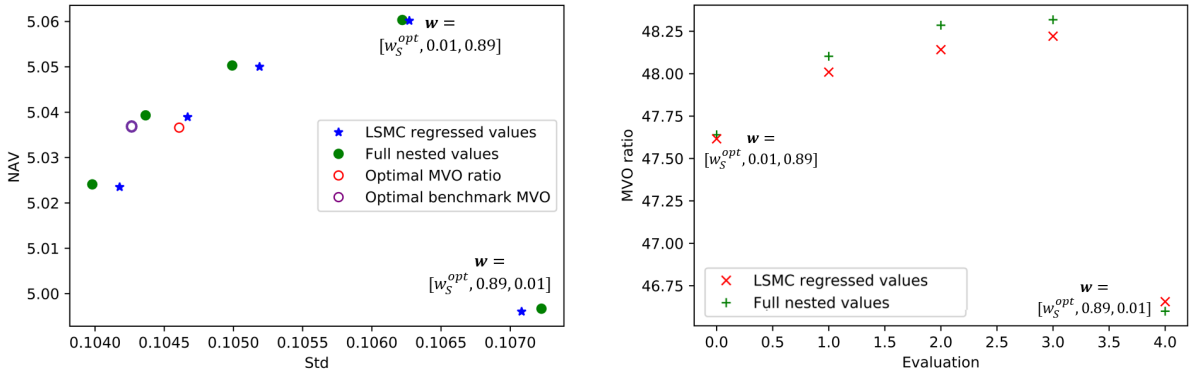

(a) (b)

Figure 5.9: *Five equidistant evaluations in LSMC set 1 vs. full nested set of (a) NAV and standard deviation (b) MVO ratio, with* $w_S^{opt} = 0.1$ *and* $w_{RF} \in [\ 0.01,\ 0.89\ ]$.

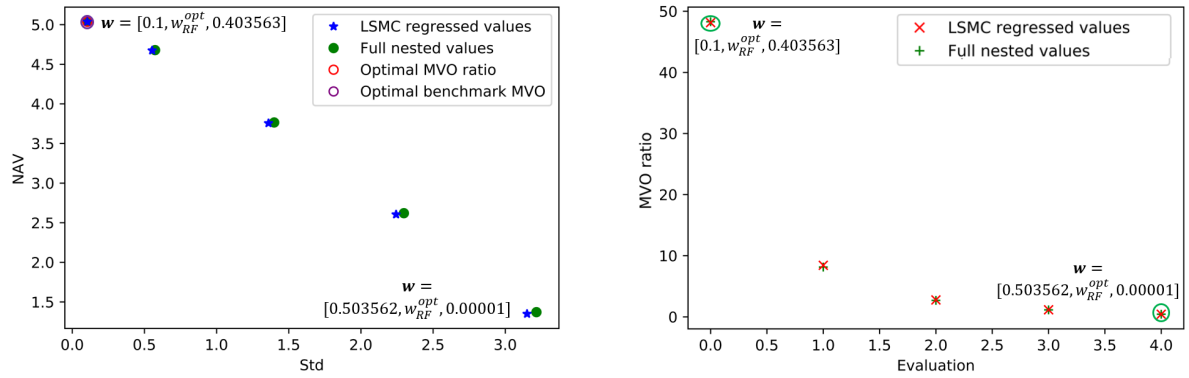

(a) (b)

Figure 5.10: *Five equidistant evaluations in LSMC set 1 vs. full nested set of (a) NAV and standard deviation (b) MVO ratio, with* $w_{RF}^{opt} = 0.496437$ *and* $w_S \in [\ 0.1,\ 0.503562\ ]$.

When keeping the amount invested into equity fixed at 10%, the small overestimation of the standard deviation discovered in section 5.2 is visible in all allocations except for the one containing the largest amount of treasury bonds, where a slight underestimation is seen. When instead fixing the amount invested into treasury bonds, the estimation error appears to be growing proportionally to the amount invested into equity, which is likely a result of the increasing dispersion.

Although slightly shifted due to the standard deviation approximation error, the benchmark and LSMC set appear to have corresponding developments in the MVO ratios. This implies that the benchmark optima is also found where the amount of treasury bonds is as high as the minimum return requirement of 3.4% allows. Further benchmark evaluations confirmed this deduction, and the benchmark optima was found where the amount of treasury bonds equals 49.75%. A plot of benchmark MVO ratio evaluations with $w_{RF} \in [\ 0.49,\ 0.5\ ]$ is found in appendix D. Consequently, this implies that optimization in the examined LSMC sets leads to a close approximation of the correct full nested optimal MVO allocation. Although, as previously mentioned, this is a particular case. Since the optima is determined by the restrictions rather than the objective function, it is hard to assess the performance of the optimization algorithm.

Chapter 6

Conclusion & Discussion

In this final chapter, the main results of the ALM optimization framework using the LSMC approach are summarized and discussed. The performance of the implemented methods are reviewed, and the resulting limitations and advantages are listed. Concluding the chapter, possible future research topics will be proposed along with some potential extensions to the current framework.

6.1 Results Summary

In this section, the main findings of the ALM optimization strategy considered in this thesis are summarized and discussed. The primary focus lies on the results of the RANAV optimization framework, while the MVO results are mainly be used to emphasize the differences between the two frameworks. The section concludes by presenting the limitations and advantages of the ALM optimization.

6.1.1 Goodness of Fit & Performance

Beginning with the goodness of fit of the LSMC regression, it was evident that the fit of the NAV proxy function was unsatisfactory for allocations containing a significant amount of equity and corporate bonds. The NAV distribution of allocations displaying significant skewness and excess kurtosis proved to be especially difficult for the LSMC regression to capture. Additionally, the regression had an insufficient fit in the lower tail of the NAV distribution. As a result, the 0.05% quantile, which is of key concern in SCR calculations, was systematically overestimated. The SCR approximation errors lead to an uncertainty regarding the optimization results, causing the optimal amount of treasury and corporate bonds to vary considerably. It was found, however, that by using the LARS/lasso method the fit of the LSMC regression was marginally improved, while the risk of over-fitting was reduced, compared to an ordinary LS regression.

The variations in the optimal allocations could be amended to some extent by simulating several LSMC sets and averaging the optimization results. The time efficiency would decrease by doing so, but the required runtime would nevertheless be nowhere near that of a full nested simulation. For an optimization over three separate sets, the LSMC method would still be almost nine times less time consuming than a full nested MC simulation.

To compensate for the poor goodness of fit, benchmark evaluations were performed alongside the evaluations on the LSMC sets. It was found that the LSMC regressed optimal treasury and corporate bond weights on average differed from those of the benchmark by 1.3%. Due to the aforementioned variation among the LSMC regressed optimas, however, it would take a far larger amount of optimizations to determine whether the error is systematic or not.

Regarding the asset class optimization, algorithms that optimize using function evaluations rather than gradients were required, as the implicit extraction of asset class weights was not possible. This decreased the accuracy of the optimizers, and one extra optimization was required to find an appropriate starting point for the algorithms. Comparing the performance of the optimizers, however, the two examined methods yielded results equal down to the fourth decimal, indicating a convergence to the same optima. While the

Powell method provided marginally higher objective function values, the considerably reduced runtime of the Nelder-Mead made it the preferred optimization method.

On a positive note, the time performance of the ALM optimization was considerably improved when implementing the LSMC method. Even excluding the full nested optimization, the simulation, LARS/lasso regression and RANAV optimization using the LSMC method was found to be almost 24 times less time consuming than a full nested MC simulation. Additionally, function evaluation using the LSMC regressed NAV proxy function was over 200 times faster than that of a full nested evaluation.

Another advantage is that the LSMC regression only has to be performed once for a determined set of asset class weights in order to obtain a proxy function that works for any set of outer scenarios. Consequently, no inner scenarios are required in future NAV calculations, which further reduces the computational burden. However, note that this only applies to the considered set of asset class weights. If a change in the underlying weights occurs, the regression would have to be redone.

Considering the significant gain in time efficiency, the ALM optimization method examined in this thesis could provide useful inputs on approximate optimal allocations, despite the unsatisfactory goodness of fit. Additionally, the runtime required to perform approximate RANAV evaluations is greatly reduced compared to a full nested evaluation, which facilitates the study of the effects from moving capital between asset classes.

6.1.2 Comparison: the RANAV and MVO Frameworks

By comparing the results from the RANAV and MVO frameworks, it was concluded that the considered risk measure has a large impact on the optimal allocations.

While the optimal MVO and RANAV allocations agreed on including an as small amount of equity as possible, the two frameworks showed significant disagreements regarding the optimal amount of risk free treasury bonds and defaultable corporate bonds. Both frameworks displayed a curved NAV-to-risk relationship, where after a certain point the risk began to increase with the amount of risk free investments. The reason behind this behaviour was the liability structure; the embedded guarantee reserve was reached for a larger number of scenarios when a large amount of risk free investments was included to the allocation, since this lowered the expected return on assets.

In section 5.2 it was concluded that the NAV of the examined allocations displayed significant skewness and excess kurtosis. As standard deviation only takes the first two moments into account, meaning a symmetric distribution is assumed, it is evident that the full risk picture is not captured for NAV distributions with the considered attributes. VaR, on the other hand, includes the additional information provided by the skewness and kurtosis to the expected maximum loss, making it a more appropriate risk measure in this context. The turning point at which the risk began to increase with the amount of risk free investments therefore occurs sooner in the RANAV framework. Consequently, the RANAV framework selected a lower optimal amount of risk free investments than the MVO framework.

Summarizing, the optimal RANAV allocation was found to hold a lower excess kurtosis and a higher positive skew than the optimal MVO allocation, leading to a lower SCR. In the MVO framework, these properties were disregarded in favour of a lowered standard deviation, which compensated for the loss in expected asset return. As a result, the RANAV framework provided an asset class portfolio superior in both RANAV and expected asset return.

6.1.3 Limitations & Advantages

In this section, the limitations and advantages of the examined ALM optimization method are listed along with some relevant comments.

Limitations

- **Goodness of fit:** The most prominent limitation of the considered LSMC method is the insufficient goodness of fit, especially regarding allocations containing a significant amount of high- and medium risk assets. In particular the poor fit of the 0.5% quantile proved problematic, as it led to significant approximation errors in SCR calculations. In section 6.2 a few suggestions on future work that could potentially improve the fit of the LSMC regression will be proposed.

- **Liability simplifications:** As discussed in section 4.3.2, the liability structure considered in this thesis is considerably simplified. Real world liabilities are often functions of a far vaster number of variables and risk drivers, for which risk quantification are considerably harder to determine. By implementing a replicating portfolio approach using basic financial instruments, and considering only one cash flow at maturity, valuations were in this thesis made more manageable at the cost of a less realistic liability function.

- **Time horizon:** As an extension to above simplifications, real world insurance liabilities often extend decades into the future. The LSMC approach considered here was found to be inadequate for simulation horizons of such magnitudes, due to hefty losses in prediction accuracy.

- **Model uncertainty:** In this application, the full nested MC simulations represent the true asset values, meaning the underlying simulation models are assumed to be correct. This is evidently an additional simplification, and it raises the question of how well the considered simulation models represent reality. A possible extension regarding the robustness to model changes is therefore proposed in section 6.2.

- **Optimization:** Since asset class weights could not be explicitly extracted from the proxy function, the NAV has to be re-valuated each time a change occurred in the weights. Consequently, only algorithms optimizing through function evaluations could be considered, which may negatively affect accuracy as well as time performance. In section 6.2, two approaches evading this issue will be proposed.

Advantages

- **Time performance:** The main advantage of the LSMC regressed proxy function was the significant improvement in time efficiency. ALM optimization using the LSMC method was found to be almost 24 times less time consuming than a full nested MC simulation. Proxy function evaluations were on average 200 times faster than full nested evaluations, making examinations of the effects from moving capital between different asset classes more accessible.

- **Only one regression per set of weights:** A factor contributing to the gain in time efficiency is that the regression only has to be performed once for a given set of asset class weights. The resulting proxy function works for any set of outer scenarios, meaning no inner scenarios are required in future NAV calculations for the considered weights.

- **Reduced risk of over-fitting:** As discussed in section 3.1.5, a too complex proxy function can lead to issues with over-fitting since it may end up fitting to the sampling error as well as the NAV. The cross-validation results in section 5.2 showed that the LARS/lasso considered in this thesis led to an improved accuracy compared an ordinary LS approach. The LARS/lasso provided a slightly higher out of sample R-square, while reducing the number of parameters included to the regression and consequently decreasing the risk of over-fitting.

- **Risk measure comparison:** By comparing the RANAV framework to an MVO approach, the impacts of the considered risk measure could be examined. Consequently, it could be determined that optimizing subject to standard deviation rather than the SCR led to significant differences in the optimal allocations. As the MVO standard deviation takes no regard to the skewness and excess kurtosis present in all examined allocations, the optimal MVO allocation displayed a higher SCR despite the lower standard deviation. The findings emphasized the importance of using an appropriate risk measure.

6.2 Future Research

In the concluding section of this thesis, possible future research topics that could potentially improve the performance of the considered LSMC method will be proposed, along with some possible extensions to the current framework.

6.2.1 Outer Scenario Sampling

The largest drawback with the LSMC method applied in this thesis was the insufficient goodness of fit, particularly in the lower tail of the NAV distribution. By sampling outer scenarios from a distribution other than the real world model used to generate the NAV, the success of the LSMC estimates can be improved, especially when the aim is accuracy in the upper tail of the liabilities or, alternatively, the lower tail of the NAV. Cathcart (2012) shows that a quasi-random sampling approach significantly improves the fit in the upper tail of a simulated liability distribution. Koursaris (2011) suggests a uniform sampling approach, which is shown to increase the overall fit of a liability distribution.

6.2.2 Basis Functions

The basis functions were in this thesis set to regular polynomial terms and cross terms. As discussed in section 3.1.4, the difference in performance between regular polynomials and orthogonal Laguerre polynomials has been found to be negligible in several similar applications. However, it has been proved that the usage of orthogonal polynomials result in parameter estimates with less mutual correlation (Cathcart, 2012). Theoretically, this leads to a smaller resultant variance associated with each individual parameter estimate, and, consequently, an improved numerical stability. For instance, Cathcart offers some evidence that employing orthogonal polynomial basis functions in combination with quasi-random sampling, in particular, might significantly improve the performance of the LSMC method.

6.2.3 SCR Aggregation

The issue with not being able to explicitly extract asset class weights from the proxy function, and thus having to re-valuate the NAV each time a change in weights occur, could be amended by using an approach similar to that of the standard formula for SCR calculation. By separately calculating the VaR for each asset class, and aggregating the results using linear correlation techniques, the overall SCR can be calculated without having to re-perform the LSMC regression. Consequently, partial derivatives can be obtained, and more reliable optimization algorithms implemented. There is an apparent drawback with this approach, however, since it is based on the assumption of linear dependency between risk factors. A modification to the correlation coefficients can to a certain extent account for potential tail dependencies and skewed distributions, but there is still a risk for aggregation errors (EIOPA, 2014).

6.2.4 Direct Estimates

Another way of resolving the issue of non-obtainable gradients is by using a direct method. By regressing over the differentiated NAV function, rather than the NAV function itself, direct estimates of the partial derivatives can be obtained despite discontinuities in the differentiated function. Consequently, optimizations requiring gradients can be performed with regard to the resulting direct estimates. Nevertheless, the gradients would still have to be re-estimated each time a change in the underlying asset class weights occurs, meaning that time efficiency would not likely improve using this method. For further information on direct estimates, see e.g. Boyle et al. (1997).

6.2.5 Robustness to Model Changes

A possible extension to the evaluation of the goodness of fit of the LSMC regression would be to test the sensitivity to changes and shifts in the underlying simulation models and parameters. As the fit of the regression proved to depend greatly on the distributional properties of the asset classes included to the allocation, it is reasonable to assume that altering these properties, or introducing a shift to the underlying process, would also have an impact on the fit. Alternatively, the underlying simulation models could be changed for different models altogether, and results could be compared to historical data. This would allow for tests of model uncertainty, as well as the performance of the LSMC regression.

6.2.6 Change of Objective Function

After implementing an MVO approach alongside the main RANAV framework, it was evident that the choice of risk measure had a significant impact on the optimal allocation. In line with this, a possible extension would be to test the corresponding impacts of using other well-known risk measures, and examine how well the results align with those obtained under Solvency II regulations. An interesting suggestion would be CVaR, which, in addition to being coherent, provides additional information on the cost of the worst loss.

This proposition could be extended to include the numerator of the objective function. A natural suggestion would in this case be to consider the expected return on NAV, rather than the expected NAV, and thereby compare the optimal RANAV allocation to the allocation with the highest RAROC.

Bibliography

Andersen, L., Jäckel, P., and Kahl, C. (2010). Simulation of square-root processes.

Bacinello, A., Millossovich, P., A., O., and E., P. (2011). Variable annuities: A unifying valuation approach. *Insurance: Mathematics and Economics, 49(3)*, pages 285–297.

Backman, F. (2015). Dependence modelling and risk analysis in a joint credit-equity frameworks.

Bakshi, G., Cao, C., and Chen, Z. (1997). Empirical performance of alternative option pricing models. *Journal of Finance, 52*, pages 2003–2049.

Bates, D. (1996). Jumps and stochastic volatility: Exchange rate processes implicity in deutsche mark options. *The Review of Financial Studies, 9(1)*, pages 69–107.

Bauer, D., Bergmann, D., and Reuss, A. (2010). Solvency ii and nested simulations - a least-squares monte carlo approach. *Proceedings of the 2010 ICA congress.*

Benzoni, L., Andersen, T., and Lund, J. (2002). An empirical investigation of continuous-time equity return models. *Journal of Finance, 57*, pages 1239–1284.

Björk, T. (2009). *Arbitrage Theory in Continuous Time.* Oxford University Press, 3 edition.

Black, F. and Scholes, M. (1973). The pricing of options and corporate liabilities. *The journal of Political Economy, 81(3)*, pages 637–654.

Boyle, P., Broadie, M., and Glasserman, P. (1997). Monte carlo methods for security pricing. *Journal of Economic Dynamics and Control, 21*, pages 1267–1321.

Brigo, D. and Mercurio, F. (2012). *Interest Rate Models - Theory and Practice.* Springer Finance, 2 edition.

Broadie, M. and Kaya, O. (2006). Exact simulation of stochastic volatility and other affine jump diffusion models. *Operations Research, 54(2).*

Cathcart, M. (2012). Monte carlo simulation approaches to the valuation and risk management of unit-linked insurance products with guarantees.

Cont, R. (2001). Empirical properties of asset returns: stylized facts and statistical issues. *Quantative Finance (1)*, pages 223–236.

Cox, J., Ingersoll, J., and Ross, S. (1985). A theory of the term structure of interest rates. *Econometrica, 53*, pages 385–407.

Cristelli, M. (2014). *Complexity in Financial Markets.* Springer.

Danielsson, J. and Gistvik, G. (2014). Estimation, model selection and evaluation of regression functions in a least-squares monte-carlo framework.

Daníelsson, J., Jorgensen, B., Samorodnitsky, G., Sarma, M., and de Vries, C. (2005). Subadditivity re–examined: the case for value–at–risk.

Duffie, D. and Singleton, K. (1999). Modeling term structures of defaultable bonds. *Review of Financial studies, 12(4)*, pages 687–720.

Efron, B., Hastie, T., Johnstone, I., and Tibshirani, R. (2003). Least angle regression.

EIOPA (2014). The underlying assumptions in the standard formula for the solvency capital requirement calculation. Technical report, European Insurance and Occupational Pensions Authority (EIOPA).

Gilbert, C. (2017). *International Actuarial Association Risk Book*. Insurance Regulation Committee of the International Actuarial Association.

Gilbert, C. L. (2004). Principles underlying asset liability management. Technical report, The Task Force on Asset Liability Management Principles.

Hastie, T., Tibshirani, R., and Friedman, J. (2001). *The Elements of Statistical Learning; Data mining, Inference and Prediction*. Springer Verlag.

Hermans, D. and Waaijer, R. (2013). Replication of a class of variable annuities for the purpose of economic capital calculations.

Heston, S. (1993). A closed-form solution for options with stochastic volatility with applications to bond and currency options. *The Review of Financial Studies, 6(2)*, pages 327–343.

Hooghwerff, S., van der Kamp, R., and Clarke, S. (2017). Judging the appropriateness of the standard formula under solvency ii. Technical report, Milliman.

Hull, J. and White, A. (1993). One factor interest rate models and the valuation of interest rate derivative securities. *Journal of Financial and Quantitative Analysis, 28(2)*, pages 235–254.

Koursaris, A. (2011). A least squares monte carlo approach to liability proxy modelling and capital calculation.

Lombardo, R. and Bailly, A. (2014). Efficient asset allocation with least-squares monte carlo. Technical report, Moody's analytics.

Longstaff, F. A. and Schwartz, E. S. (2001). Valuing american options by simulation: A simple least-squares approach. *Review of Financial studies, 14(1)*, pages 113–147.

Markowitz, H. (1952). Portfolio selection. *The Journal of Finance. 7 (1)*, pages 77–91.

McKinnon, K. (1999). Convergence of the nelder–mead simplex method to a non-stationary point. *SIAM J Optimization, 9*, pages 148–158.

Merton, R. (1976). Option pricing when underlying stock returns are continuous. *Journal of Financial Economics, 3*, pages 125–144.

Nelder, J. and Mead, R. (1965). A simplex method for function minimization. *Computer Journal, 7*, pages 308–313.

Osborne, J. and Waters, E. (2002). Four assumptions of multiple regression that researchers should always test. *Practical Assessment, Research Evaluation, 8(2)*, pages 1–9.

Pedregosa, F., Varoquaux, G., Gramfort, A., Michel, V., Thirion, B., Grisel, O., Blondel, M., Prettenhofer, P., Weiss, R., Dubourg, V., Vanderplas, J., Passos, A., Cournapeau, D., Brucher, M., Perrot, M., and Duchesnay, E. (2011). Scikit-learn: Machine learning in Python. *Journal of Machine Learning Research*, 12:2825–2830.

Pelsser, A. and van Haastrecht, A. (2008). Efficient, almost exact simulation of the heston stochastic volatility model.

Powell, M. (1964). An efficient method for finding the minimum of a function of several variables without calculating derivatives. *Computer Journal, 7(2)*, pages 155–162.

Press, W., Teukolsky, S., Vetterling, W., and Flannery, B. (2007). *Numerical recipes - The art of scientific computing*. Cambridge University Press, 3 edition.

Riccioletti, S. (2016). *Backtesting Value at Risk and Expected Shortfall*. Springer.

Singer, S. and Nelder, J. (2009). Nelder-Mead algorithm. *Scholarpedia*, 4(7):2928. revision #91557.

S&P (2016). 2016 annual global corporate default study and rating transitions. Technical report, Standard Poor's.

Vasiček, O. (1977). An equilibrium characterization of the term structure. *Journal of Financial Economics, 5(2)*, pages 177–188.

Appendix A

Hull-White Analytical Solution

Let $r(t)$ hold the Hull-White dynamics expressed in 3.20. An analytical solution for every $0 \leq s \leq t$ to the resulting SDE is given by:

$$r(t) = r(s)e^{-a(t-s)} + \int_s^t e^{-a(t-u)}\theta(u)du + \sigma \int_s^t e^{-a(t-u)}dW^Q(u) \tag{A.1}$$

Since $\theta(t)$ is calibrated to the initial forward curve $f(0,t)$ in order to fit the current term structure, the complicated part of solution A.1 is to evaluate the deterministic integral:

$$\int_s^t e^{-a(t-u)}\theta(u)du \tag{A.2}$$

From the calibration of $\theta(t)$ expressed in 3.21, the forward curve can be derived as (Björk, 2009):

$$f(0,t) = e^{-at}r(0) + \int_0^t e^{-a(t-u)}\theta(u)du - \frac{\sigma^2}{2a^2}(1-e^{-at})^2$$

Multiplying the entire expression by e^{at} allows us to rewrite it in the following way:

$$\int_0^t e^{au}\theta(u)du = e^{at}f(0,t) + e^{at}\frac{\sigma^2}{2a^2}(1-e^{-at})^2$$

By evaluating the resulting expression for an earlier time points $s < t$, and subtracting it from the above expression we obtain:

$$\int_s^t e^{au}\theta(u)du = e^{at}f(0,t) + e^{at}\frac{\sigma^2}{2a^2}(1-e^{-at})^2 - e^{as}f(0,s) + e^{as}\frac{\sigma^2}{2a^2}(1-e^{-as})^2$$

Lastly, we find an expression for the deterministic integral A.2 by again multiplying the entire expression by e^{at}:

$$\int_s^t e^{-a(t-u)}\theta(u)du = f(0,t) - e^{-a(t-s)}f(0,s) + \frac{\sigma^2}{2a^2}((1-e^{-at})^2 - e^{-a(t-s)}(1-e^{-as})^2)$$

By inserting this equation into A.1, we gain access to an analytical solution that can be expressed in terms of a Vasiček process complemented by an independent deterministic function:

$$\begin{aligned} r(t) = &\underbrace{r(s)e^{-a(t-s)} + \sigma \int_s^t e^{-a(t-u)}dW^Q(u)}_{\text{Vasiček process}} \\ &+ \underbrace{f(0,t) - e^{-a(t-s)}f(0,s) + \frac{\sigma^2}{2a^2}((1-e^{-at})^2 - e^{-a(t-s)}(1-e^{-as})^2)}_{\text{Deterministic terms}} \end{aligned} \tag{A.3}$$

Appendix B

RANAV Optimization Results

Set	w_S^{opt}	w_{RF}^{opt}	w_{CR}^{opt}	Runtime (s)	RANAV	Asset return (%)
1	0.1	0.33445	0.56555	262	18.141087	3.848901
2	0.1	0.288158	0.611842	206	18.168987	3.966486
3	0.1	0.292585	0.607415	256	18.171248	3.960083
4	0.1	0.289224	0.610776	234	17.884240	3.957963
5	0.1	0.304434	0.595566	255	18.011392	3.923074
6	0.1	0.264663	0.635337	350	18.189810	4.040247
7	0.1	0.308053	0.591947	216	18.343504	3.917750
8	0.1	0.378711	0.521289	261	17.950315	3.753626
9	0.1	0.347764	0.552236	258	18.171248	3.960083
10	0.1	0.372983	0.527017	236	18.080989	3.770206

Table B.1: *Optimal asset class weights and approximate RANAV obtained using Nelder-Mead method in ten LSMC sets, with* $\boldsymbol{w}^0$ *given by 5.1.*

Appendix C

MVO Optimization Results with no Asset Return Restriction

Set	w_S^{opt}	w_{RF}^{opt}	w_{CR}^{opt}	Runtime (s)	MVO ratio	Asset return (%)
1	0.1	0.664990	0.235010	311	48.222471	3.034777
2	0.1	0.660557	0.239443	303	48.443595	3.049383
3	0.1	0.631399	0.268601	267	48.480985	3.175403

Table C.1: *Optimal asset class weights and approximate MVO ratio obtained using Nelder-Mead method in three LSMC sets, with no minimum return on assets requirement and* $\boldsymbol{w}^0$ *given by 5.7.*

Appendix D

Benchmark Evaluations

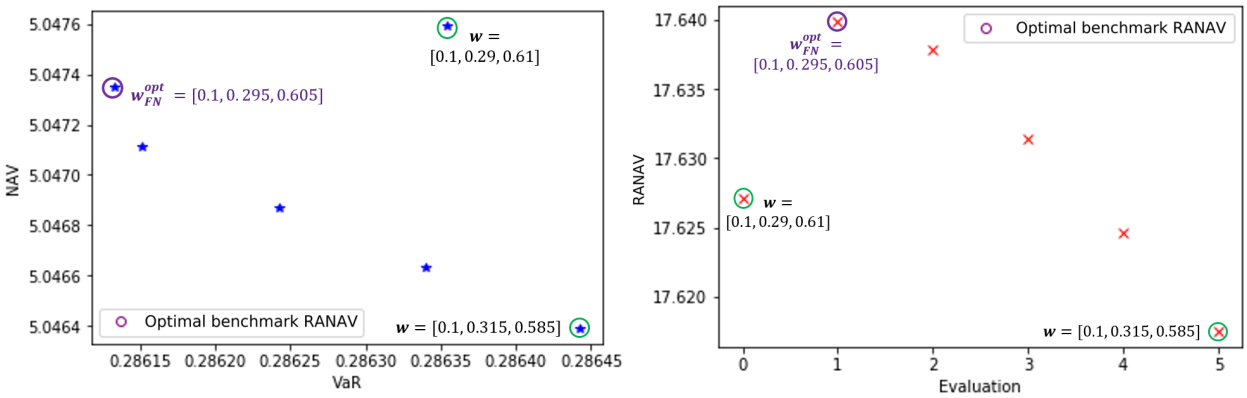

(a) (b)

Figure D.1: *Equidistant evaluations in full nested set of (a) NAV and VaR (b) RANAV, with* $w_S = 0.1$ *and* $w_{RF} \in [\ 0.29,\ 0.315\ ]$.

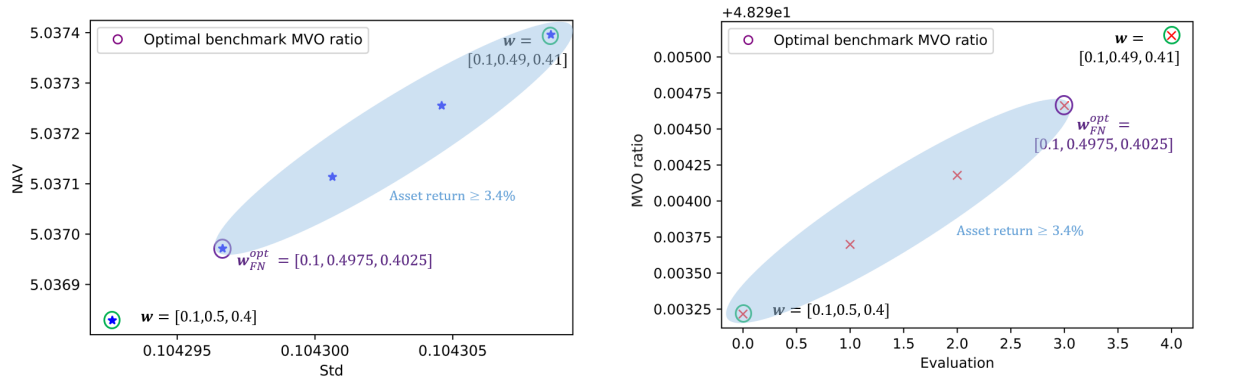

(a) (b)

Figure D.2: *Equidistant evaluations in full nested set of (a) NAV and standard deviation (b) MVO ratio, with* $w_S = 0.1$ *and* $w_{RF} \in [\ 0.49,\ 0.5\ ]$.